Athens Journal of Technology & Engineering

Quarterly Academic Periodical, Volume 9, Issue 3, September 2022
URL: https://www.athensjournals.gr/ajte
Email: journals@atiner.gr
e-ISSN: 2241-8237 DOI: 10.30958/ajte

Front Pages

TADO JURIĆ
Predicting Refugee Flows from Ukraine with an Approach to Big (Crisis) Data: A New Opportunity for Refugee and Humanitarian Studies

SIPHO MAKGOPA
Examining Student Support in Implementing Open Distance Learning during COVID-19

TOBIAS HELD, JENS PETH & CHRISTOPH FRIEDRICH
Preload Stability of Modern Bolted Joints

ENES YASA
The Interaction of Wind Velocity and Air Gap Width on the Thermal Comfort in Naturally Ventilated Buildings with Multiple Skin Facade

Athens Journal of Technology & Engineering

Published by the Athens Institute for Education and Research (ATINER)

The ***Athens Journal of Technology & Engineering (AJTE)*** is an Open Access quarterly double-blind peer reviewed journal and considers papers from all areas engineering (civil, electrical, mechanical, industrial, computer, transportation etc), technology, innovation, new methods of production and management, and industrial organization. Many of the papers published in this journal have been presented at the various conferences sponsored by the Engineering & Architecture Division of the Athens Institute for Education and Research (ATINER). All papers are subject to ATINER's Publication Ethical Policy and Statement.

The Athens Journal of Technology & Engineering
ISSN NUMBER: 2241-8237- DOI: 10.30958/ajte
Volume 9, Issue 3, September 2022
Download the entire issue (PDF)

Front Pages i-viii

Predicting Refugee Flows from Ukraine with an Approach to Big (Crisis) Data: A New Opportunity for Refugee and Humanitarian Studies 159
Tado Jurić

Examining Student Support in Implementing Open Distance Learning during COVID-19 185
Sipho Makgopa

Preload Stability of Modern Bolted Joints 197
Tobias Held, Jens Peth & Christoph Friedrich

The Interaction of Wind Velocity and Air Gap Width on the Thermal Comfort in Naturally Ventilated Buildings with Multiple Skin Facade 213
Enes Yasa

Athens Journal of Technology & Engineering
Editorial and Reviewers' Board

President's Message

All ATINER's publications including its e-journals are open access without any costs (submission, processing, publishing, open access paid by authors, open access paid by readers etc.) and is independent of presentations at any of the many small events (conferences, symposiums, forums, colloquiums, courses, roundtable discussions) organized by ATINER throughout the year and entail significant costs of participating. The intellectual property rights of the submitting papers remain with the author. Before you submit, please make sure your paper meets the basic academic standards, which includes proper English. Some articles will be selected from the numerous papers that have been presented at the various annual international academic conferences organized by the different divisions and units of the Athens Institute for Education and Research. The plethora of papers presented every year will enable the editorial board of each journal to select the best, and in so doing produce a top-quality academic journal. In addition to papers presented, ATINER will encourage the independent submission of papers to be evaluated for publication.

The current issue is the third of the ninth volume of the *Athens Journal of Technology & Engineering (AJTE),* published by the Engineering & Architecture Division of ATINER.

Gregory T. Papanikos, President, ATINER.

Athens Institute for Education and Research

A World Association of Academics and Researchers

13th Annual International Conference on Civil Engineering
19-22 June 2023, Athens, Greece

The Civil Engineering Unit of ATINER is organizing its **13th Annual International Conference on Civil Engineering, 19-23 June 2023, Athens, Greece** sponsored by the Athens Journal of Technology & Engineering. The aim of the conference is to bring together academics and researchers of all areas of Civil Engineering other related areas. You may participate as stream leader, presenter of one paper, chair of a session or observer. Please submit a proposal using the form available (https://www.atiner.gr/2023/FORM-CIV.doc).

Academic Members Responsible for the Conference

- **Dr. Dimitrios Goulias**, Head, Civil Engineering Unit, ATINER and Associate Professor & Director of Undergraduate Studies Civil & Environmental Engineering Department, University of Maryland, USA.

Important Dates

- Abstract Submission: **21 November 2022**
- Acceptance of Abstract: 4 Weeks after Submission
- Submission of Paper: **22 May 2023**

Social and Educational Program

The Social Program Emphasizes the Educational Aspect of the Academic Meetings of Atiner.

- Greek Night Entertainment (This is the official dinner of the conference)
- Athens Sightseeing: Old and New-An Educational Urban Walk
- Social Dinner
- Mycenae Visit
- Exploration of the Aegean Islands
- Delphi Visit
- Ancient Corinth and Cape Sounion

Conference Fees

Conference fees vary from 400€ to 2000€
Details can be found at: https://www.atiner.gr/fees

11th Annual International Conference on Industrial, Systems and Design Engineering, 19-22 June 2023, Athens, Greece

The Industrial Engineering Unit of ATINER will hold its **11th Annual International Conference on Industrial, Systems and Design Engineering, 19-23 June 2023, Athens, Greece** sponsored by the Athens Journal of Technology & Engineering.The aim of the conference is to bring together academics, researchers and professionals in areas of Industrial, Systems, Design Engineering and related subjects. You may participate as stream leader, presenter of one paper, chair of a session or observer. Please submit a proposal using the form available (https://www.atiner.gr/2023/FORM-IND.doc).

Important Dates

- Abstract Submission: **21 November 2022**
- Acceptance of Abstract: 4 Weeks after Submission
- Submission of Paper: **22 May 2023**

Academic Member Responsible for the Conference

- **Dr. Theodore Trafalis**, Director, Engineering & Architecture Division, ATINER, Professor of Industrial & Systems Engineering and Director, Optimization & Intelligent Systems Laboratory, The University of Oklahoma, USA.

Social and Educational Program

The Social Program Emphasizes the Educational Aspect of the Academic Meetings of Atiner.

- Greek Night Entertainment (This is the official dinner of the conference)
- Athens Sightseeing: Old and New-An Educational Urban Walk
- Social Dinner
- Mycenae Visit
- Exploration of the Aegean Islands
- Delphi Visit
- Ancient Corinth and Cape Sounion

More information can be found here: https://www.atiner.gr/social-program

Conference Fees

Conference fees vary from 400€ to 2000€
Details can be found at: https://www.atiner.gr/fees

Athens Journal of Technology and Engineering - Volume 9, Issue 3, September 2022 – Pages 159-184

Predicting Refugee Flows from Ukraine with an Approach to Big (Crisis) Data: A New Opportunity for Refugee and Humanitarian Studies

By Tado Jurić[*]

This study was created due to the need to predict the migration flows of refugees from Ukraine to the EU in the absence of official data. We present a descriptive analysis of Big Data sources, which are helpful in determining, as well as for estimating and forecasting refuge emigration flows from Ukraine and help crisis managers. The objective of this study was to test the usefulness of Big Data and Google Trends (GT) indexes to predict further forced migration from Ukraine to the EU (mainly to Germany). The primary methodological concept of our approach is to monitor the digital trace of Internet searches in Ukrainian, Russian and English with the GT analytical tool. The control mechanism for testing this sort of Big Data was performed by comparing those insights with the official databases from UNHCR and national governments, which were available two months later. All tested migration-related search queries (20) about emigration planning from Ukraine show a positive linear association between the Google index and data from official UNHCR statistics; R2 = 0.1211 for searches in Russian and R2 = 0.1831 for searches in Ukrainian. Increase in migration-related search activities in Ukraine, such as "граница" (Rus. border), кордону (Ukr. border); "Польща" (Poland); "Германия" (Rus. Germany), "Німеччина" (Ukr. Germany) and "Угорщина" and "Венгрия" (Hungary) correlate strongly with officially UNHCR data for externally displaced persons from Ukraine. The results show that one-fourth of all refugees will cross into Germany. According to Big Data insights, the estimated number of expected refugees until July 2022 is 5.9 Million refugees and mid-2023 Germany can expect 1.5 million Ukrainian refugees.

Keywords: *refugee, forecasting refugee flows, Ukraine, big data, Google trends, forced migration, UNHCR*

Introduction[1]

The Ukraine war that started on 24 February 2022 destroyed civilian infrastructure and forced people to flee their homes to seek safety, protection, and assistance. According to UNHCR (2022c), more than a million refugees from Ukraine crossed borders into neighbouring countries in the first week since the war outbreak (2.5 Mil. in the second week), and many more are on the move both inside and outside the country. As the situation unfolds, an estimated 4 million people may flee Ukraine (UNHCR 2022a). The UNHCR estimated on February 27 that there would be 7.5 million internally displaced people in Ukraine in two months. According to the UNHCR, 18 million people are affected by the conflict, and 12 million people will require health care (UNHCR 2022a).

[*]Associate Professor, Catholic University of Croatia, Croatia.

[1]The pre-print version of this study is published on 16 March 2022 on pre-print server *MedrXiv*, https://doi.org/10.1101/2022.03.15.22272428.

Nobody knows how long the war will last, what kind of conflict this will develop into, and the civilian toll. This crisis is just one of many during which having reliable data would have assisted UNHCR and UN agencies in preparing high-quality projections for emergencies. But such data are often either unavailable or only available with a considerable time lag, which renders them useless for operations and emergency preparedness (UNHCR Global Data Service 2021).

This study was created due to the need to predict the migration flows of refugees from Ukraine to the EU. We present a descriptive analysis of Big Data sources, which could be helpful in determining, as well as for estimating and forecasting refuge emigration flows from Ukraine.

The expression "Big Data" has been spreading since 2011; the term is used in academia, industry and the media, but it is not even today precisely clear what it means. In this study, the term "Big Data" refers to the interdisciplinary method for deriving new understanding from massive aggregations of the information sampled through Google analytical tools Google Trends. We refer to the term Big (Crisis) Data as the subset of Big Data sources that have been applied in the humanitarian work of UNHCR (UNHCR 2021).

Since there has been a substantial increase in internet access compared to creating credible migration monitoring registration systems (Spyratos et al. 2018), the development of statistical tools that combine traditional and new sources of information is likely to become an accepted approach for monitoring migration and refugee flows. In demography, researchers have begun to use non-traditional or alternative data (mobile phone records, social media use, satellite maps, and internet-based platforms) to understand migration and mobility in light of new methodological approaches (Wanner 2020). This study will show that the analytical tool Google Trends (GT) can give valuable complementary data in the field of migration and refuge studies and be useful in the current refugee crisis.

The structure of the paper is as follows: after briefly showing the results of relevant studies, we explain this study's methods and show the limitations of the method. We then discuss Ukraine refugee flows and reveal the results achieved via this approach. In the section on results, we show the correlation between the Google search index and the official UNHCR statistics and discuss how to forecast refugee flows with Google Trends.

Forced Migration from Ukraine

Ukraine was one of 15 republics of the Soviet Union and became an independent state in 1991[2] (Britannica.com); it had a population of approximately 44 million. Since the end of the Soviet Union, the country had been a country of origin, transit and arrival for forced migration, as well as a provider of "durable solutions" for ethnic Ukrainians returning to the country from which they had been

[2]Britannica. *Ukraine: History*. Britannica Online Encyclopedia. Retrieved from: Britannica.com [Accessed 6 March 2022]

exiled during the Soviet era (Bergtora and Garnier 2022). In the 1990s, the ethnic composition of Ukraine changed significantly. Many ethnic Russians left, and many ethnic Ukrainians returned, including Tatars originally from Crimea, whose returned population increased fivefold between 1989 and 2001. The suspension of negotiations of the EU association agreement by a pro-Russia government in 2013 led to the Maidan protests in Kyiv and a pro-European regime change the following year, rapidly followed by Russia's occupation of Crimea (2014) (Bergtora and Garnier 2022). 5.2 million people were affected by the conflict, and 1.6 million were displaced within and outside Ukrainian borders (Bergtora and Garnier 2022). As of 2019, there were 1.4 million internally displaced people in Ukraine. Most Ukrainians sought refuge in Russia, but many also went to EU countries.

In refugee, migration and humanitarian studies, little attention has been given to the continued refugee resettlement of Ukrainians (c.f. UNHCR 2022b). A larger body of work can be found in area studies (cf. Bergtora and Garnier 2022), including research on the Ukrainian internally displaced people (IDP) (Kuznetsova and Mikheieva 2020) in Crimea (Charron 2020) and Donbas (Sereda 2020) and the humanitarian crisis (Scrinic 2014).

In the recent exodus from Ukraine, UNHCR estimates that over 4 million people could flee from Ukraine and seek protection and support across the region (UNHCR, Ukraine 2022) (Table 1). Our estimates obtained with Big Data show that there will be at least 5.4 million refugees. According to data from UNHCR, the speed of the exodus is already more extensive than the migration crisis of 2015, when 1.3 million asylum seekers from Syria, Iraq, Afghanistan and Africa, fleeing poverty and wars, entered Europe (UNHCR, 2016). "This is the fastest-moving refugee crisis in Europe since the end of the second world war" (The Guardian 2022).

Most Ukrainians (53%) fled in the first week to Poland, which welcomed at 04 March 2022 about 756,303 people, followed by Hungary, with 157,004. The number of refugees is also high in Hungary, Romania, Slovakia and Moldova. But not everyone decides to stay in the countries they first arrive in from Ukraine. For example, 140,000 people who came to Romania during the first eight days of the war travelled to other countries, leaving about 60,000 in Romania, according to the UNHCR (2022a) (Figure 1).

Figure 1. *Refugee from Ukraine (UNHCR)*

Source: UNHCR, https://data2.unhcr.org/en/situations/Ukraine (08.03.2022).

Table 1. *A Total Projected Refugee from Ukraine by July 2022 (UNHCR)*

Hosting Countries	**Total projected refugee population by July 2022***
Hungary	250,000
Moldova	100,000
Poland	1,500,000
Romania	250,000
Slovakia	60,000
Other Countries	1,840,000
Total	4,000,000

Source: UNHCR. *Ukraine situation regional refugee response plan.* Retrieved from: https://data2.unhcr.org/en/situations/Ukraine. [Accessed 8 March 2022].

Refuge Welcome Policy in the EU

In just one week, into the EU came so many refugees as in the entire so-called Yugoslav war (cf. Radelić et al. 2006). In the light of the current crisis, we believe that it is useful here to look back at the breakup of Yugoslavia and try to predict the course of the refugee crisis from lessons from the past. During the Homeland War in Croatia, 150,000 Croatians, or 3% of Croatia's population, emigrated to Germany, while about 250,000 arrived from BiH. Of that, 1/3 remained there forever, 1/3 returned because their temporary stay (so-called *Duldung*) expired, while 1/3 returned of their own free will (cf. Jurić 2021a).

If we draw a parallel between the war in Ukraine and the Homeland War and assume that the same number of Ukrainians as former Croatians under the pressure of war will escape to Germany, we expect that at least 1.5 Million Ukrainians will emigrate to Germany. We assume that further migration waves will occur in the years to come when men are allowed to leave the country and

emigrate to Germany due to family reunification and other reasons (for now, men between the ages of 18 and 60 cannot leave the country).

There are numerous differences in the welcome policy of Germany today and Germany in the 1990s. For entry to Germany during the Homeland war in Croatia, Croats asked the so-called letter of guarantee, i.e., proof that one of the relatives, etc., would guarantee the care of refugees. At the supranational level in the current crisis, the EU has triggered the adoption of the EU temporary protection directive for the first time. The directive grants immediate protection to Ukrainians fleeing to war for three years (Bergtora and Garnier 2022). Ukrainians do not require Schengen visas to enter the EU, and there is no other restriction. The EU admits Ukrainians without valid passports if they pass an individual assessment conducted by border officials. Moreover, Germany openly encourages the immigration of Ukrainians. Namely, Ukrainian nationals will be given the right to live and work in the European Union for up to three years without claiming asylum (Visitukraine 2022).

What has changed from the 1990s to today in Germany? In short, the demographic picture. Today, due to the demographic crisis in its own country, the lack of labour force of all profiles and young people in general, Germany needs to import about 400,000 employees every year to maintain its pension and health care system, according to a study by Bertelsmann Stiftung (2015). According to projections, the potential labour force in Germany will decrease by 16.2 million workers between 2012 and 2050 for purely demographic reasons (Arbeitsagentur 2020). The German generations with the highest birth rates will have left working life around 2035. According to model calculations, the net migration with countries of the EU will soon drop significantly from the current number to slightly below 300,000 (Arbeitsagentur 2020). For the next 36 years, an average of between 276,000 and 491,000 people would have to immigrate from third countries every year to Germany for the labour force potential to remain constant (Arbeitsagentur 2020).

Our primary hypothesis is that up to one-third of all refugees will cross into Germany. Surely, no refugee from Ukraine will be forced to stay in Germany, as neither are Croats during the Homeland War, but the combination of fear, a better standard and open hospitality will influence this decision.

The German Trade Union Confederation (DGB) and the German Employers' Union (BDA) issued a joint statement calling on the German government to urgently remove "legal and bureaucratic" obstacles to the rapid integration of Ukrainian refugees into German labour market. "Companies and works councils are ready to take their share of responsibility in order to take over these people as soon as possible, train or retrain them and thus integrate them into the labour market," the joint statement said (Deutsche Welle 2022).

Furthermore, the German Railways (Deutsche Bahn), three days after the start of the war, already on 27 February, put at its disposal trains for free transport of all Ukrainians from Poland to Germany (Deutsche Bahn 2022).

Some authors state that refugees from Syria and Africa have received worse treatment than refugees from Ukraine (Abcnews 2022). In the 2015 European migrant crisis (Almustafa 2021), when 1.3 million people came to the continent to

request asylum (BMI 2015), the welcome policy was completely different - for example, many EU members have lifted the razor wire on their borders. In March 2016, Turkey agreed to close its border to the EU in exchange for money and diplomatic favours, which effectively stopped the further passage of refugees through Eastern and South-eastern Europe (Berkay 2020).

Innovative Data Sources in the Refuge and Migration Studies

Human migration within Europe is difficult to measure due to the lack of efficient statistical systems in numerous EU countries (cf. Jurić 2022a). Numerous researches have shown (Böhme et al. 2020) that obtaining timely, evidence-based information on potential migratory movements is of the utmost importance to develop early-warning strategies and set up the necessary reception mechanisms in transit and receiving countries.

Traditional data sources, based either on surveys or registers, generally fail to provide statistical information on refugee flows quickly and do not facilitate the accurate short-term anticipation of these flows (Wladyka 2017). This limitation is one reason underlying the development of new methods based on alternative sources, so-called Big Data (Jurić 2022a).

The potential of Big Data to facilitate early warning of crises lies in its ability to provide granular, almost real-time information in locations where there are few other data sources. According to UNHCR, some Big Data sources can have the power to fill some of the information gaps left by conventional data acquisition channels, especially during crises (UNHCR Blog et al. 2022). According to Ibáñez Sales (2021), there are three main types of Big Data sources that are highly relevant to complement traditional migration and refugee data sources: communication services (calls records and texts messages), geo-localised activity as well as Internet-based exchanges (social media activity, online searching preferences, and online money transfers).

The main advantages of this approach for refugee studies are that those data are easily collected and generated in real-time, they are incredibly robust, and they provide a profound insight into migrants' or refugees' opinions (cf. Jurić 2021c). This data can be used to gather insights into what was going on in the user's mind in a non-invasive manner (see section Restrictions about ethical concerns) (Wang et al. 2018). Moreover, digital traces provide documentation of both movement and activities, which can help researchers bypass possible sources of error in survey data, such as inability to recall, bias, and the like (Jurić 2021a). Finally, digital traces can provide access to groups that are difficult to reach or are generally underrepresented by traditional research techniques (Cesare et al. 2018).

According to Jurić (2022c) and Choi and Varian (2012), Google Trends data have been used in various types of research: US unemployment, flu outbreak, predicting consumer behaviour, predicting inflation rates, predicting the housing market, predicting stock market changes, modelling tourism demand, etc. All the research results showed that GT analytical tools could reveal valuable insights about intentions (Önder 2017).

Several case studies have demonstrated that the inclusion of Big Data sources significantly improves the power and accuracy of predictive models of refugee flows (Agrawal et al. 2016). A study by Singh et al. (2019) on internally displaced persons (IDPs) movements between provinces in Iraq shows that a mix of social media data and traditional register data improves the predictive quality compared to predictions based on register data alone. Therefore, Big Data hold huge potential for humanitarian organisations to improve their early warning systems and generate better contingency planning figures (UNHCR Global Data Service 2021, p. 11). Although previous research has established that digital data can be employed to study migration, there are still significant methodological issues and scepticism regarding the feasibility of using alternative data sources (Jurić 2022a).

In 2014 the UN conducted the first research on the use of Big Data for demographic research, with its report released in 2018 (United Nations 2014). These data were shown to provide useful insights into the quantitative and qualitative characteristics of international and other migrations (United Nations 2019). Since the UN confirmed the relevance of these data, explorations have been carried out on social networks (Zagheni et al. 2014, Zagheni et al. 2017, Zagheni and Weber 2015), and several studies have used Big Data sources to analyse migration-related phenomena directly (e.g., Dubois et al. 2018, Hawelka et al. 2014, State et al. 2014, Jurić 2021a, 2022a,b).

The European Commission concluded similarly to the UN that a) Big Data sources do not replace traditional data sources but can complement them, b) they can still be used to assess trends (Jurić 2021c). Furthermore, it has been established that both kinds of data sources can complement each other (Spyratos et al. 2018). "In addition to being extremely robust, these data are easily collected, are generated in real-time, and provide significant insights into the opinions of individuals" (Jurić 2022a).

According to Gabrilovich (2020), would-be migrants often use online searching to get answers about the country they plan to emigrate to, and according to Wanner (2020), Google is the first source of information for most users planning relocate. Several studies have used immense data sources to analyse migration-related phenomena directly. The first successful analysis of this type of data was in 2009, and the first study in the field of migration examined during the 2015 Migration Crisis searches for particular terms in Arabic in Turkey and Germany according to selected terms such as "Greece" or "Germany" (Connor 2017). A study by the PEW - research centre showed that digital prints left by internet searches could provide insight into the movement of migrants. Namely, during their travels in 2015 and 2016, many migrants used smartphones that provided access to information and maps and travel tips via social media. It was then unequivocally proven that these indicators could be used to predict migration (Jurić 2022b). Compared to approaches using social media, the advantage of Google Trends is that limitations related to fake accounts are not prevalent (Jurić 2022a).

Undoubtedly, the Internet penetration rate is for this method significant. When it comes to the use of Internet services, Ukrainians are generally comparable to the EU average (with a slightly lower share) (Internet World Stats

2022). Migrants and refugees are nowadays increasingly using mobile devices and digital interactions on social media to communicate with relatives and send them news and pictures. Migrants use smartphones to facilitate their movements across borders, stay up to date with weather predictions, get last-minute information in transit and destination countries, or send and receive international remittances (Ibáñez Sales 2021). Moreover, it is proven that the refugees are more interested in information from the Internet than the average and that they generally use smartphones during migration (cf. Connor 2017).

Methodological Concept

In this study, we present a descriptive analysis of Big Data sources, which could be useful for predicting refugee flows from Ukraine to the EU and especially to Germany. The primary methodological concept of our approach is to monitor migration-related searches with the analytical tool Google Trends (GT)[3] during the Ukraine war crisis. This tool shows the popularity of a specific term and shows if a trend is rising or falling. GT does not provide information on the actual number of keyword searches - instead, it standardises search volume on a scale of 0 to 100 over the period being examined, with higher values indicating the time when the search volume was greatest, allowing for verifiable metrics (Jurić 2021b). In previous studies, it was a significant limitation that each of these searches was conducted for its reason and did not answer researchers' questions, so "googling" the term "Germany" was not necessarily an implication that someone wants to move to Germany, but may be interested in tourist information or just looking for the German Bundesliga (Jurić 2022a). However, in this crisis, it is quite certain that no one is interested in the Bundesliga when googling the word Germany. However, it is essential to pay attention to the overall context by interpreting the results.

The Google search Index cannot estimate the exact number of searches, so with the help of this tool, the exact number of emigrants cannot be calculated, but the increase in the trend can be noticed very precisely (Jurić 2021a). This method we have already tested in our previous studies with quite good predictive indicators (Jurić 2021c, Jurić 2022a). The justification for using the GT method for the assessment of refugee flows is that mismatch between intention and actual behaviour, which is one of the most significant restrictions of this approach, is, in the case of refugees from Ukraine, not to such an extent represented as in the case of predicting migrations in peacetime (cf. Jurić 2021a).

For this method, it is essential to establish the time flow from the expressed intention to the realisation of migration. We hypothesise that an increase in the number of Google searches will, following a delay of about one to three days, translate to a rise in the number of refugees. According to Curry et al., trigger events happen immediately before migration, usually within a time frame of 1-2

[3]Google Trends. https://trends.google.com/trends/?geo=HR.

days before emigration occurs and are events that the individual perceives as threatening their integrity (Curry et al. 2018).

To standardise the data for Google Trends, we extracted data from 24 February 2021 to 24 February 2022. We then divided the keyword frequency for each migration-related word, which gave us a search frequency index that we then compared with official statistics using a linear regression method (cf. Wanner 2020, Wilde et al. 2020). In order to estimate the model, linear regression was used to measure the correlation between the number of searches (x) and the number of moves (y) evidenced by the official UNHCR statistics, which were available one to two months later, to prove the significance of our results.

Initially, keywords were chosen by brainstorming possible words that we believed to be predictive, specific, and common enough to forecast refugee flows (Table 2). After the significance test, we selected followed keywords and topics.

Table 2. *List of Keywords*

English	Ukrainian	Russian
asylum	*притулок*	*убежище*
border	*кордону*	*граница*
border control	*прикордонний контроль*	*пограничный контроль*
migrant	*мігрант*	*мигрант*
refugee	*біженець*	*беженец*
interpreter	*перекладач*	*переводчик*
weather forecast	*прогноз погоди*	*прогноз погоды*
Schengen	*Шенген*	*Шенген*
visa	*віза*	*виза*
job	*робота*	*работа*
PCR	*ПЛР*	*ПЦР*
consulate	*консульство*	*консульство*
Poland	*Польща*	*Польша*
Germany	*Німеччина*	*Германия*
Romania	*Румунія*	*Румыния*
Hungary	*Угорщина*	*Венгрия*
Moldova	*Молдова*	*Молдова*
Slovakia	*Словаччина*	*Словакия*

It is to note that we observed that Ukrainians use the Russian language more often to search for terms than Ukrainian. This phenomenon is numerous: During the 19th century, the Russian government and in the 20th century, the Soviet Union promoted the spread of the Russian language among the native Ukrainian population by suppressing the Ukrainian (Magoscy 1996). In independent Ukraine, although Russian is not an official language, it is widely spoken, particularly in regions of Ukraine where Soviet Russification policies were the strongest, notably most of the urban areas of the east and south (Donetsk, Luhansk and Crimea) (Magoscy 1996).

It is also necessary to consider the overall social context and that even before the war, many Ukrainians emigrated to Poland. 1.4 million Ukrainians lived in

Poland before the war broke out (most fled after the Crimea crisis) (The Guardian 2019).

Limitations of the Methodological Concept

Like all data sources, Big Data also come with limitations. According to UNHCR, issues with Big Data mostly come from three sources: bias, inaccuracy, and low scalability (UNHCR Blog 2022). GT has some specific limitations when applied in the context of forced displacement. Namely, many displaced people do have not the time to conduct detailed searches on the Internet for a potential host country (UNHCR Global Data Service 2021, p. 19). But the biggest weakness of GT data, which is biased due to limited access to the Internet, is in the case of refugees from Ukraine not represented. As already mentioned, it is proved proven that refugees are ready to allocate the most resources for smartphones, i.e., connection with relatives and friends, but also the Internet.

Although penetration rates of the Internet are increasing globally, they still do not reach 100% of the Ukrainian population. Rural communities, women, children, and the elderly are underrepresented population segments and risk becoming invisible in Big Data sources (UNHCR Global Data Service 2021, p. 7). On the other hand, there are numerous indications that potential migrants and refugees largely gather or refine information through Google searches before emigrating (Wladyka 2017). According to EUROPOL (2018), there has been an exponential growth in the use of the Internet and social media by refugees and migrants arriving in Europe in the last few years. Even the UNHCR has concluded that smartphones, the Internet and social media are now a key tool for migrants, who spend up to a third of their total budget on staying connected (UNHCR 2017).

Although the data obtained with GT are robust data with large samples, which provide information qualitatively different from what can be obtained from the official databases, they are not representative of the observed population (Jurić 2022a). A significant restriction is that GT does not provide data on which population was sampled or how it was structured (Wladyka 2017). A problem also exists in the researchers' education who must be skilled in computational methods, be transparent about their methods to ensure repeatability, and be accustomed to the interdisciplinary environment (Jurić 2022b).

We are also aware that refugees may use other methods to gather information on living and working conditions in Poland and Germany, such as the accounts of friends or family members who have already immigrated to these countries. A further aspect is the availability of humanitarian help in a potential host country, a network within an existing diaspora in the likely host country, and available information on flight routes and corridors from earlier migrants (UNHCR Global Data Service 2021, p. 11).

This study has a descriptive character and is limited by the lack of data due to the actuality of the phenomenon being observed. The exponential growth in the first phase of the war needs to be modelled via the second phase to detrend the time series. The whole process should be checked with significance tests to make conclusive statements about the observed quantities.

Twitter data is only effective if the user uses the geotagging option, typically using only 3% of users. Furthermore, the basic idea of monitoring the moves of refugees from country to country through geotagged messages usually requires a more extended period, which in our study, due to actuality, could not be done.

Regarding ethical issues, since the vast majority of Big Data is generated automatically by mobile and Internet users without informed consent and knowledge for what purpose those data are collected, its use may violate privacy and data protection (Ibáñez Sales 2021, p. 8). This situation also raises concerns about public-private cooperation because governments may become dependent on Big Data collection (Bircan and Korkmaz 2021).

Results

Use of the Google Trends Analytical Tool to Forecast Refugee Flows from Ukraine

Searching for queries in Ukrainian, Russian and English from Ukraine "border crossing", "кордону" (Ukr. border), "граница" (Rus. border) from 7 December 2021 to 3 March 2022 (Figure 2) shows an upward trend since the outbreak of war. This is a strong indication that more and more Ukrainian citizens will emigrate, i.e., flee from Ukraine.

Figure 2. *Search Queries in Ukrainian, Russian, German and English from Ukraine "Border Crossing", "кордону" (Ukr. border), "граница" (Rus. Border) (7 December 2021 – 3 March 2022)*

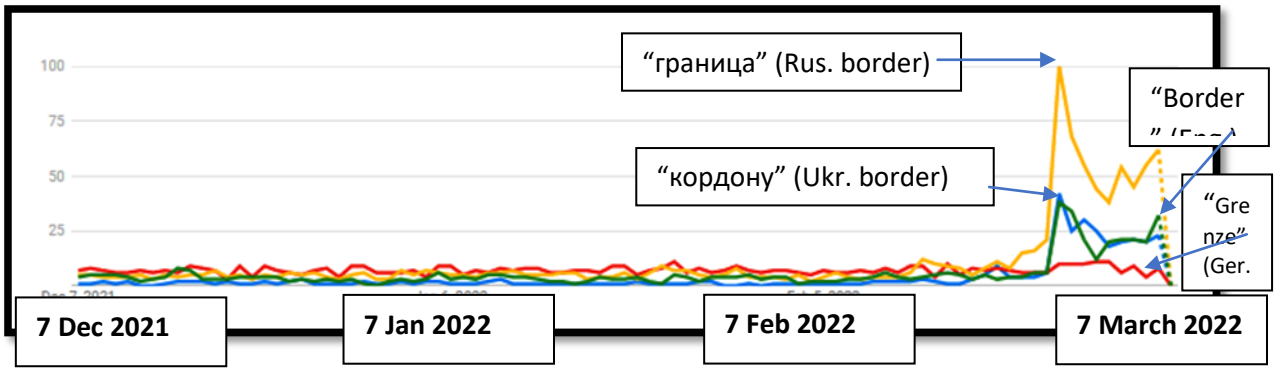

Source: Jurić (2022d).

A further indication is searching for terms related to registration in Poland, Hungary and Germany.

Figure 3. *Fastest Growing Google Search Terms in Ukraine: Western Union, Asylum, refugee, Schengen (7 December 2021 to 7 March 2022)*

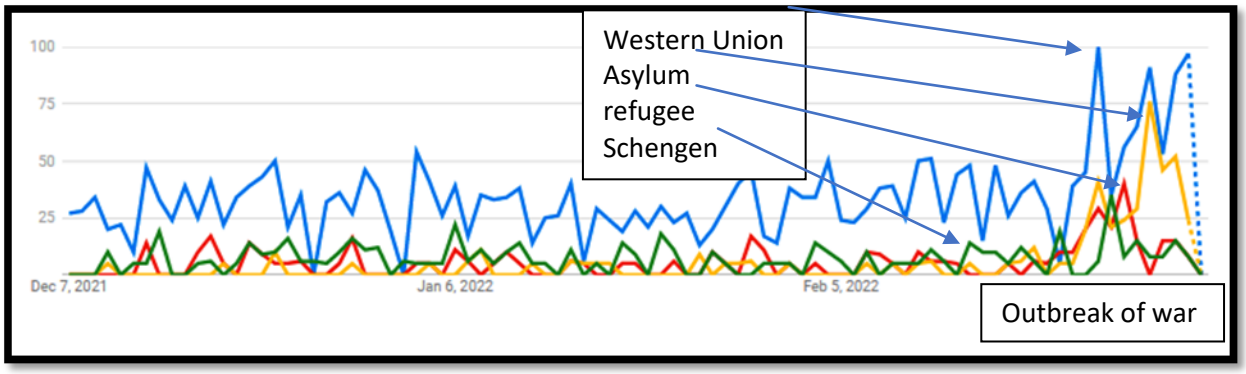

Figure 3 shows that the fastest-growing Google search terms in Ukraine (7 December 2021 to 7 March 2022), except mentioned term "border", are Western Union, asylum, refugee and Schengen.

When looking at the showed interest in emigration countries, we notice that the internet traces correspond to the official data of the UNHCR. Namely, the GT, just like the UNHCR, shows that the interest is focused primarily on Poland, Hungary, Slovakia and Germany (UNHCR still does not confirm information about Germany, 11 March 2022).

Figure 4. *Search queries in Ukrainian from Ukraine "Польща", "Німеччина" "Угорщина", "Молдова" "Словаччина" (Poland, Germany, Hungary, Moldova, Slovakia) (7 January 2021 – 3 March 2022)*

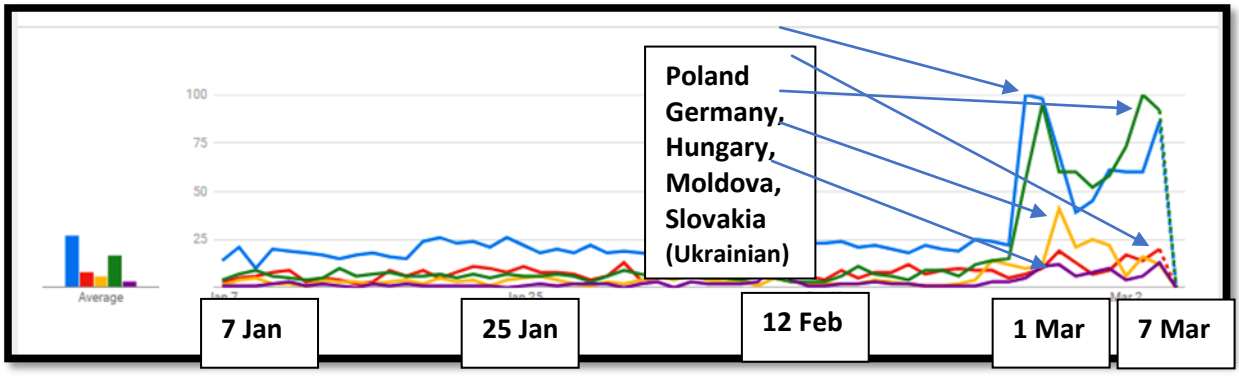

Source: Jurić, T (2022d) Big (Crisis) Data in Refugee and Migration Studies – Case Study of Ukrainian Refugees, Comparative Southeast European Studies (forthcoming)

Figure 4 shows that the most searched countries from Ukraine in Ukrainian are Poland and Hungary. As already mentioned, the citizens of Ukraine use Russian during Internet searches more than Ukrainian. This could be explained, as mentioned, that the citizens of Ukraine probably expect more information in Russian, which is known as a world language, but also that the vast majority of Ukrainians learn and use Russian (cf. Jurić 2022d).

Figure 5. *Search Queries in Russian from Ukraine "Польша", "Германия", "Румыния", "Венгрия", "Молдова" (Poland, Germany, Hungary, Moldova, Slovakia) (7 January 2021 – 3 March 2022)*

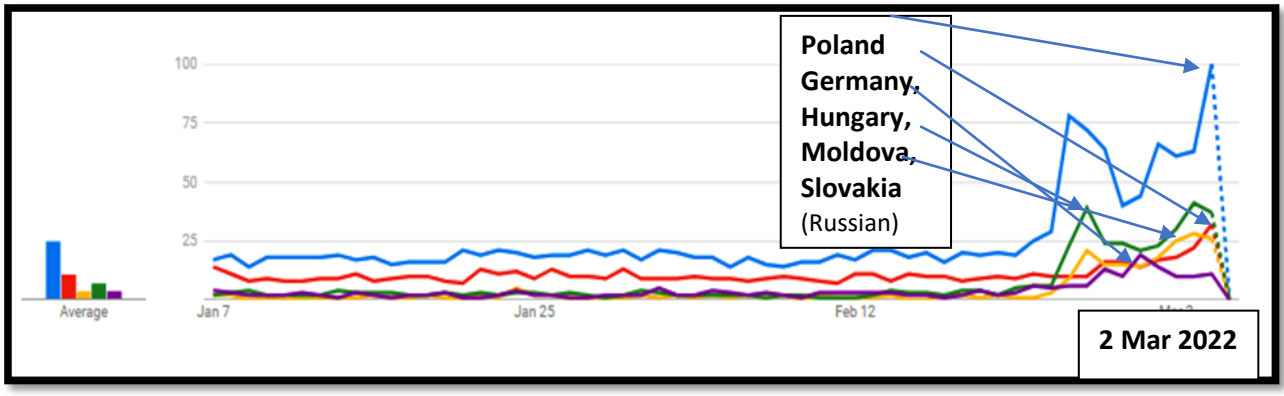

Figure 5 shows that Poland and Moldova are the most searched countries in Ukraine in Russian. The following Figure 6 shows that *Poland* and *Romania* are the most searched countries in English.

Figure 6. *Search Queries in English Poland, Germany, Hungary, Moldova, Slovakia from Ukraine (7 January 2021 – 3 March 2022)*

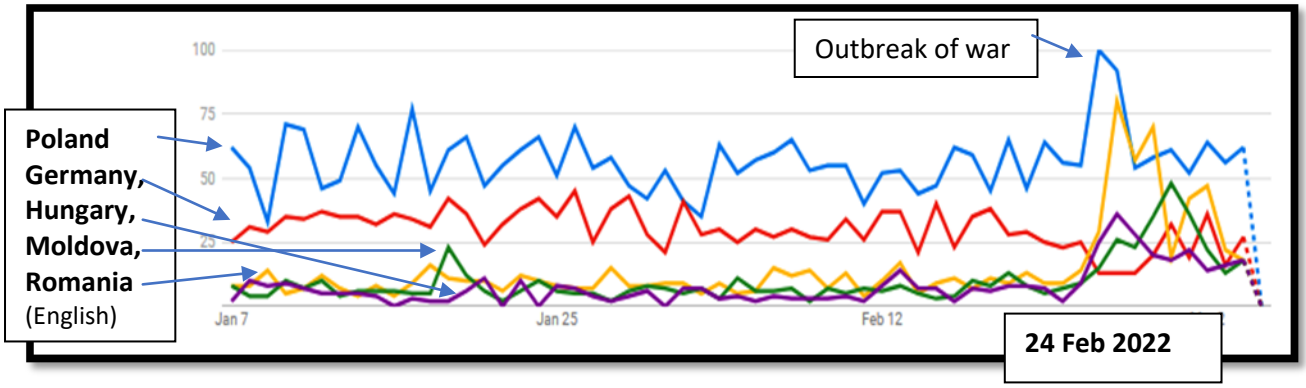

Figures 4, 5 and 6 show the increase in Internet searches for all neighbouring countries in Russian, Ukrainian and English; all three languages show that the search interest for Poland is the highest. Other languages, including German, are not significantly represented.

Our basic hypothesis is that one-third of all refugees from Ukraine will emigrate further to Germany after arriving in the original EU countries. As we stated in the introduction, this assumption is based on the movement of refugees during the Homeland War in Croatia, when it turned out that most Croatian citizens, after fleeing to nearby countries, Hungary and Slovenia, continued to Germany. Undoubtedly, the economic power of the receiving country and the assessment of when the war could stop also play an important role in this prediction. The data we received with the GT application undoubtedly show a high increase in interest in Germany (Figure 7), but also a set of inquiries related to the so-called "German way of life", jobs opportunities, children's enrolment in school

and other indicators that undoubtedly indicate the intention of refugees to stay longer in Germany.

Figure 7. *Interest in the Search Term "Germany" in Ukraine in English, German, Russian and Ukrainian since the Outbreak of War (28 February to 06 March 2022)*

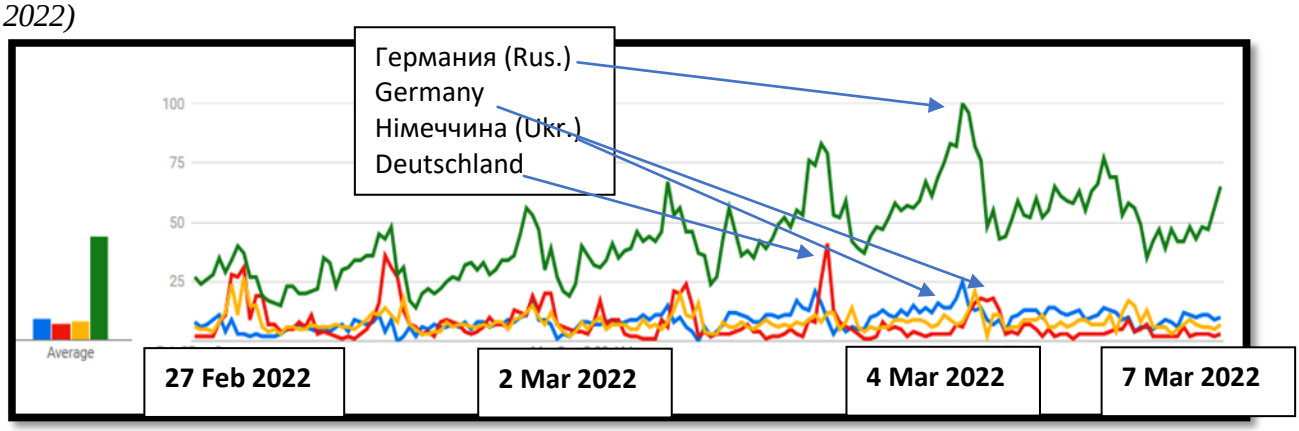

Source: Jurić, T (2022d)

Further confirmation of this hypothesis is the increase in specific searches that undoubtedly reveal the intention to move or flee to Germany (Figure 8). One of the most common searches is just focused on the question "Германия принимает беженцев из Украины" (Does Germany accepts refugees from Ukraine?).

Figure 8. *Increase in Search Query in Ukraine "Германия принимает беженцев из Украины" (Does Germany Accepts Refugees from Ukraine) (6 December 2021 - 08 March 2022)*

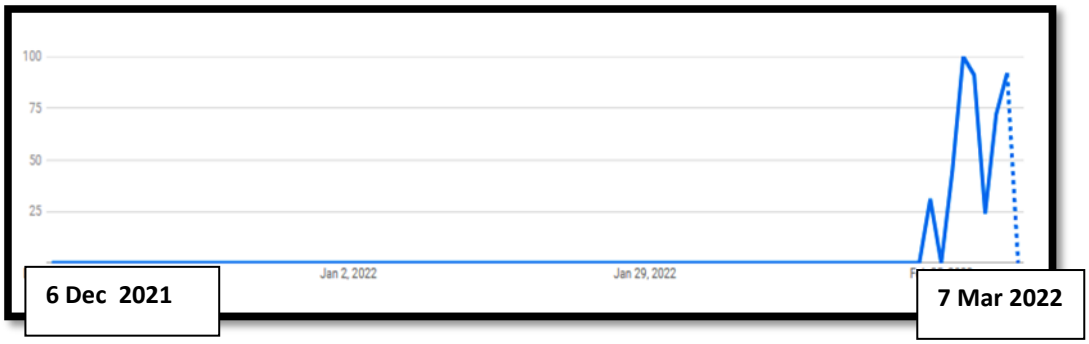

This specific search also correlates with the regions most affected by the war, such as Donetsk, Luhansk, Kharkiv, Odesa and Kyiv (Figure 9).

Figure 9. *Correlation of Google Search "border+Poland" with the Regions in Ukraine Most Affected by the War, such as Donetsk, Lugansk, Harkiv, Odesa and Kyiv (6 March 2022)*

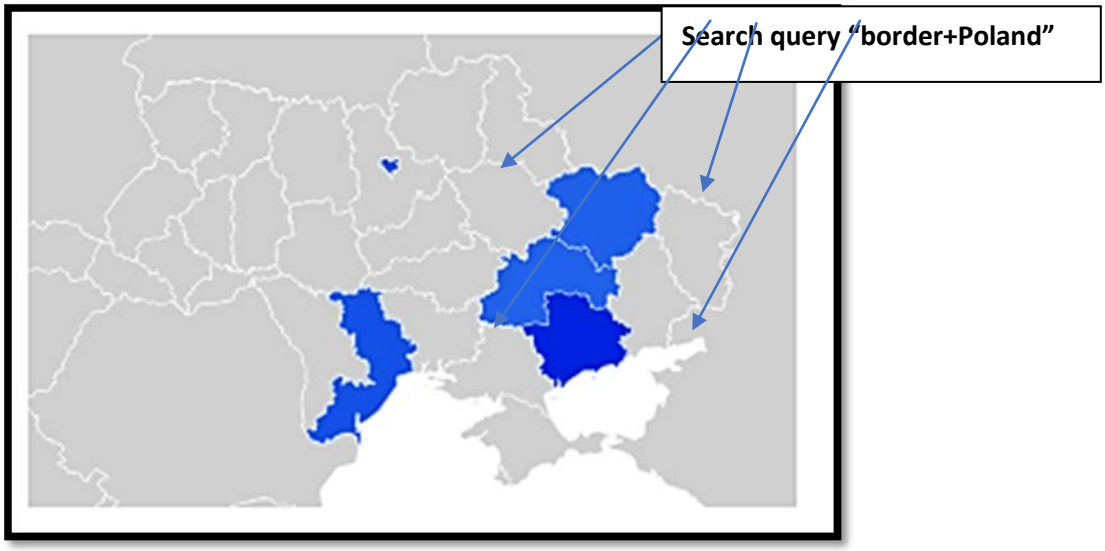

As time goes on, refugees usually realise that the war and its consequences will last longer than they expected. When they notice this, they continue their emigration to a country that offers the highest economic and financial security. In this case, as in the case of the Homeland War in Croatia, this is Germany. This assumption confirms the high growth of interest in Poland for the search query "Germany" (Figure 10).

Figure 10. *The Search Term "Німеччина, Германия" (Germany) in Poland (from 11 July 2021 to 08 March 2022)*

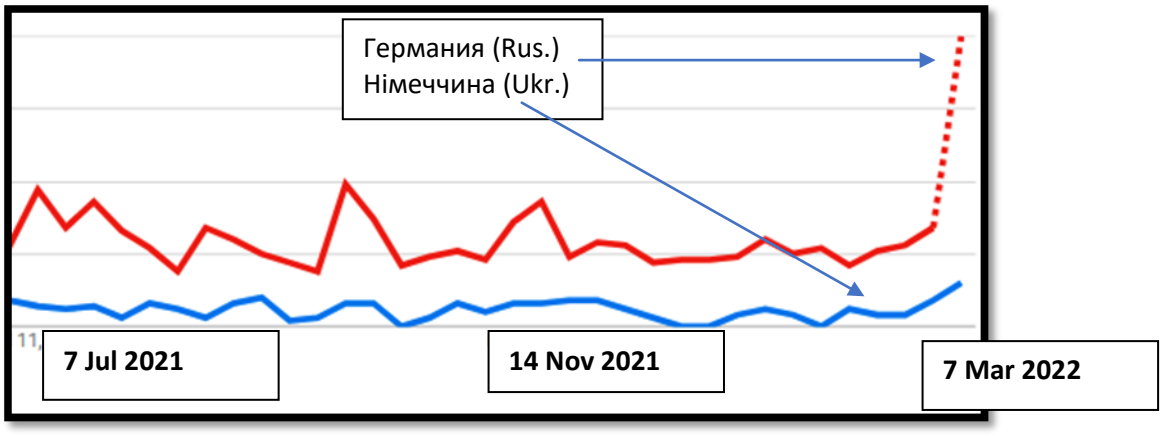

The most frequent search in Poland since the outbreak of the Russian-Ukrainian war is "Border crossing+Germany" (Figure 11) (cf. Jurić 2022d).

Figure 11. *A Most Common Internet Search in Poland: "Border crossing+ Germany", "border crossing", "кордону" (Ukr. Border), "граница" (Russ. Border) (7 December 2021 to 7 March 2022)*

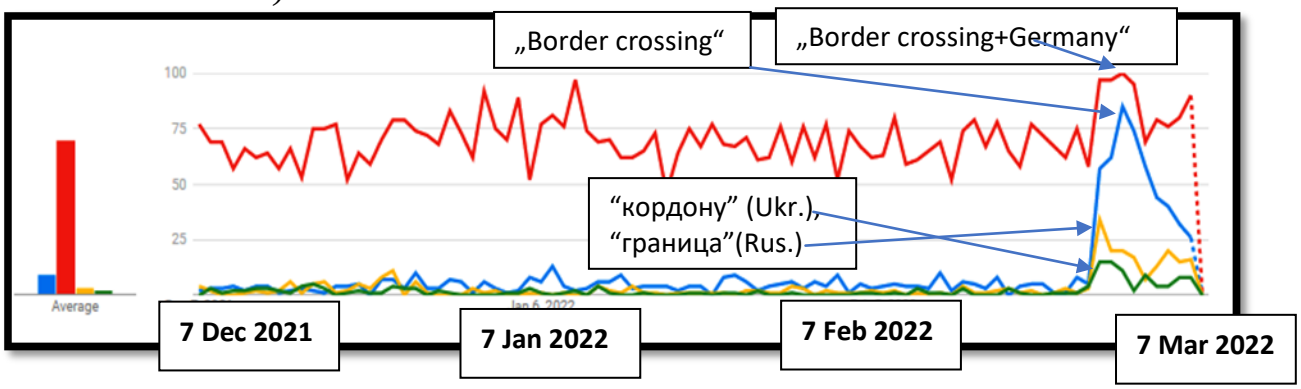

Source: Jurić, T. (2022d)

According to the German Federal Ministry of the Interior, 37,786 war refugees from Ukraine were registered in Germany by midday on 6 March 2022 (BMI 2022). The search for terms related to crossing the border into Germany in Poland is growing precisely in the regions located near Ukraine (Figure 12).

Figure 12. *Regions in Poland Where Interest for "the German border" is Growing (6 March 2022)*

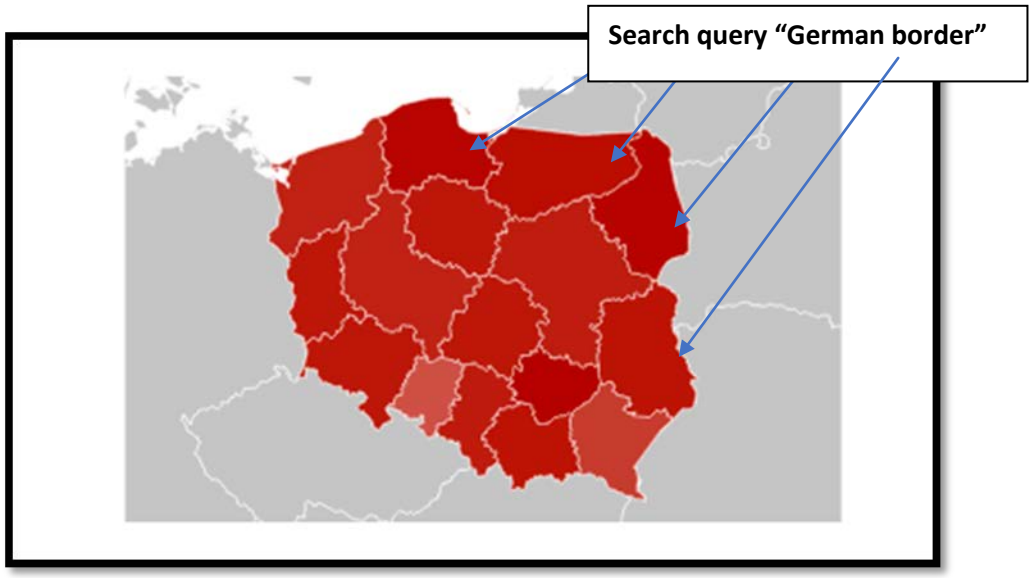

Note: Dark red colour indicates an increase in the frequency of search keywords.

According to Düvell (2022), there are currently up to 24 million people affected by the war. Half of the population was displaced in the Crimea-Donbass conflict. According to the UNHCR, 2.3 million citizens were displaced in Ukraine during the Crimean crisis. Of that, 1.5 million escaped from Crimea (800,000 were of Russian ethnicity) (UNCHR nd). If half of the affected population flees like the

Crimean occupation in 2014, there will be up to 12 million Ukrainian refugees (Düvell 2022). That this hypothesis could be correct, we see when we compare the search query "Германия принимает беженцев из Украины" (Does Germany accepts refugees from Ukraine) during the Annexation of Crimea in 2014 with the current crisis.

Figure 13. *Comparison of the Search Queries "Германия принимает беженцев из Украины" (Germany Accepts Refugees from Ukraine) During the Annexation of Crimea in 2014 with the Current Crisis in 2022*

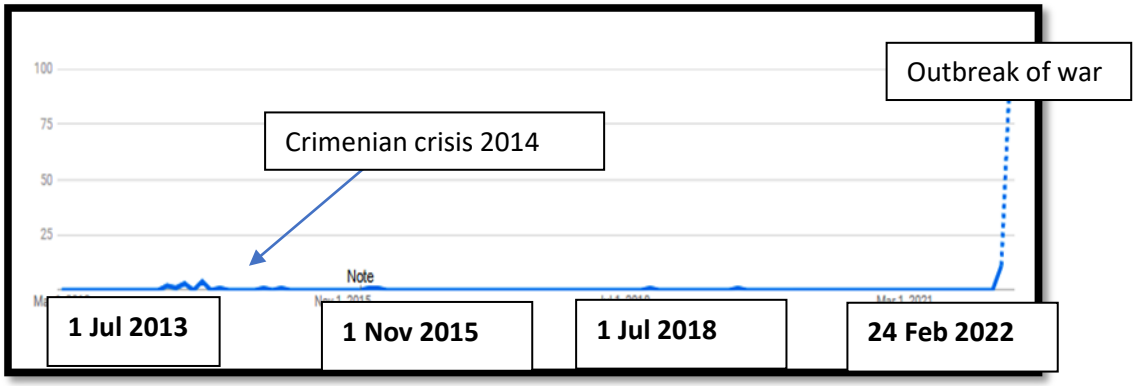

Figure 13 shows that during the peak of the Crimean crisis in 2014, the search index for query "Германия принимает беженцев из Украины" (Germany accepts refugees from Ukraine) was 4, and in 2022 it is 12, that is, the interest in fleeing the country is now three times higher.

Further keywords we tested in Germany were *Ukrainian-German translator* and *English-Ukrainian translator* (Figure 14). At 13 March 2022 all queries shows rapid increasing "точний перекладач з української на німецьку" (+250%), "перекладач з англійської на українську" (+190%), "українсько-німецький перекладач" (+150%) compared to a month ago (Jurić 2022d).

Figure 14. *Querie "перекладач" (Ukr. translator) and "переводчик" (Rus. translator) in Germany (from 23 December 2021, to 13 March 2022*)

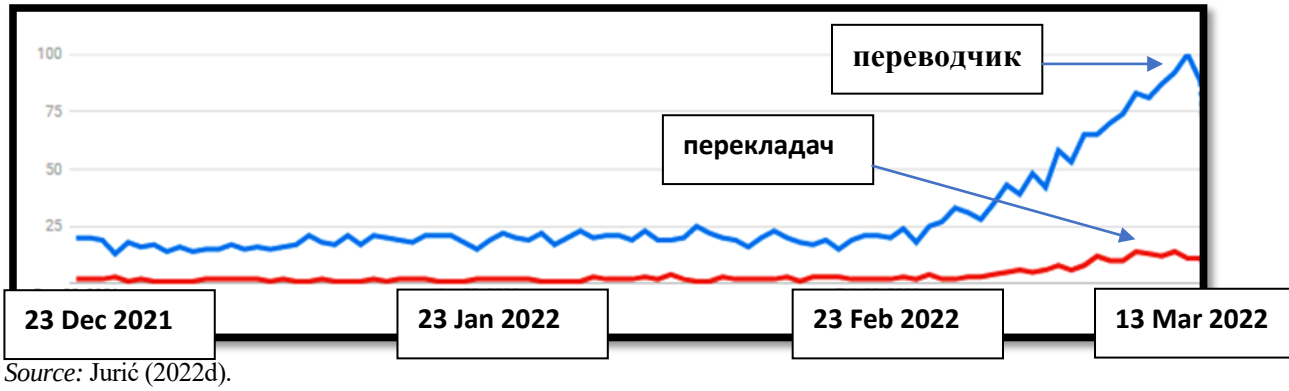

Source: Jurić (2022d).

In further proceedings to standardise the data, we requested the data from 01 February to 11 March 2022, and divided the keyword frequency for the most

searched terms "граница" and "кордону" (border) and compared this search index with later available official statistics from UNHCR to prove the signification of results (Table 3) (cf. Jurić 2022d).

Table 3. *Refugees from Ukraine in Poland, Hungary and West European Countries*

Datum	Poland	Hungary	Other European countries (West)
11. Mar 2022	1,524,903	225,046	282,497
08. Mar 2022	1,204,403	191,348	210,239
04. Mar 2022	756,303	157,004	133,876
28. Feb 2022	280.000	85.000	34,600
Total: 2,504,893 (Data as 11 March 2022)			

Source: UNHCR, https://data2.unhcr.org/en/situations/ukraine and UNHCR, Ukraine Situation Regional Refugee Response Plan, https://data2.unhcr.org/en/situations/ukraine, authors creation.

Figure 15. *Correlation Between Google Search Index for Query "граница" (border) in Russian and the UNHCR Statistics for Externally Displaced persons from Ukraine to Poland (24 February – 11 March 2022)*

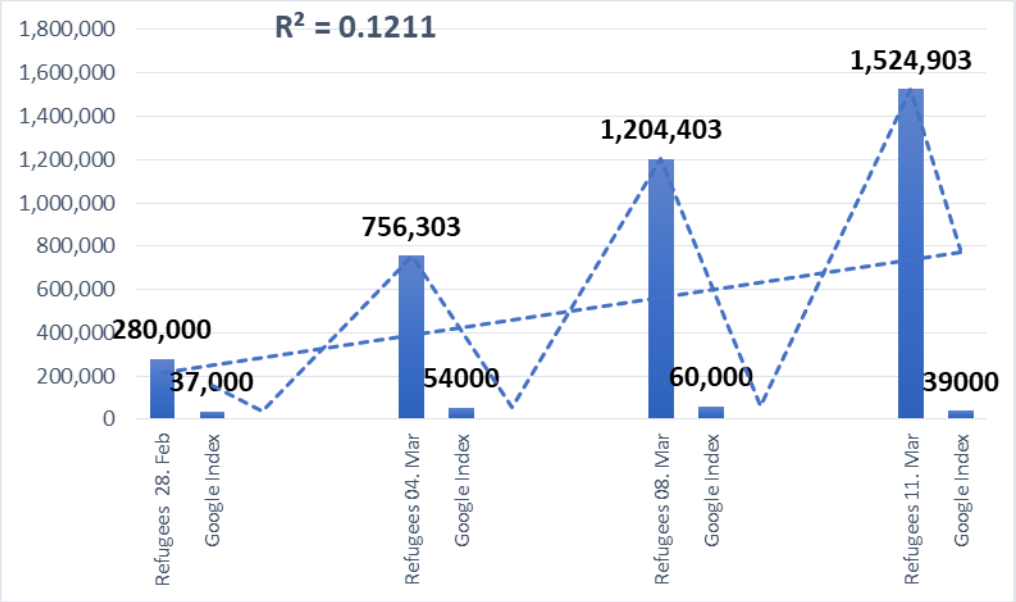

Source: Jurić (2022d).

Figure 15 shows that the increase in Google search for the query "граница" (border) in Russian correlates with the increase of externally displaced persons from Ukraine to Poland (Feb 24 – Mar 11, 2022). R2 is 0.1211 and shows a positive correlation. A p-value is statistically significant (Jurić 2022d).

Figure 16. *Correlation Between Google Search Index for Query "кордону" (Border) in Ukrainian and the UNHCR Statistics for Externally Displaced Persons from Ukraine to Poland (24 February – 11 March 2022)*

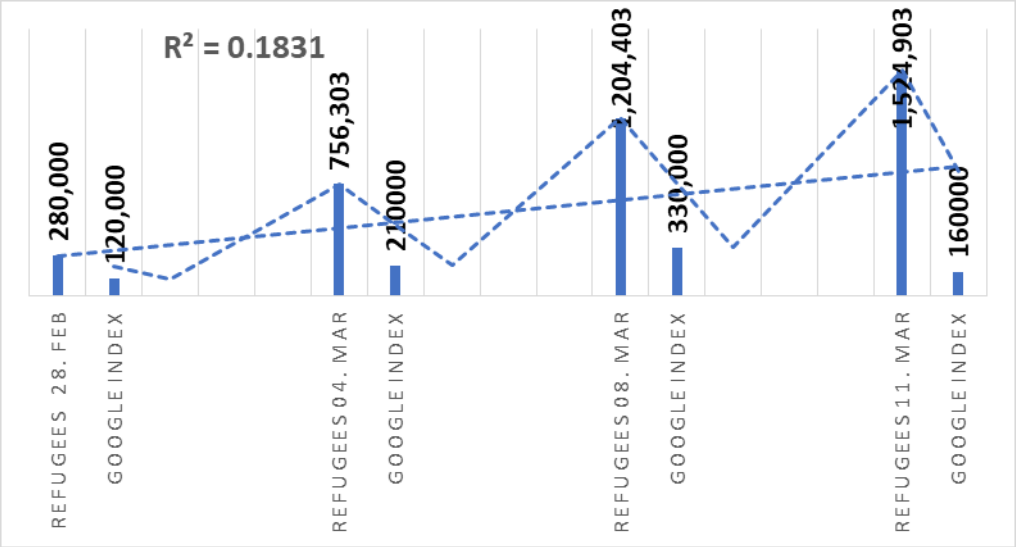

Figure 16 shows that there is a positive correlation as in the case of Google searches in Russian. The increase in Google search for the query "кордону" (border) in Ukrainian correlates with the rise of externally displaced persons from Ukraine to Poland (24 February – 11 March 2022). R2 is 0.1831 and shows a positive correlation. A p-value is not statistically significant (Table 4).

Table 4. *Correlation Analysis ANOVA*

Regression Statistics	
Multiple R	0.417921
R Square	0.174658
Adjusted R Square	-0.23801
Standard Error	603084.3
Observations	4

ANOVA

	df	*SS*	*MS*	*F*	*Significance F*
Regression	1	1.54E+11	1.54E+11	0.423237	0.582079
Residual	2	7.27E+11	3.64E+11		
Total	3	8.81E+11			

	Coefficients	*Standard Error*	*t Stat*	*P-value*	*Lower 95%*	*Upper 95%*	*Lower 95.0%*	*Upper 95.0%*
Intercept	431691.1	839512.2	0.514217	0.658282	-3180438	4043820	-3180438	4043820
X Variable 1	2.486396	3.821891	0.650567	0.582079	-13.9579	18.93067	-13.9579	18.93067

Our previous studies (Jurić 2021a, Jurić 2022c) have shown that, in contrast, when the Google search decreases, there will be a decrease in externally displaced

persons from Ukraine. There is a positive linear association between the Google index and data from official statistics, UNHCR, enabling estimates and forecasting for the future.

Discussion

All tested migration-related search queries (20), which indicate emigration planning, show a positive linear association between the Google index and data from official statistics, UNHCR; $R^2 = 0.1211$ for queries in Russian and $R^2 = 0.1831$ for queries in Ukrainian (cf. Jurić 2022d).

The increase in Google search is correlated with the rise in the number of refugees in the EU. In contrast, according to our previous studies, the decrease in Google search will show a decrease in externally displaced persons.

Our testing shows an increase in Internet searches for all neighbouring countries in Russian, Ukrainian and English; all three languages show that the interest in *Poland* is the highest. It should be emphasised that when refugees arrive in nearby countries, the search for terms related to *Germany*, such as "crossing the border + Germany", etc., is proliferating. This result confirms our hypothesis that up to one-third of all refugees will cross into Germany.

Regarding the estimated number of expected refugees, we compared the Crimean crisis in 2014 and the current crisis. During the peak of the Crimean crisis in 2014, the search index for the query "Германия принимает беженцев из Украины" (Germany accepts refugees from Ukraine) was 4, and in 2022 it is 12, that is, the interest in fleeing the country is now three times higher. Therefore, according to Big Data insights, it is to expect 5.9 Million refugees until July 2022.

The presented method contributes in a way that proves the feasibility of predicting further refugees waves from Ukraine, which allows reliable forecasts for the future and helps prepare humanitarian aid and civil infrastructure. This procedure also presents a new methodological approach to how data obtained through GT can be standardised for comparison with official UNHCR databases. The insights are particularly relevant for EU policymakers and can help governments to design appropriate strategies and prepare and better respond to this crisis in the future. Namely, even if the war ends quickly, Croatia's previous experience with the war (Radelić et al. 2006) shows that the crisis in Ukraine will continue for many years to come, and it is to be expected that the abolition of military service will lead to the emigration of large numbers of men from the country.

This study has important limitations. It has a descriptive character and is limited by the lack of data due to the actuality of the observed phenomenon. Therefore, many more other studies are needed to perfect this method. The exponential growth in the first phase of the war needs to be modelled via the second phase to detrend the time series. The whole process should be checked with significance tests to make conclusive statements about the observed quantities.

Conclusion

This study was created due to the need to predict the migration flows of refugees from Ukraine to the EU and help crisis managers to prepare the humanitarian infrastructure and conditions for eventual integration. The usefulness and the main advantage of this approach is the timely identification of external migrations from Ukraine, which can be used to model projections and predict future trends.

Our approach to Big Data and analysis of digital traces showed that Ukrainian refugees most often searched for the term "border". The data generated by our approach regarding the direction of refugee flows from Ukraine correlates with official UNHCR data, but there were available one to two months later after Big Data insights. Furthermore, our insights showed timely that 27% more refugees are expected than the UNHCR predicted in early stage of crisis. Here presented method showed that mid 2022 it is to expect 5.9 Million refugees and mid 2023 Germany can expect 1.5 Million Ukrainian refugees.

According to geolocations, the tested crosschecks of migration-related searches correspond to the subsequently published UNHCR data. Big (Crisis) Data show that the main regions of emigration from Ukraine are the provinces directly affected by the war (as expected). However, Ukrainian refugees will not necessarily stay in the countries of first immigration, and almost one fourth will continue their journey to Germany.

This study showed that Big (Crisis) Data has many advantages, but there are still significant open methodological issues. At the same time, more and more studies argue that samples obtained from Big Data do not significantly differ from samples obtained from more traditional recruitment and sampling techniques (Kalimeri et al. 2020). Therefore, Big Data holds enormous potential for humanitarian organisations, governments and crisis managers to improve their early warning systems, especially now in the Ukrainian refugee crisis.

Compliance with Ethical Standards

In this work, we use only anonymous, aggregate data. All data are collected following the applicable GDPR and ethical principles of personal data handling. This project's database retains no information about the identity, IP address, or specific physical location of any user.

References

Abcnews (2022) *Europe welcomes Ukrainian refugees — Others, less so*. Retrieved from: https://abcnews.go.com/International/wireStory/europe-welcomes-ukrainian-refugees-83153021 [Accessed 30 March 2022]

Agrawal A, Sahdev R, Davoudi H, Khonsari F, McGrath S (2016) *Detecting the magnitude of events from news articles*. Retrieved from: https://ieeexplore.ieee.org/document/7817051. [Accessed 24 February 2022]

Almustafa M (2021) *Reframing refugee crisis: a "European crisis of migration" or a "crisis of protection"?* Available at: https://doi.org/10.1177/2399654421989705.

Arbeitsagentur (2020) *Gemeldete Arbeitsstellen nach Berufen (Engpassanalyse)* (Registered jobs by occupation). Retrieved from: https://statistik.arbeitsagentur.de/Statistikdaten/. [Accessed 24 February 2022]

Bergtora SK, Garnier A (4 Mar 2022) *Forced displacement from Ukraine: notes on humanitarian protection and durable solutions*. Retrieved from: https://reliefweb.int/report/ukraine/forced-displacement-ukraine-notes-humanitarian-protection-and-durable-solutions. [Accessed 7 March 2022]

Berkay M (2020) *Sharing the burden: revisiting the EU-Turkey migration deal*. Retrieved from: https://www.crisisgroup.org/europe-central-asia/western-europemediterranean/turkey/sharing-burden-revisiting-eu-turkey-migration-deal. [Accessed 25 February 2022]

Bertelsmann Stiftung (2015) *Zuwanderungsbedarf aus Drittstaaten in Deutschland bis 2050.* (Need for immigration from third countries in Germany by 2050). Retrieved from: https://bit.ly/3cyw0u1. [24 February 2022]

Bircan T, Korkmaz EE (2021) Big data for whose sake? Governing migration through artificial intelligence. *Humanities Social Sciences Communications* 8(Oct): 241.

BMI (2015) *A test for our country*. Retrieved from: https://www.bmi.bund.de/SharedDocs/kurzmeldungen/EN/2015/09/measures-on-asylum-and-refugee-policy.html. [Accessed February 2022]

BMI (2022*) Befragung ukrainischer Kriegsflüchtlinge*. (Interrogation of Ukrainian war refugees). Retrieved from: https://bit.ly/3Q8krZw. [Accessed 6 March 2022]

Böhme MH, Gröger A, Stöhr T (2020) Searching for a better life: Predicting international migration with online search keywords. *Journal of Development Economics* 142(Jan): 102347.

Cesare N, Lee H, McCormick T, Spiro E, Zagheni E (2018) Promises and pitfalls of using digital traces for demographic research. *Demography* 55(5): 1979–1999.

Charron A (2020) Somehow, we cannot accept it: drivers of internal displacement from Crimea and the forced/voluntary migration binary. *Europe-Asia Studies* 72(3): 432–454.

Choi H, Varian H (2012) Predicting the present with google trends. *Econ Record* 88(s1): 2–9

Connor P (2017) *The digital footprint of Europe's refugees. Methodology*. Pew Research Center. Retrieved from: https://www.pewglobal.org/2017/06/08/online-searches-eu-refugees-methodology/. [Accessed 28 February 2022]

Curry T, Croitoru A, Crooks A, Stefanidis A (2018) Exodus 2.0: crowdsourcing geographical and social trails of mass migration. *Journal of Geographical Systems* 21(Sep): 161–187.

Deutsche Bahn (2022) *"Helpukraine" ticket allows refugees to travel to any station in Germany free of charge.* Available at: https://www.deutschebahn.com/en/presse/press_releases/-helpukraine-ticket-allows-refugees-to-travel-to-any-station-in-Germany-free-of-charge-7315140.

Deutsche Welle (2022) *Ukrajinske izbjeglice kao konkurencija useljenicima sa zapadnog Balkana?* (Ukrainian refugees as competition to immigrants from the Western Balkans). Retrieved from: https://www.dw.com/bs/ukrajinske-izbjeglice-kao-konkurencija-useljenicima-sa-zapadnog-balkana/a-61045150. [Accessed 1 March 2022]

Dubois A, Zagheni E, Garimella K, Weber I (2018) Studying migrant assimilation through Facebook interests. *Lecture Notes in Computer Science* 11186(Sep): 51–60.

Düvell F (2022) *Krieg in der Ukraine: Wie ist die Flüchtlings-Situation?* (War in Ukraine: what is the refugee situation like? Universität Osnabrück, Mediendienst Integration. Retrieved from: https://mediendienst-integration.de/artikel/krieg-in-der-ukraine-wie-ist-die-fluechtlings-situation.html. [Accessed 7 March 2022]

EUROPOL (2018) *Two years of EMSC: activity report January 2017 – January 2018*. European Migration Smuggling Centre, EUROPOL. Retrieved from: https://www.europol.europa.eu/cms/sites/default/files/documents/two_years_of_emsc_report.pdf. [Accessed 10 March 2022]

Gabrilovich E (2020) *Using symptoms search trends to inform COVID-19 research*. Google Health. Retrieved from: https://blog.google/technology/health/using-symptoms-search-trends-inform. [Accessed 28 February 2022]

Hawelka B, Sitko I, Beinat E, Sobolevsky S, Ratti PKC (2014) Geo-located Twitter as proxy for global mobility patterns. *Cartography and Geographic Information Science* 41(3): 260–267.

Ibáñez Sales M (2021) *Big data at the crossroads: seizing the potential of Big data to guide the future of EU migration policy*. Euromesco Policy brief, n. 116.

Internet World Stats (2022) *Internet users distributions in the world - 2021*. Retrieved from: https://www.internetworldstats.com/stats.htm. [Accessed 2 March 2022]

Jurić T (2021a) *"Gastarbeiter Millennials": exploring the past, present and future of migration from Southeast Europe to Germany and Austria with approaches to classical, historical and digital demography*. Hamburg: Verlag Dr. Kovač.

Jurić T (2021b) Google trends as a method to predict new COVID-19 cases and socio-psychological consequences of the pandemic. *Athens Journal of Mediterranean Studies* 8(1): 67–92.

Jurić T (2021c) Medical brain drain from Southeastern Europe: using digital demography to forecast health worker emigration. *JMIRx Med* 2(4): e30831.

Jurić T (2022a) Forecasting migration and integration trends using digital demography – A case study of emigration flows from Croatia to Austria and Germany. *Comparative Southeast European Studies* 70(1): 1–28.

Jurić T (2022b) Facebook i Google kao empirijska osnova za razvoj metode digitalnog praćenja vanjskih migracija hrvatskih građana (Facebook and Google as an empirical basis for the development of a method of digital monitoring of external migration of Croatian citizens). *Ekonomski pregled* 73(2).

Jurić T (2022c) Google search analysis in interdisciplinary research (case studies: COVID-19, birth rate and tourism demand), 4. In *Međunarodna naučna konferencija o digitalnoj ekonomiji DIEC 2021 - Zbornik radova*, 5–25. Tuzla, 2022.

Jurić T (2022d) Big (crisis) data in refugee and migration studies – Case study of Ukrainian refugees. *Comparative Southeast European Studies* (forthcoming).

Kalimeri KA, Beiro MG, Bonanomi A, Rosina A, Cattuto C (2020) Traditional versus Facebook-based surveys: evaluation of biases in self-reported demographic and psychometric information. *Demographic Research* 42(5): 133–148.

Kuznetsova I, Mikheieva O (2020) Forced displacement from Ukraine's war-torn territories: intersectionality and power geometry. *Nationalities Papers* 48(4): 690–706.

Magoscy R (1996) *A history of Ukraine*. Toronto: University of Toronto Press.

Önder I (2017) Forecasting tourism demand with Google trends: accuracy comparison of countries versus cities. *International Journal of Tourism Research* 19(6): 648–660.

Radelić Z, Marijan DN, Barić A, Bing, Živić D (2006) *Stvaranje hrvatske države i Domovinski rat*. (The creation of the Croatian state and the Homeland War). Školska knjiga Zagreb 2006.

Scrinic A (2014) Humanitarian aid and political aims in Eastern Ukraine: Russian involvement and European response. *Eastern Journal of European Studies* 5(2): 77–88.

Sereda V (2020) Social distancing' and hierarchies of belonging: the case of displaced population from Donbas and Crimea. *Europe-Asia Studies* 72(3): 404–431.

Singh L, Wahedi L, Wang Y, Wei Y, Kirov C, Martin S, et al. (2019) Blending noisy social media signals with traditional movement variables to predict forced migration. In *KDD '19: Proceedings of the 25th ACM SIGKDD International Conference on Knowledge Discovery & Data Mining*, 1975–1983.

Spyratos S, Vespe M, Natale F, Weber I, Zagheni E, Rango M (2018) *Migration data using social media: a European perspective*. JRC Technical Reports European Commission. Luxembourg: Publications Office of the European Union.

State B, Rodriguez M, Helbing D, Zagheni E (2014) Migration of professionals to the U.S. evidence from LinkedIn data. *Lecture Notes in Computer Science* 8851: 531–43.

The Guardian (2019) *"A whole generation has gone": Ukrainians seek a better life in Poland*. Retrieved from: https://www.theguardian.com/world/2019/apr/18/whole-generation-has-gone-ukrainian-seek-better-life-poland-elect-president. [Accessed on 14.04.2022]

The Guardian (2022, March 5) *Ukraine has fastest-growing refugee crisis since second world war, says UN*. Retrieved from: https://www.theguardian.com/world/2022/mar/06/ukraine-fastest-growing-refugee-crisis-since-second-world-war. [Accessed 10 April 2022]

UNHCR (2016) *Global trends. Forced displaments in 2015. https://www.unhcr.org/576408cd7.pdf (accessed 1 April 2022).* [Accessed 8 March 2022]

UNHCR (2017) *From a refugee perspective: discourse of Arabic speaking and Afghan refugees and migrants on social media from March to December 2016*. Retrieved from: https://www.unhcr.org/publications/brochures/5909af4d4/from-arefugee-perspective.html; https://reliefweb.int/sites/reliefweb.int/files/resources/58018.pdf. [Accessed 10 March 2022]

UNHCR (2022a) *Ukraine RRR*. Retrieved from: https://www.unhcr.org/ukraine-emergency.html [Accessed 4 March 2022].

UNHCR (2022b) *Internally displaced persons (IDP)*. Retrieved from: https://www.unhcr.org/ua/en/internally-displaced-persons. [Accessed 29 February 2022]

UNHCR (2022c). *Ukraine situation regional refugee response plan.* Retrieved from: https://bit.ly/3bBmIxp. [Accessed 8 March 2022]

UNHCR Blog, Pellandra A, Henningsen G (2022) *Predicting refugee flows with big data: a new opportunity or a pipe dream?* Retrieved from: https://www.unhcr.org/blogs/predicting-refugee-flows-with-big-data-a-new-opportunity-or-a-pipe-dream/.

UNHCR Global Data Service (2021) *Big (crisis) data for predictive models: a literature review*. UNHCR Global Data Service.

United Nations (2014) *The data revolution for human development*. Retrieved from: http://hdr.undp.org/en/content/data-revolution-human-development. [Accessed 28 February 2022]

United Nations (2019) *Report of the global working group on big data for official statistic*s. The Economic Social Council of the United Nations, UN Global Working Group on Big Data.

Visitukraine (2022, March 5) *Refugees from Ukraine received the right to live in the EU for 3 years*. Retrieved from: https://visitukraine.today/blog/154/refugees-from-ukraine-received-the-right-to-live-in-the-eu-for-3-years. [Accessed 11 March 2022]

Wang R, Wang W, daSilva A, Huckins JF, Kelley WM, Heatherton TF, et al. (2018) Tracking depression dynamics in college students using mobile phone and wearable sensing. In *Proceedings of the ACM on Interactive, Mobile, Wearable and Ubiquitous Technologies* 2(1): 43.

Wanner P (2020) How well can we estimate immigration trends using Google data? *Quality and Quantity* 55(Oct): 1181–202.

Wilde J, Chen W, Lohmann S (2020) *COVID-19 and the future of US fertility: what can we learn from Google?* IZA Discussion Papers 13776.

Wladyka D (2017) Queries to Google Search as predictors of migration flows from Latin America to Spain. *Journal of Population and Social Studies* 25(4): 312–327.

Zagheni E, Garimella VRK, Weber I, State B (2014) Inferring international and internal migration patterns from Twitter data. In *WWW '14 Companion: Proceedings of the 23rd International Conference on World Wide Web*, 439–444.

Zagheni E, Weber I (2015) Demographic research with non-representative Internet data. *International Journal of Manpower* 43(9).

Zagheni E, Weber I, Gummadi K (2017) Leveraging Facebook's advertising platform to monitor stocks of migrants. *Population and Development Review* 43(4): 721–734.

Athens Journal of Technology and Engineering - Volume 9, Issue 3, September 2022 – Pages 185-196

Examining Student Support in Implementing Open Distance Learning during COVID-19

By Sipho Makgopa[*]

In times of crisis and the global spread of the COVID-19 pandemic, the world has observed exponential growth of online education as educators and students are required to stay at home and resume with online learning entirely. With the new norms in education, come new experiences and challenges. The demands in online learning have pushed both students and educators to maximise their information communication technology (ICT) skills and caused some to be unwillingly ready for the new normal. The purpose of this study is to describe the student support of registered students in open distance learning (ODL) institutions during the COVID-19 era. Active learning theory is adopted as a theoretical lens for the interpretation of the data. This study used a quantitative research method approach to gather insights regarding the student experience pertaining to technology integration in the ODL context during COVID-19. The findings uncovered challenges associated with online student support in ODL context. This paper provide recommendations to key stakeholders in higher learning institutions and future research directions.

Keywords: *active learning theory, COVID-19, information communication technology, open distance learning, student support*

Introduction

Msweli (2012) maintains that ODL is higher education provides access to students disqualified physical distance, personal restrictions or the full-time employment and family responsibilities. ODL further extends to provide tertiary education to previously disadvantaged students with limited financial resources that are unable to attend face-to-face higher education institutions. In offering access to higher education to students, ODL institutions offer student support to all registered students. It should be noted that South African Bill of Rights stipulates that every person has the right to education, therefore, barriers should not stop individuals from furthering their studies (South African Bill of Rights 1996). Hence, ODL contributes to overcoming identified barriers. Msweli (2012) highlights that many ODL institutions function in a blended mode of both online and physicality with regards to their module offerings; however, for an ODL institution to function effectively, proper processes must be put in place to support the students.

The sustainability of distance learning relies on quality services, therefore, it is imperative that institutions comprehend and recognise the nature of the quality of services being offered. Understanding this will assist institutions to select

[*]Curriculum and Learning Development Specialist, University of South Africa, South Africa.

appropriate measures when determining the quality of support services, or how to start improving the quality thereof, and this, should be regarded as the key element in in order to deliver quality student support services. Mankoe and Ntsaba (2019) maintain that open and distance learning institutions are responsible for aiding students in academic and administrative matters (which will be critically discussed in the following topics) to improve the trust of students and their sense of confidence, and to overcome feelings of isolation and reduce the drop-out rate.

Theoretical Background and Review of Previous Studies

COVID-19

In 2020, a deadly COVID-19 virus emerged. The number of infected cases increased rapidly and spread across the world, which resulted in many fatalities. Due to the disturbing situation, the World Health Organization (WHO) declared COVID-19 a global pandemic on 11 March 2020. Precautionary measures are necessary to limit the spread of the diseases (Mailizar et al. 2020). The South African government enforced Movement Control Measures, new health protocols, guidelines, and restrictions on all sectors of the economy, including the education sector. One of the precautionary control measures pertaining to COVID-19 included the closure of schools and institutions of higher learning in order to flatten the curve of the pandemic. In addition, institutions of higher learning had to adopt technology in order to facilitate learning and offer student support to registered students during COVID-19 pandemic.

Defining Open Distance Learning (ODL)

Mayanja, Tibaingana and Birevi (2019) stated that the concept of open distance learning describes the offering of education at a distance where students are physically separated from the educational institution to instruct students in the absence of tutor and student interactions. Ravhudzulo (2014) maintains that ODL involves the ability to study at a distance from the higher learning institution and thus, provide a flexible learning model and allow students to access educational opportunities. Msweli (2012) maintains that open distance learning is seen as a learning system that incorporates student support, curriculum and instructional design, learning versatility, the elimination of barriers to entry, previous learning credit, and other instructional practices. These instructional design practices include the implementation and evaluation of programmes to meet students' diverse needs who generally come from different cultural, social and religious backgrounds (Msweli 2012). In the context of this study, the preceding definition is adopted and supports the view that ODL is targeted at anyone who is willing to further their studies in an open distance learning institution, and offering student tuition support despite the age. individual differences and geographic dispensation.

Active Learning Theory

This study adopted active learning theory as a theoretical lens for the interpretation of data as it forms the basis of deep active learning. Active learning is relevant in this study as it relates to the paradigm shift from teaching to learning. This is due to the fact that changes outside teaching environment are likely to bring change to how teaching and learning are facilitated in higher learning institutions including those operate in ODL context. Bonwell and Eison (1991) argued that although it is difficult to define active learning the point is that "when you take a position in a stationary object (T1) and next you see the object start to move (T2), you observe the gradual movement from T1 to T2. This movement is action and thus active. From this standpoint, learning (action) is always active, and passive learning cannot exist". In this study, the author share the same sentiments that learning is an action that need to be active teaching which can be supported by student support activities even during trying times of Covid-19. The point is that academic staff needs to engage with students to facilitate learning in ODL context.

Previous Studies on Student Support in the ODL Context

Arifin (2018) highlights that student support can be regarded as the range of services available to individuals and students in groups, and complements the course material or learning resources that are appropriate for all learners. Mpofu (2016) posits that student support is a very important component of open distance learning programmes, including systemic, affective and cognitive factors that are intended to scaffold the student to achieve their academic success. Mpofu (2016) further states that ODL student support consists of three categories: a course and design dimension (course design and content delivery), educational support services (student groups, tutor support, academic service centres and technical services) and university support services (orientations, achievement and retention programmes, university support services, scholarships and awards, library resources, and computing and technology). Arifin (2018) suggests that technological infrastructure, scale and geography are also important in developing student support systems, and the importance of knowing which technologies are used by students is very vital. Technological innovation plays an important role in our lives, particularly social media networks, hence, social media is an effective tool that can be used to provide student support. Netanda et al. (2017) alluded that the value of providing support services for students is to allow students to meet various academic demands, to help them with their academic prospects, and to maintain them until they successfully complete their studies. Therefore, this paper acknowledges the importance of student support for student success and aims to focus on student support in the ODL context amid the COVID-19 pandemic.

Arifin (2018) maintains that student support can be accomplished through three support mechanisms, namely, systemic, affective, and cognitive support. These should be accompanied by the transformation of institutional attitudes affecting all staff at all levels in an attempt to set retention targets and establish approaches, motivators and incentives for achieving them. Netanda et al. (2017)

suggest that lectures should establish appropriate and meaningful educational content to promote the participation of students in learning processes and their achievements. Previous studies have shown that the use of support programmes for students provides more complementary benefits to both the students and the institution. Dependable and effective student support programmes that best address student needs can advance students' learning and learning experiences by affecting immersion and achievement in learning. Netanda et al. (2017) argue that ODL higher institutions should be competitive in a global higher education environment by providing students with support services that maximise student enrolment and retention rates until they successfully complete their studies. Makoe and Nsamba (2019) identified different modes of student support services that can be found in open distance learning institutions. These include the following: (1) Counselling, which provides career, academic and personal support to students; (2) Student regional centres that provide academic and financial advice, meet other students, make use of academic services and computers, and have conversations with counsellors in registration services; (3) Academic learning support through e-tutors, module design and library services (Makoe and Nsamba 2019). Student email addresses are also created for all registered students, to obtain updates on all the modules they registered for.

Mankoe and Nsamba (2019) compared students' expectations and perceptions through support services to determine the gaps in the quality of services offered. A questionnaire analysis was conducted consisting of four proportions, namely, tangibility, reliability, delivery and assurance. The results revealed that the aspirations of the students were greater than their perceptions in three dimensions of service quality, with the measurable dimension having the greatest gaps. The findings of the overall study from the perception and expectation assessment of quality from students' perspectives uncovered that there are discrepancies within an ODL institution's student support programme. This study also established that support systems should be more accessible and aimed at students' needs, and should not be a standard universal approach across the board. This study recommends that distance education institutions should set official quality standards and different types of services should be considered to decide what works and what does not work. Paniagua and Simpson (2018) recommended that to be efficient, institutional induction programmes should have systematic and on-going processes throughout the students' first year, to generate authentic networked learning.

The number of studies conducted on the role of student support in ODL institutions is increasing, but with diverse and inconclusive findings regarding some variables. Simsons et al. (2020) reported on the dimension of tutor support in student support services. The results of the study conducted by Simsons et al. (2020) show that students seem to highly respect the input they receive from their tutors on their evaluated work and describe it as a forward-thinking encouragement and motivation. The study further highlighted the positive impact on students, which was evident to students when they experienced stressful circumstances in their lives. Due to difficulties forcing the students to abandon their studies, they sought the assistance and support of their tutors who granted them extensions and

postponements on due dates, where circumstances were beyond the students' control. This support enabled the students to still accomplish their goals to complete their studies.

Mpofu (2016) posits the self-efficacy dispositions of students in relation to studying in the ODL context. The study suggests that student support plays an important rolein ODL context, while student achievement is influenced by anticipated outcomes and further moderated by efficacy dispositions. Self-efficiency dispositions such as coping skills, proactivity, ingenuity, problem solving abilities and tenacity are also crucial in ODL institutions. However, further to the study of Mpofu (2016), Netanda et al. (2017) posit student autonomy as the degree of independence displayed by students in the student relationship to assess learning participation, goals and decisions to assess the learning programme, in summary students who commit to their studies are more likely to succeed in their studies. Simsons et al. (2020) added that working students, or students with other commitments make use of ODL institutions. Therefore, ODL is the best alternative way in which to further higher learning studies since they do not have to attend the institution every day for tutoring lessons. Arko-Achemfour (2017) provides a definition of the 'distance' that is found in ODL institutions as the 'transactional distance' – this is found in Moore's theory, which refers to all the gaps that exist in educational ties, especially, geographically. However, the distance is measured by the amount of contact between the academic instructor and students, and the amount of structure in the course design. Educational processes in an ODL can be applied by using the transactional presence approach as stated by Arko-Achemfour (2017), which highlights the different modes that are offered by an institution to support the learner. Support services may include tutoring mediated programmes to allow students to achieve and realise their academic objectives and goals. He further defined transactional presence as the degree to which learners perceive the quality and accessibility of an ODL institution and its staff, as well as the learning centre's coordinators, tutors, peer learners, and other related persons.

In another study, Msweli (2012) found that ODL encourages the ideals of more independent methods of study and work, open education for all, and continuing professional development through its goals. Goals include: access to learning; and breaking down geographic barriers of time and space to meet learners' needs in a world characterised by new values and social trends; knowledge sharing and collaborative learning; and reaching economic goals. However, in today's fast changing world, societies are faced with conditions with a need to adapt to the Fourth Industrial Revolution. The revolution is influenced by our technological advances that replace most functionalities that are developed by humans. Pham and Ahn (2018) found that green or sustainable systems evolves under the support of cyber-physical systems (or digital twins) based on ICT technology. Mayanja et al. (2019) maintain that the evolution of the world economic change requires institutions to stay abreast of the current technological trends, which will enable them to provide the best services to their students, meet the expectations of students, and meet their institutional objectives as outlined in their missions and visions. Information and communication technologies such as

computers, emails, mobile phones, social media applications, radio and television are the barrier points between students, facilitators and institutions.

Paniagua and Simpson (2018) investigated an ODL system with specific reference to share expertise about how effective, or not, technology has been for developing innovative, advanced and quality student support services to large or small groups. The findings of this study uncovered that one of the greatest challenges experienced by ODL institutions is the large number of enrolled students, which calls for strong and well-organised student support programmes at an institutional level. The study further discovered that student support is fundamental to ODL and influences the quality of the entire system. Paniagua and Simpson (2018) suggest that for this reason, each quality assurance model in ODL incorporates specific indicators pertaining to the suitability of student support services at both institutional and course level.

Mayanja et al. (2019) explored the use of ICT services for student support in an ODL institution, namely, Makerere University. The study revealed the challenges students face as they struggle to obtain relevant research tools, which affects academic performance. Therefore, student study supervision is carried out through face-to-face interactions that require students to travel far distances, and incur costs due to these distances travelled, in order to meet their superiors at the University. At times, these meetings are cancelled after the students have travelled far distances. The findings of this study revealed that integrating ICTs in the various phases of the learning life cycle of the students can increase the students' satisfaction regarding the university programmes. In another study, Msweli (2012) explored on ODL strategy that supports the ODL framework, various components and how resources are distributed to facilitate learning. Msweli (2012) adds that each component of the ODL programme can and should be internationalised in order to obtain the full ODL outcomes, including extended and equal access to education and training, and improved student outputs..

Problem Statement

Regarding the afore-mentioned context, it is evident that the literature review revealed the processes about how students are supported in an ODL context, along with the different types of student support services that are offered. The literature review also indicated the relationship between student support and student experiences on the issue of access to student support services. Many studies have focused on examining the casual relationships of student support in an ODL context using a universal approach on students rather than focusing on the individual needs of students. The role of student support in open distance learning institutions needs to consist of informational approaches to enhance student achievement, and student retention needs to be considered.

Arifin (2018) maintains that the higher education sector plays an important role in the economy by empowering students to graduate and become employable in the labour market. Higher education institutions that operate in an ODL context, have concerns pertaining to student retention, as the global labour market provides

increased career opportunities for skilled professionals with specialised qualifications. Research conducted by Paniagua and Simpson (2018) has shown that success rates at ODL institutions are considered lower than conventional education offered by residential institutions. Arko-Achemfuor (2017) posits physical distance as the challenge faced by ODL students. Previous studies identified various success factors that lead to proper execution of student support in ODL institutions.

Fewer studies have been found on the relationship between student support services offered in ODL institutions and students in marginalised groups, with specific reference to students who are in rural areas in South Africa. Arko-Achemfour (2017) found that there are many challenges faced by students who are in rural areas, such as the lack of technological devices like computers, which also implicates financial challenges of tuition fees, whereas if they had proper access to laptop or computer with internet they would limitless and appropriate information on different types of financial assistance programmes and their providers. Arko-Achemfour (2017) add that there is a scarcity of information available on how different biographical groups differ in their perceptions of ODL institutions and student support, hence, this current study aims to address this gap in academic literature. This study also aims to enhance the understanding of ODL institutions in conceptualising the student support services provide to students through the use of technological devices to students both in urban and rural areas. The relationships between these variables should provide an understanding that will guide retention practices and strategies for students in ODL institutions in South Africa. The study should enlighten future research into the role that these variables play in retaining students and reaching suitable graduate success rates from different biographical and geographical groups. In summary, this study seeks to answer the following research questions:

- What are the different types of student support services that are offered to students in implementing ODL during COVID-19?
- What are the benefits enjoyed by students due to implementation of ODL during COVID-19?
- What are the challenges experienced by students due to the implementation of ODL during COVID-19?

Contribution of the Study

This study makes contribution to active learning theory by focusing on online student support platforms adopted by academic teaching staff in ODL context in engaging students in the process learning by identifying challenges experienced by the students. In practice teaching and learning methods in institutions of higher learning have changed due to the COVID-19 pandemic. As a result, this challenge in teaching methods is likely to present challenges to both students and academics as they have to embrace numerous new methods of teaching and learning on various online learning environments. The results of this study can assist academics to choose the most effective and convenient platform preferred by students, which

consequently will assist in identifying the most appropriate approach in the preparation of ODL materials in the midst of the COVID-19 pandemic. In addition, the study aimed to make an academic contribution by addressing gaps in literature pertaining to student support amid the unprecedented COVID-19 pandemic.

Research Methodology

A descriptive quantitative approach was followed, using a structured questionnaire to achieve the research objective. A quantitative research approach was chosen as an appropriate research approach, since it permitted the participants to share their opinions and perspectives on student support in the ODL context during COVID-19 pandemic. A purposive sampling method was used in the study; this sampling method requires that participants are chosen by considering some defining characteristics that make them the holders of the data needed for the study (Tustin et al. 2005). Registered undergraduate students at various South African universities were selected as the unit of analysis. An online survey was used to capture data regarding the students' profiles and their experiences relating to student support during COVID-19 pandemic in implementing ODL. Descriptive statistics were used in this study to analyse the primary data on demographic variables of students, and student support tools were used to ensure the data was of good quality with no missing values. The reliability of the measurement scales was assessed by measuring internal consistency using Cronbach's alpha values. Cronbach alpha is used to measure the internal consistency reliability, which is the average of all possible split-half coefficients resulting from the scale items being split differently. (Malhotra 2010). The validity of the measurement scales was assessed looking at face or content validity and used scales, which that proved to be valid, previously.

Results and Discussion

304 undergraduate student respondents (registered for either a diploma or undergraduate degree) throughout South Africa participated and shared their feedback on the ODL implementation in their respective universities. The response rate was satisfactory, and this was the result of the online convenient survey used during the data collection process. The data analysed includes the demographic profiles of respondents and data on the students' perspectives have covered feedback on the ratings of online tools or platforms used to implement ODL, and the benefits derived from the online tools. The respondents of the study consisted of 38% males and 62% females. The next item analysed on the demographic profile was the location of the respondents and 66% were at home residing in cities, and 34% of these respondents were dispersed in rural areas.

In line with research objective one of the study which aimed to identify different types of student support services offered in implementing ODL during

COVID-19, students were asked to identify the different types of student support services that were offered to them. Majority of students (94%) indicated that online student support services are offered by lecturers using Learning Management Systems (LMS), Microsoft Teams Meeting, YouTube videos, Zoom Meeting. However, only 6% of students alluded that online support service are offered through the use of WhatsApp social media platform. The results of the current study concur with the view by Arifin (2018) that technological infrastructure, scale and geography are also important in developing student support systems. The results regarding the use of social media platforms to offer student support concur with Arifin (2018) that argued that technological innovation can be utilised to play an important role in lives, particularly social media networks, as tool to provide student support.

To achieve research objective two, students were also asked to identify the benefits derived in studying via the ODL teaching model. 87% of respondents agreed that ODL teaching model supported by online platforms allows them to understand learning outcomes of the subject matter due to the convenience and flexibility of ODL while 13% of students disagreed. The results of this paper concur with Ravhudzulo (2014) in that ODL provides the opportunity to study at a distance through a higher learning institution, and provides a flexible learning model, in addition to allowing students to access educational opportunities. The results also support the view by Msweli (2012) that the ODL learning system incorporates student support. Students were asked to rate their internet connection quality in ODL context as a possible challenge in implementing ODL. In addition, 69% of the respondents indicated they were satisfied with the efforts made by lecturers to offer student support in conducting the lessons through online platforms, such as Learning Management Systems (LMS), Microsoft Teams Meeting, YouTube videos, Zoom Meeting. However, 31% mentioned that they did not prefer teaching to be carried out on online platforms (Microsoft Teams Meeting, YouTube videos, Zoom Meeting). The results of this study add new insight in literature by revealing the students' satisfaction regarding the student support offered by lecturers during unprecedent era of COVID-19 era.

To realise research objective three, students were asked to identify challenges linked to implementation of ODL model amid COVID-19. The majority of respondents 68% had good internet connection quality while a minority of 32% experienced poor internet connection quality. The preceding results regarding poor internet connection as a barrier to effective implementation of ODL add insights for academic literature related to open distance learning, specifically, in COVID-19 era. In addition, 58% of students indicated that late response on administrative queries pose a challenge for the effective implementation of ODL during COVID-19 pandemic era. These results are in support of Makoe and Nsamba (2019), these authors argued that administrative support is crucial for effective implementation of ODL.

Moreover, 64% of students alluded that offering online student support is appreciated, but face-to face classroom interaction is lost due to COVID-19 and study material content cannot be explained in details. In addition, majority of students 68% agreed that online student support pose a challenge with regard to

high data costs for downloading study material while minority of students 32% cared less about data costs.

Conclusions

In this paper, the respondents confirmed that different types of student support services were offered to them by lecturers using Learning Management Systems (LMS), Microsoft Teams Meeting, YouTube videos, Zoom Meeting. Furthermore, the results of this paper revealed that students are satisfied with ODL teaching model which is supported by online platforms as they allow them to understand learning outcomes of the subject matter due to the convenience and flexibility. These results add significant contribution to ODL literature by identifying the mentioned techological platforms used to offer online student support in ODL context. Moreover, the results of this paper add insight to literature by uncovering data connectivity as a one of challanges related to online stude support. In addition, the results of this study revealed that students are faced with a challenge of high data cost associated with viewing and dowloading of study material content. The results of this paper add new insight to literature by identifying additional challenges such as internet connectivity specifically in rural areas, and downloading data costs as a barriers for effective in implemention of ODL and online student support during COVID-19 era.

Recommendations

Despite the challenges faced in ODL implementation in the past, the opportunity to innovate teaching is available to the instructors to explore. On a positive note, ODL as the post COVID-19 new norm, has proven that learning has no boundaries. Instead of conducting lessons within four walls in the traditional way, the implementation of ODL will take teaching and learning to a whole new level and unleash creativity for both learners and instructors. In order to have effective student support and to improve students' performance at institutions of higher learning, which follow an ODL teaching model, various recommendations are made. First, online or virtual induction programmes in ODL learning institutions should be conducted for new students and new lecturers to empower them. Secondly, lecturers training workshops should be conducted on a regular basis to improve online lecturing and facilitation skills. Thirdly, students should be offered financial support with data to make studying effective and for downloading of study material. Furthermore, it is recommended that academics upload support material that consumes less data.

Future Research Directions

Future research should focus on obtaining insights on how to blend both online and offline student support tools to cater for the needs of students in rural areas characterised by poor quality network connections. In addition, future research should aim to analyse how to develop interactive teaching and learning materials. Moreover, future research should consider obtaining insights on the training needs of academics to ensure the effective implementation of interactive teaching methods for the ODL context.

References

Arifin MH (2018) The role of student support services in enhancing student persistence in the open university context: lesson from Indonesia open University. *Turkish Online Journal of Distance Education* 19(3): 156–168.

Arko-Achemfour A (2017) Student support gaps in an open distance learning context. *Issues in Educational Research* 27(4): 658–676.

Bonwell CC, Eison JA (1991) *Active learning: creating excitement in the classroom.* ASHE-ERIC Higher Education Report No. 1.

Mailizar M, Almanthari A, Maulina S, Bruce S (2020) Secondary school mathematics teachers' views on e-learning implementation barriers during the COVID-19 pandemic: the case of Indonesia. *Eurasia Journal of Mathematics, Science and Technology Education* 16(7): em1860.

Makoe M, Nsamba A (2019) The gap between student perceptions and expectations of quality support services at the University of South Africa. *American Journal of Distance Education* 33(2): 132–141.

Malhotra NK (2010) *Marketing research: an applied orientation*. 6th Global Edition. Upper Saddle River, NJ: Pearson.

Mayanja J, Tibaingana A, Birevu PH (2019) Promoting student support in open and distance learning using information and communication technologies. *Journal of Learning for Development* 6(2): 177–186.

Mpofu N (2016) What can we still offer? Understanding student support in distance education teacher preparation programmes. *Progressio* 38(2): 33–46.

Msweli P (2012) Mapping the interplay between open distance learning and internationalisation principles. *The International Review of Research in Open and Distributed Learning* 13(3): 97–116.

Netanda RS, Mamabolo J, Themane M (2017) Do or die: student support interventions for the survival of distance education institutions in a competitive higher education system. *Studies in Higher Education* 44(2): 397–414.

Paniagua AS, Simpson O (2018) Developing student support for open and distance learning: the EMPOWER project. *Journal of Interactive Media in Education* 1(9): 1–10.

Pham A, Ahn H (2018) High precision reducers for industrial robots driving 4th industrial revolution: state of arts, analysis, design, performance evaluation and perspective. *International Journal of Precision Engineering and Manufacturing-Green Technology* 5(4): 519–533.

Ravhudzulo A (2014) Enhancing teaching and learning in open and distance learning: A mechanism to facilitate student success. *International Journal of Education Science* 6(1): 27–32.

Simsons J, Leverette S, Beaumont K (2020) Success of distance learning graduates and the role of intrinsic motivation. *Open Learning: The Journal of Open and Ditsance Learning* 35(3): 277–293.

South African Bill of Rights (1996) *Chapter 2*. Available at: https://www.gov.za/documents/constitution/chapter-2-bill-rights.

Tustin DH, Ligthelm A, Martins JH, van Wyk HdeJ (2005) *Marketing research in practice*. University of South Africa, Pretoria: Unisa Press.

Athens Journal of Technology and Engineering - Volume 9, Issue 3, September 2022 – Pages 187-212

Preload Stability of Modern Bolted Joints

By Tobias Held[*], Jens Peth[±] & Christoph Friedrich[°]

The design of screw joints is very important for fastened components to ensure reliable transmission of mechanical or thermal loads between components. Suitable fastener selection and proper design are required for increasing product performance while reducing size, weight and cost ratios. A fastening system is basically characterized by component geometry, materials and tightening level. Robust clamping of components depends on time dependent clamp force, which can be represented by Bolt's preload change. In any fastening system preload loss takes place. The contribution shows, why (seating, load plastification, creeping). Furthermore, the loss may not be too large to provide suitable behaviour over time. This means, a higher tightening preload cannot be utilized, if most of the advantage is compensated by preload loss. Important influences are clamped materials, tightening level (from assembly method) and type of thread engagement. For various combinations long time measurements of preload loss over time are shown. The paper shows also how the measurement is done. The outcome of all the combinations is that preload loss significantly exceeds the estimations of existing guidelines, e.g., VDI 2230. The reason is, that in time of development of the guidelines mainly steel components have been used and preloading was moderate. So the conclusion is to extend the calculation with a better and more flexible approach for today´s requirements. Overall, the contribution combines explaining mechanisms for preload loss, results from measurements for analysis as well as calculation for prediction in advance to extend guidelines.

Keywords: *bolted joints, preload loss, influences, prediction, guideline for design*

Introduction to Preload Relaxation and Methods of Measuring

Bolted joints are an important way of connecting components, they are widely used in all sectors of mechanical engineering. The unique combination of high clamping forces and the fact, that such a connection is detachable and reusable, leads to a growing number of screw joints in many modern mechanical devices. Another reason for the growing usage is the increasing use of light metals like aluminum or CFRP, which are difficult for welding. In Germany for example, more than 500,000 tons of steel are annually used for screw production. Only when a sufficient level of preload is ensured in the screw about the entire life

[*]Scientific Assistant, Department of Mechanical Engineering, Institute of Engineering Design – MVP, University of Siegen, Germany.
[±]Scientific Assistant, Department of Mechanical Engineering, Institute of Engineering Design – MVP, University of Siegen, Germany.
[°]Professor, Department of Mechanical Engineering, Institute of Engineering Design – MVP, University of Siegen, Germany.

cycle, the function of the fastening system can be guaranteed. If not, failures can take place from breaking, opening, corrosion or self-loosening (for latest details see Guggolz (2019)).

As mentioned in the abstract above, the loss of preload in a clamped bolted joint can be mainly accomplished by the following three mechanisms. It is able to summarize them as “preload losses due to relaxation”:

1. Seating: While the assembly and tightening process, the different rough clamping parts are getting into contact. Even fine manufactured parts are having roughness peaks (maxima) and corresponding minima. Seating means a flattening of those peaks of the clamped parts, screw (under the head, in the thread) and nut thread during and afterwards the tightening process. The flattening is caused by local plastifications of the peaks. This leads to a reduction of the compression (extension) of the clamped parts (the screw), which again leads to a loss of preload, the seating loss. Its amount can be calculated with a simple formula given in the VDI 2230-1 (2015) guideline. The seating effect begins directly after the finished assembly procedure and continues at maximum to 48 hours, the main part of 80% is relaxed within the first hour in operation. In detail, the seating processes are acting already during the assembly process, but are getting equalized by the more and more increasing preload.
2. Load plastification: Local plastic deformations at the highest stressed areas (bearing surfaces under the screw head and nut position as well as thread contact and component contact zone) in the bolted joint, initialized by thermal and/or additional loads. Thereby, the preload increases first, but if the additional factors are gone, it supposes a lower amount as before. This process occurs, if the surfaces are overloaded above their plastic limit, this leads in the further development to a loss of preload in the screw.
3. Creeping: Longtime global plastic deformations of the solid materials in the entire clamping system because of the mechanical stress and especially increased thermal loads. This effect runs clearly stronger above 40% of the melting temperature of the clamped materials. For aluminum, those effects can occur already at temperature levels from T = 100°C (Peth and Friedrich 2018). This is especially of interest, because aluminum alloys are often used for modern lightweight applications. The difference between creeping and load plastification is, that for creeping the yield strength of a material is not reached. The creep plastification of a screw connection (and the resulting preload loss due to creep) cannot be estimated from uniaxial creep tests. One of the reasons is the difference of stress distribution. While the uniaxial creep sample usually has a circular stress area, the parts of the screw connection have an inhomogeneous stress distribution in the component contact and furthermore also over the length of the clamped parts and threads. Additionally the resilience of the screw and clamped parts lead to less plastic deformation as a plastification will directly reduce the preload and therefore reduce the stress and temperature driven creep mechanisms.

In Figure 1, these mechanisms are illustrated schematically for two types of bolted joints. For this, the preload level is plotted versus time. In the first system (top), steel based clamping parts were used, aluminum based in the second one (bottom). All other parameters like clamping length or assembly preload are already equal.

Figure 1. *General Approach for Determining Preload Loss with Two Different Systems (Hubbertz and Friedrich 2013)*

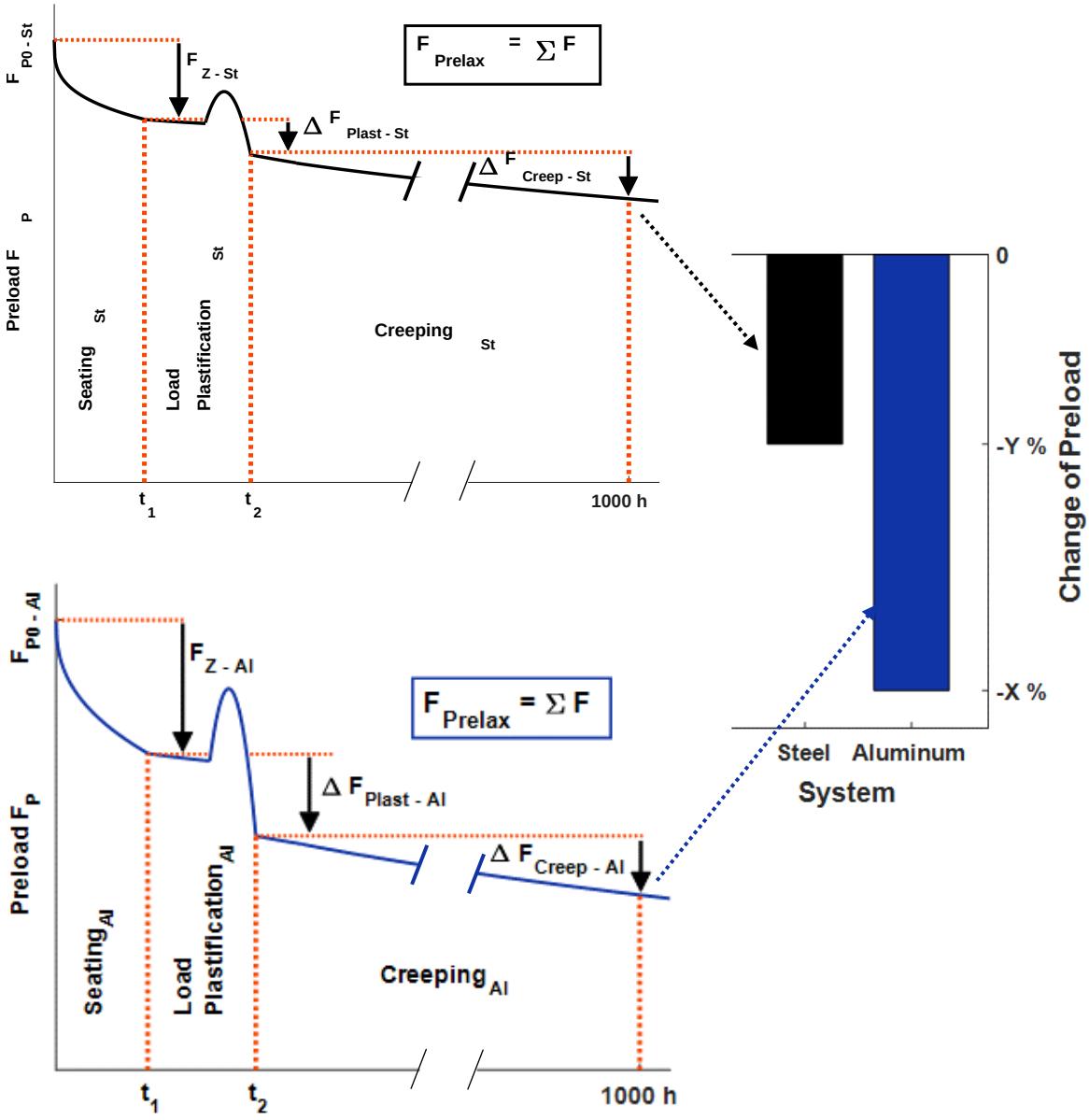

The bar graph below illustrates, that the preload losses because of relaxation processes are significantly higher for an aluminum system than for a steel system. Further it can be seen, that each Phase 1-3 within t_1 - t_3 has an own contribution to loss of preload, which ensures to differ the single phases (F_Z, ΔF_{Pplast}, ΔF_{Pcreep}).

The sum of them can be expressed as ΔF_{Prelax}, the above mentioned "preload losses due to relaxation". Besides this, it can be seen very good, that the preload increases, if the seating processes are finished and additional loads are acting.

The established guidelines are mainly focusing on the assembly process of a bolted joint or even on a short time after it. The loss of preload of such a connection can be estimated based on measurements, engineering standards or special literature, but in many cases, the loss is higher than the given information in these instruction textbooks. This is especially the case for modern lightweight - connections (e.g., aluminum) or if critical parameters are additionally acting, e.g., an increased temperature. Another important problem is that these guidelines are providing equations for the preload losses due to seating processes only, the additional mechanisms load plastification and creeping are not considered with the help of equivalent terms. For example, the very well respected and often used engineering standard VDI 2230-1 (2015) just says about rules for load plastification and creeping: "Due to the variety of influencing factors it is not possible to lay down any rules of universal validity nor even formulate any equations for evaluating the preload loss due to relaxation". It will be shown, that the losses of preload can be much bigger though. However, this paper will consider all of these processes and give further information to them, all are accompanied with a loss of the preload force. For the measurement of the preload itself, there are numerous methods available (Jenne et al. 2015), the different sources of literature of this paper are using divers methods. An interesting and modern way is the measurement with strain gauges (applied on or in the screw), which is a current research focus of MVP. The main benefits are the realistic and continuous in-situ recording of the forces as well as the unchanged screw system (clamping length). However, other ways of preload measurement like ultrasound (utilizing the duration between sending and receiving a sound wave in a sample, used in Hörnig (2016)), micrometer screw (utilizing the correlations between force, resilience of the screw and the belonging elongation, used in Peth (2021)) or load cell (combinations of strain gauges in a special cell, used for Figure 4) are as well reliable as accepted by professionals.

In this paper, various combinations of longtime measurements will be shown and different systems will be presented. Longtime means a considered time period of t = 1,000 h, the loss of preload will always be compared at this point. The different systems are all existing out of a steel screw and clamping parts made of steel, aluminum or CFRP.

Literature Review

The subject area of bolted joints is a research focus of MVP for many years, especially the loss of preload for different systems and conditions (Jenne et al. 2014, Hörnig 2016, Peth 2021). Regarding this, also different methods for preload measurements are investigated (Jenne et al. 2015). This results in the diagrams below.

Experimental Results

As introduction to this chapter, the abbreviations used below will be explained at first:

- M : metric thread
- T : level of thermal load
- F_{P0} : assembly preload
- D_A : outside diameter of the samples
- d : nominal screw diameter
- l_k : clamping length
- t_e : length of thread engagement
- N : quantity of single experiments

Impact of Different Clamping Materials in Combination with a Thermal Load

The classical, often used bolted joint system is consisting out of a steel screw in combination with steel clamping parts. The calculation rules and standards are elaborated well for this situation. Modern bolted joints are still using steel screws, but the clamping parts are getting substituted apart from steel. But for the estimated preload losses, the material of the clamping part is having an influence. Especially, if an additional thermal load is acting. Figure 2 illustrates the difference between a screw joint using steel and aluminum clamping parts for a longtime period in combination with a thermal load. Therefore, the time t is plotted versus the relative preload F_P/F_{P0}. Generally, the first 48 hours (-48 h until 0 h) of the experiment was conducted by a temperature of T_1 = 20 °C (Room temperature RT). Then the thermal load was increased to the amount of T_2 = 150 °C (120 °C) for the rest of the period. Three curves were recorded, the assembly preload was in all cases F_{P0} = 30 kN.

It can be seen that the steel curve shows a very low loss of preload across the measurement although a higher temperature level was acting. Also the explicit loss of preload can be mentioned for the aluminum systems combined with the increased temperatures. Facing a thermal load of T = 120 °C, the dotted line loses up to 25% of initial preload, even around 52%, when the temperature is increased for another 30 °C to T = 150 °C (triangular markers). This is a problem for many modern bolted joints, because due to the effort of generating light connections as much as possible with clamped parts using light alloys, the loss of preload for often-used bolted joints are very high and need to be considered already in design state. If a thermal load occurs additionally, an aluminum system will lose even more of its initial preload. This means, that the prediction of preload loss must be taken into account of a material and temperature dependency. Thereby, the temperature - caused characteristics between materials like steel und light alloys like aluminum are differing: For metals (steel and aluminum), the beginning of the creeping processes are being stated generally at around a homologous temperature $T_H = T/T_M$ = 0.4. The homologous temperature is the ratio between the temperature of an element and its melting temperature (Kelvin scale), so it is a dimensionless parameter. For steel, the corresponding value is $T_{Creep\ St} \approx 724$ K (450 °C), for aluminum $T_{Creep\ Al} \approx 373$ K (100 °C). This explains the development of the lowest

curve while facing T = 150 °C in Figure 2. Therefore, the first message is that the preload loss of lightweight systems using light alloys is much bigger than the loss for a classical steel system, especially under high thermal loads. Another notable statement is, that bolted joints using steel clamping parts can be used without any problems at increased temperatures like T = 150 °C, because this temperature is much smaller than $T_{Creep\ St}$.

Figure 2. *Impact of the Material of the Clamped Parts and an Additional Thermal Load for the Measuring via Micrometer Screw (The Samples Were Cooled Down to Room Temperature)*

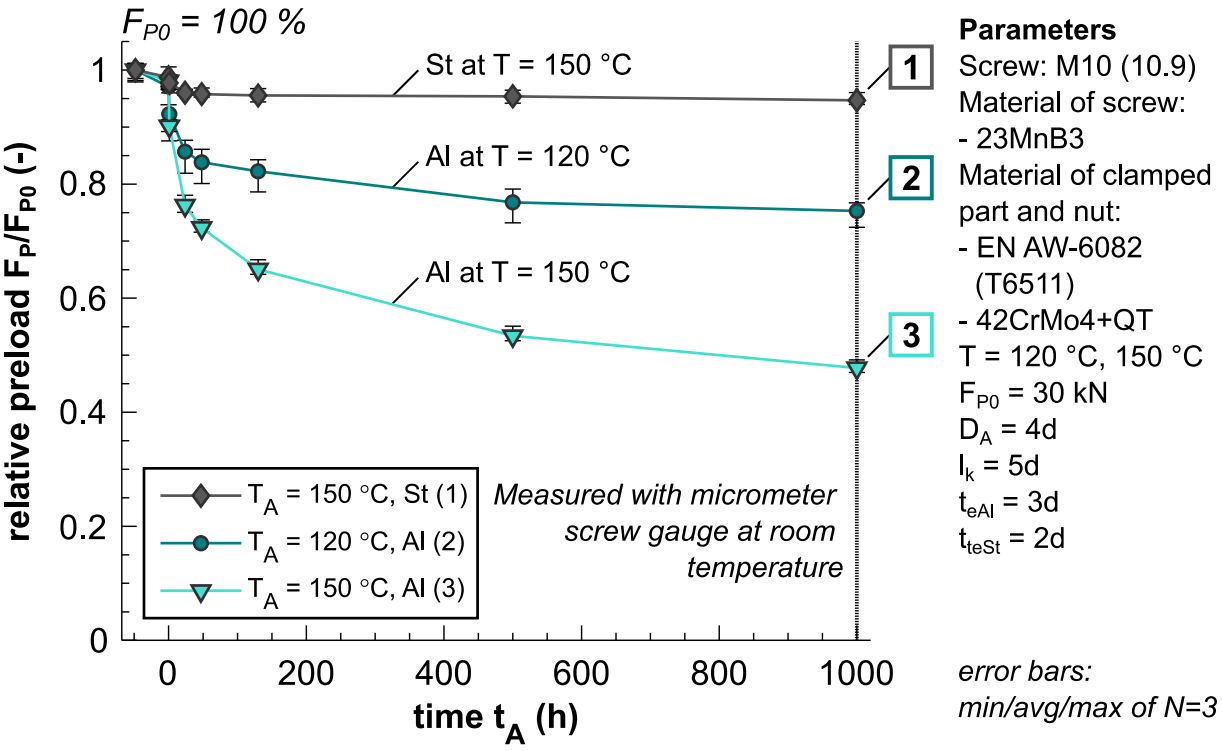

Impact of Different Assembly Preload

Variable assembly preloads can result easily out of the different ways to tighten a bolted joint. In detail, this is described by the tightening factor $\alpha_A = F_{Mmax}/F_{Mmin}$. The bigger α_A, the bigger the difference between minimal (F_{Mmin}) and maximal (F_{Mmax}) assembly preload. Of course it is interesting to use a method, which generates a small value of α_A (like yield-point-controlled tightening, $\alpha_A \approx 1.2$), because the resulting preload is even more precise. An example for an imprecisely method is the torque-controlled tightening ($\alpha_A \approx 1.6$), which is often used in mechanical engineering. Besides this, the value of the assembly preload has an influence on the three mechanisms seating, load plastification and creeping, and with them for the loss of preload, too. This is shown in Figure 3.

Figure 3. *Impact of Different Assembly Preloads for the Measuring via Micrometer Screw (The Samples Were Cooled Down to Room Temperature)*

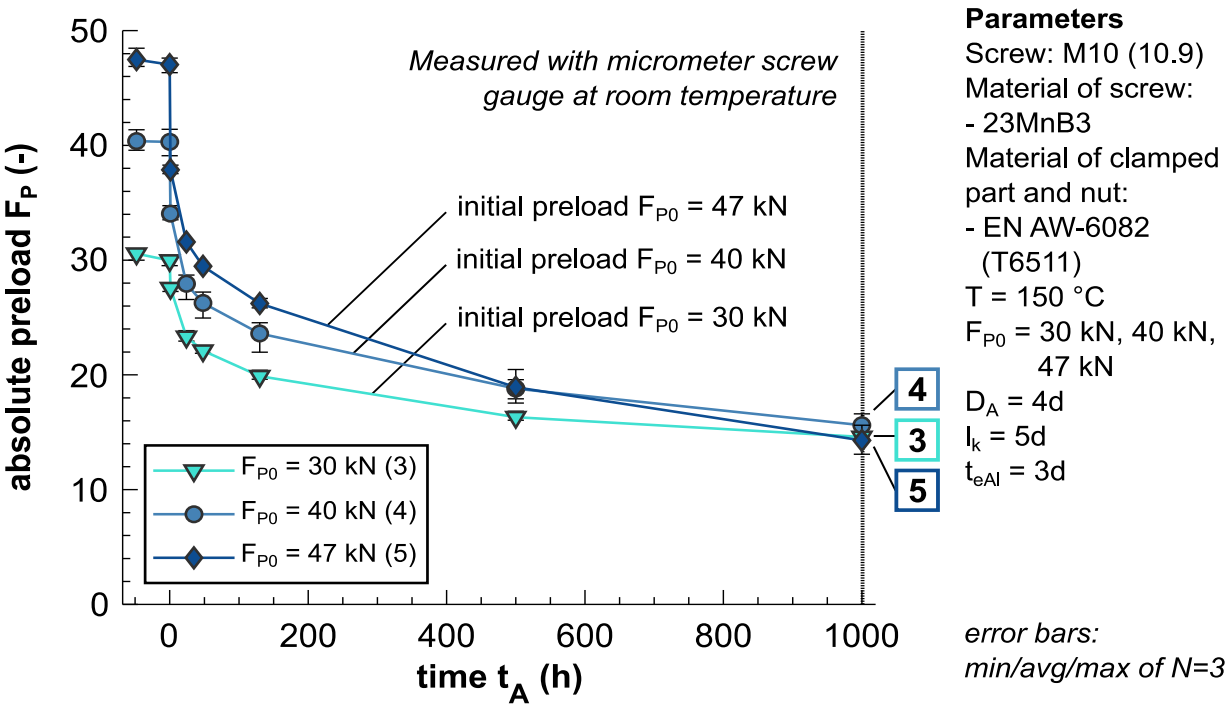

In Figure 3, the preload (scale using absolute, not percentage values) is again plotted versus time, three different curves are shown. The dark blue (light blue, turquoise) belongs to an assembly preload of F_{P0} = 47 kN (40 kN, 30 kN), a thermal load of T = 150 °C was acting in all cases. At the beginning the assembly preload differs, but at exposure of t = 1,000 h deviations are gone. This behavior is typical for systems with large preload loss. So the higher the assembly preload, the higher the loss of it in a period of t = 1,000 h under a thermal load of T = 150 °C. The reason is that the creeping processes are not just depending on the height of the thermal load, but also on the value of the surface pressure. For F_{P0} = 47 kN, this amount is larger than for F_{P0} = 30 kN, the effects are stronger. MVP - research studies have shown that the screw in combination with a high preload level contributes to a preload loss due to load plastification processes (Peth 2021).

At MVP, further experiments were done to examine the influence of different assembly preloads on the processes of preload relaxation. The aspect, which should be investigated, was the behavior of the actual preload, if the level of the thermal load is rising (From T = RT until T = 120 °C) respectively decreasing (From T = 120 °C until T = RT). Therefore, a load cell was used, which enabled the continuous recording of the preloads values. Just like Figure 3, Figure 4 compares different assembly preloads (10 kN, 30 kN, 40 kN & 47 kN) versus time. Similarly to Figure 3, clamping parts and nut were made from aluminum. The profile of the thermal load versus time is stated under the diagram. It must be considered, that the different way of preload measurement affects the result (higher clamp length

by using a load cell), but mainly Figure 4 emphasizes further topics in addition to Figure 3.

Figure 4. *Further Impact of Different Assembly Preloads in Combination with Thermal Load*

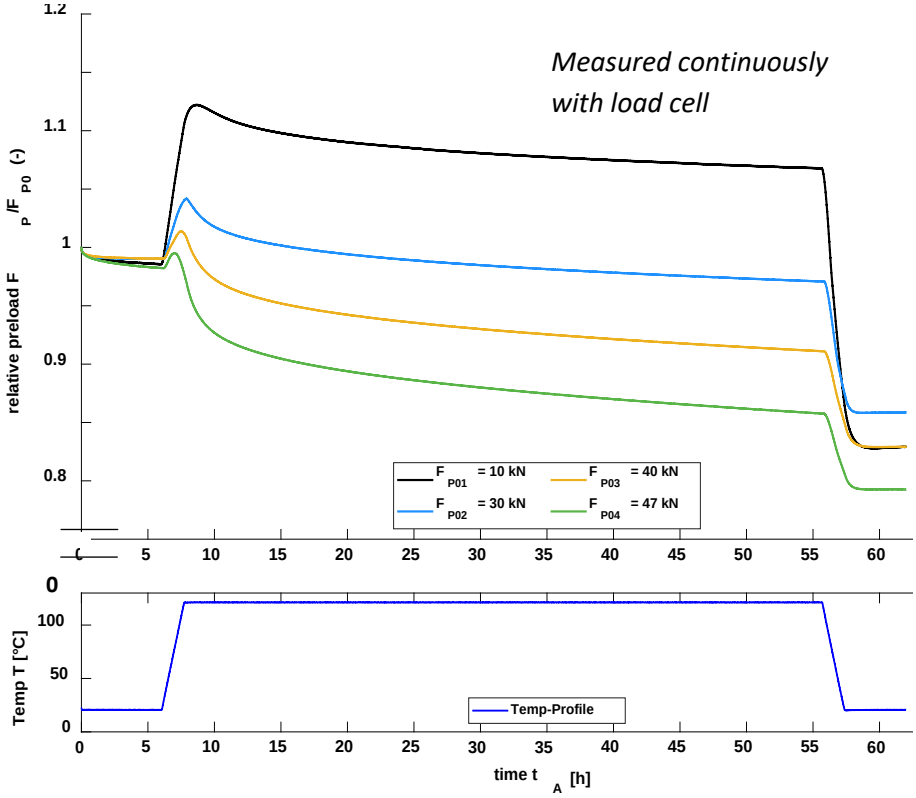

Parameters
Screw: M10 (10.9)
Material of screw:
- 23MnB3
Material of clamped part:
- EN AW-6082 (T6511)
Material of nut:
- EN AW-6082 (T6511)
T = 120 °C
F_{P0} = 10 kN, 30 kN, 40 kN, 47 kN
D_A = 4d
l_k = 7d
t_e = 2d
N = 1

It can be seen that the preload loss due to seating are almost equal for all curves in the first 6 hours since beginning of the measurement. This is caused by the low level of roughness (R_Z = 3 µm). If the temperature increases, the preload of a screw system with a higher amount of F_{P0} will not rise as much as a system with a lower. The reason is that plastification processes are already taking place in the high preloaded screw joint systems. The screw as well as the higher loaded contact surfaces are beginning to yield, which leads to a loss of preload.

Impact of Nut Type and Length of Thread Engagement

In this section it will be shown that the material of the nut as well as the length of thread engagement in combination with aluminum clamping parts has an impact on the expected loss of preload as well. Generally, screw joints can be separated in the two classes tapped thread joints (TTJ) and through-bolt joint (TBJ). Using a TTJ, a threaded hole will be drilled in the lower clamping part, so that the connection will not have an additional nut. Using a TBJ, a classical nut is going to be installed. The general characteristics between these classes are always differing (e.g., different resiliencies between a TTJ and TBJ because of a different clamping

length). You have to consider, that a TTJ can be tightened in the most cases only on the side of the screw head. For lightweight applications, the facility of TTJ's is very interesting, because it reduces the nut at of bolted joint. Considering a car for example, several hundred individual screw connections are assembled, the use of TTJ's will lead to weight reduction which is desirable. Figure 5 shows a comparison of screw systems using steel and aluminum nuts, partly with higher length of thread engagement, facing an increased thermal load of T = 150 °C:

Figure 5. *Impact of the Nut Type and Length of Thread Engagement for the Measuring via Micrometer Screw (The Samples were cooled Down to Room Temperature)*

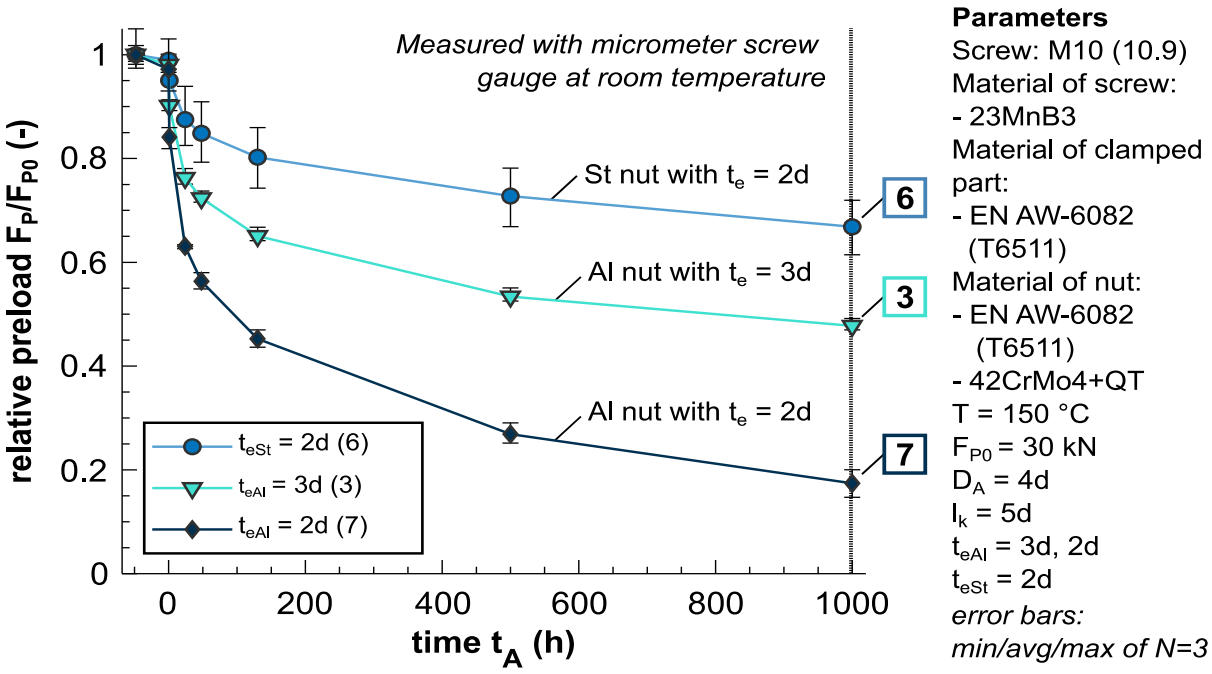

In Figure 5, the relative preload (percentage scale) is plotted versus time, this scheme was already used at Figures 2 and 4. All experiments were done with aluminum clamped parts. The first thing, which can be seen, is the lowest loss of preload (≈ 30%) by using a steel nut (length of thread engagement: 2•d). For the same parameters, just using an aluminum nut, the preload loss is significantly higher (around 80%), so that the function of the connection will be clearly not given further. By increasing the length of thread engagement to t_e = 3•d, the loss is decreasing, but it is even reaching around 50% of the assembly preload. The reason for the high losses are not just creeping processes, a damaging of the aluminum nut can occur as well. If the length of thread engagement is being reduced, the acting preload is dividing to a smaller area in the nut thread, which leads to a rise of specific stress in the thread. If the stress is getting to high or/and a higher thermal load applies additionally, a damage case and with it a loss of preload can happen.

Impact of Clamped Materials Made of CRFP

Additional to the mentioned aluminum systems above, further information about the preload loss of another modern systems will be given at this point. CFRP (short for Carbon Fiber Reinforced Plastic) clamped parts are very interesting for modern future lightweight applications. In comparison to aluminum for example, the density is about 33% lower (Al: 2700 kg/m³ - CFRP: ≈ 1500 - 1800 kg/m³), which enables to design even lighter components. Basically, CFRP are providing complete different material attributes compared to steel or aluminum based materials, so these attributes have to be investigated carefully. Generally, the common aspect from all CFRP-types is the combination of carbon fibers, which are embedded in a synthetic plastic matrix. Due to the impact of heat and pressure, these two components are getting merged together to a very light and stiff material. The plastic matrix can and should be designed for the desired use case. Today´s prices for CFRP are still comparatively high, but they will become cheaper in future because of new and enhanced ways of manufacturing. Like every material, there are as well cheaper and more expensive types of CFRP. The version "EP (Epoxy Resin - Matrix)" is an example for a low cost CFRP. On the other hand, an example for an expensive type of CFRP, is the CFRP "PEEK (Polyether Ketone, a thermoplastic material)", which can be rather used by higher thermal loads (look at the following diagram). A notable attribute of every CFRP is the anisotropic character of their material constants. The Young's modulus for example is around 140 GPa parallel to the carbon fibers, but rectangular to them only at around 12 GPa. The different types of CFRP, to be more precise their matrices, are providing an influence on the estimated loss of preload, too. Especially, if an increased thermal load is acting. The following Figure 6 shows the different behavior of bolted joints, which are clamped with several materials, considered for a period of t = 1,000 hours. Information about clamping aluminum types were given above, Figure 6 claims additionally further information about using aluminum and magnesium clamping parts. The interesting statement here are the curves for the two different CFRP types "PEEK" and "EP". In that, three single curves from three individual experiments are bundled to one common line (arithmetic mean), which are plotted versus time (here we need to consider, that the X-Axis is not subdivided in a linear time-scale like all other diagrams). The colored and numbered boxes were added additionally. The illustrated Al-curves do not belong to the ones shown above.

Figure 6. *Impact of Different CFRP-Materials in a Bolted Joint (acc. to Hubbertz (2020)) (The Colored and Numbered Boxes Were Added Additionally)*

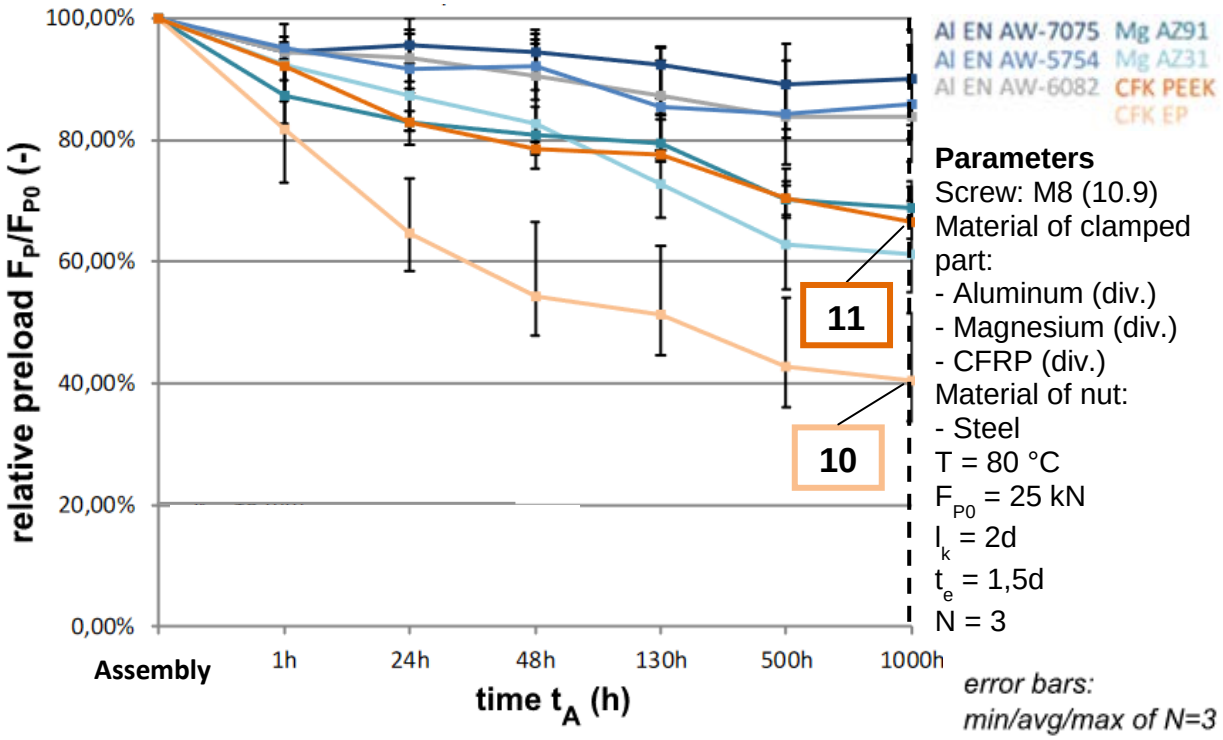

A thermal load (T = 80°C) was additionally acting. Figure 6 illustrates, that the individual kind of CFRP is having a unique behavior of losing preload while facing a thermal load. While the PEEK-Matrix-CFRP loses a smaller amount of preload during the time of exposure, the CFRP with EP-Matrix loses a higher percentage value already directly after assembly. The reason is the matrix itself, in which the carbon fibers are embedded. For increased temperatures, the EP is getting softer, the material is getting more and more rubber-like. However, this can be described by the "glass transition temperature" (Hubbertz 2020). In contrast, the PEEK-Matrix stays harder, so the PEEK-CFRP is rather useful by higher temperature levels instead of the EP-CFRP. Summarized, using PEEK-Matrix-CFRP the preload of the screw rather sustains, and with it the function of the connection.

Impact of Thread Inserts

The function of every screw joint is achieved by a thread engagement between screw and nut. The thread can be part of a nut as well as a part of the clamping components (TTJ or TBJ, mentioned above). The lightweight design approach in modern mechanical engineering requires the development of components, which are not only light weighted, but also efficient. It has to be ensured that the weight reduction of a part (e.g., due to lowering of wall thickness) does not affect the

function of the component. This explains the growing commitment of (heat-treated) aluminum alloys in many sectors. On one hand, the material constants of aluminum (e.g., the tensile strength) are clearly lower as values corresponding to steel, on other hand, the occurring loads are increasing more and more, so screws with even higher strength classes are chosen for the design process. Because of the (often reduced) values of the wall thickness and the substitution from steel to aluminum, the thread engagement of the screw system is not as sustainable as in the classical cases. Problems can occur regarding the necessary length of thread engagement, which leads to general problems for the functioning connection. Only deep enough assembled screws are enabled to guarantee the function. To correct this, thread inserts can be used: the screw is assembled in this insert, the insert again gets assembled in the clamping part. This is called a "multiple thread engagement" (MTE), a benefit for modern lightweight constructions is given (Hörnig 2016). Furthermore, these multiple thread engagements are having a positive impact on the loss of preload for general screw joint systems over time as well. It can be shown, that this loss over an estimated time of t = 1,000 h in combination with an additional temperature load of T = 100 °C is significant lower during the use of MTE instead of STE, especially, when the length of thread engagement is increased from 1•d to 2•d. Figure 7 shows this.

Figure 7. *Difference between Single Resp. Multiple Thread Engagement (acc. to [2]) (The Colored and Numbered Boxes Were Added Additionally)*

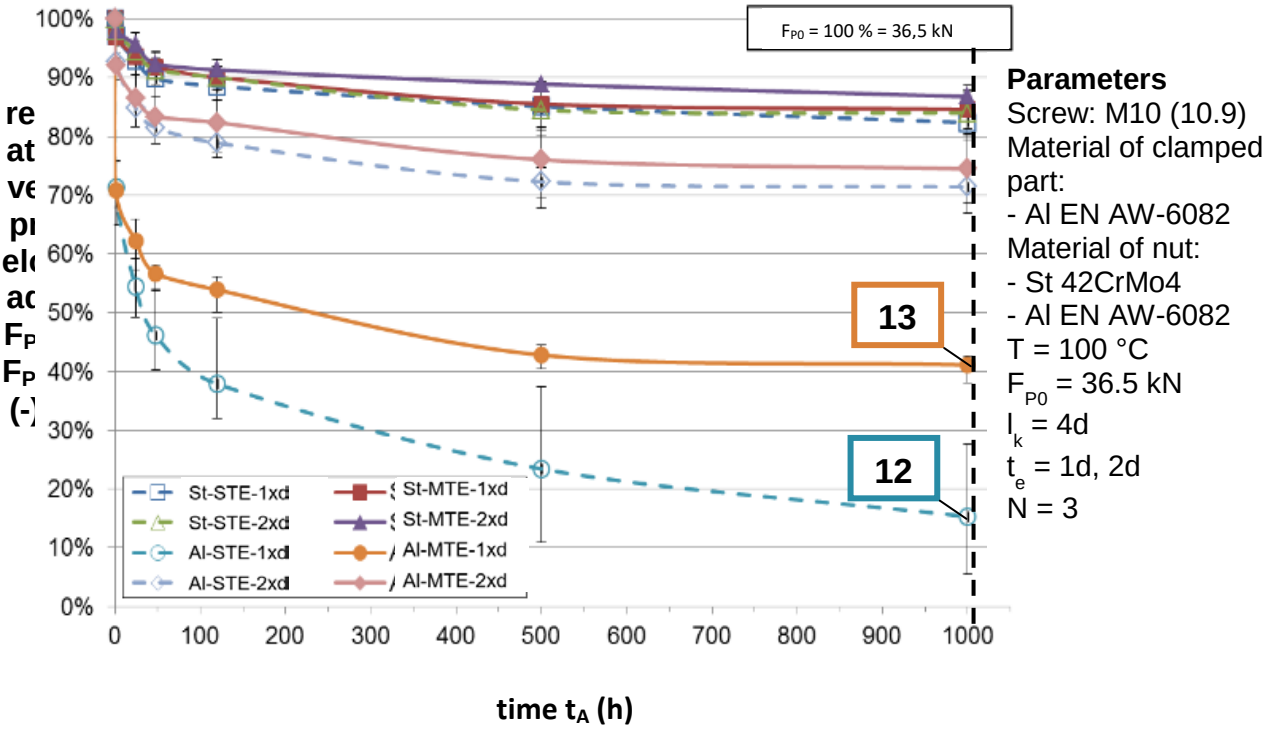

In Figure 7, the relative preload is plotted versus time. Curves for two thread types are shown: first, the screw is assembled directly into the clamping part

(STE), second, the screw is combined with a thread insert made of steel (MTE), which again is assembled in the clamping part. Besides, the length of thread engagement (clamping part material) is variated between 1•d and 2•d (St 42CrMo4 and Al EN AW-6082), so that 8 graphs are demonstrated overall. Now, this figure mainly points out the following aspects:

1. By comparing to STE, the use of MTE leads to a lower loss of preload during the time of t = 1,000 h. This is the case as well for inserts combined with aluminum and steel based materials. All curves for MGE are exceeding the corresponding curves for STE.
2. The length of thread engagement of the screws in the inserts is having a big influence on the estimated preload loss as well: The deeper the screws are assembled, the lower the influence on the following measured preload loss. The reason is that the acting preload can distribute on a larger area, the specific mechanical stress is lower.
3. In comparison to steel systems, aluminum screw systems are far more vulnerable for preload losses. The usage of MTE can partly mitigate the preload loss.

The points 2. and 3. were already shown in the upper chapters. Summarized, the use of thread inserts in combination with a higher length of thread engagement is a good possibility to reduce the estimated losses of preload, even when longer time periods are favored or an additional thermal load is acting. This is an important point for modern lightweight design (LWD) shown by the impacts above.

Conclusion

Finally, the illustrated and described systems and their unique values of preload loss will be compared in a percentage way with the help of a bar graph, look at Figure 8. Additionally, a calculation of the estimated loss for a classical Steel system at room temperature (seating losses F_Z) according to VDI 2230 was conducted (black bar, left). Directly aside, the result of the measured preload loss for the identical system is stated (grey bar).

Figure 8. *Comparison of the Illustrated Mechanisms*

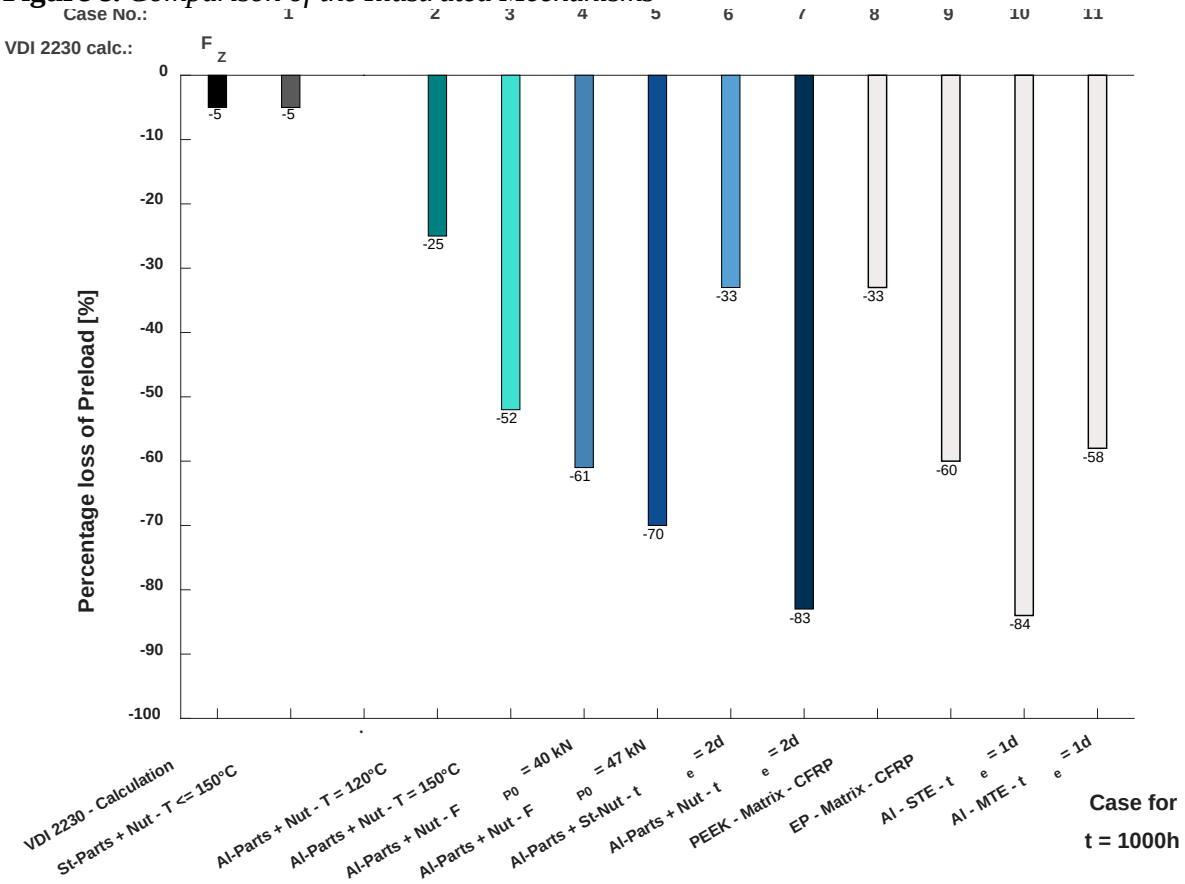

Due to Figure 8, several aspects can be identified: It can be seen, that the temperature influence is determining the preload loss, especially in combination with aluminum parts (or LWD materials). In contrast, components made of steel are not as problematic for those aspects. The homologous temperature for steel materials in relation to creeping processes (724 K ≙ 450 °C) is not being reached. In this case, the calculation for the estimated loss of preload according to VDI 2230-1 (2015) caused by seating (F_Z) is equal to the measured value. Eminently high losses could be expected while clamping aluminum parts with STE and low length of thread engagement, EP-Matrix-CFRP or aluminum parts with an aluminum nut with an increased assembly preload, all in combination with a thermal load. However, a comparing statement is possible though.

Generally, bolted joints need a stable level of preload during the entire life cycle. There are three meaningful mechanisms, which are leading to a decrease of preload (seating, load plastification, creeping processes). In fact, there are numerous literatures of rules and standards, which engineers can try to use for the design of a bolted joint, but these are mainly focusing on the assembly process. Equations for the preload loss due to seating processes are provided, further terms for the estimation of losses due to load plastification or creeping are missing though. So the sum of the preload loss is excelling VDI 2230-1 (2015) clearly. An important

point is that today's material combinations apart from steel do not play an adequate role in guidelines. An adaption is consequently necessary.

In this paper, with the help of different screw systems it was analyzed, that the longtime loss of preload could be meaningful higher, as the established guidelines are supposing. This is especially the case for an aluminum system. The belonging systems and the individual influencing factors were shown and compared, always for a longtime measurement of t = 1,000 h. Another focus of this paper were configurations using modern CFRP clamping parts. It was illustrated, that the preload loss of those systems is different for each type of CFRP. Useful methods against a strongly loss of preload are named, e.g., the use of multiple instead of single thread engagement or increasing the length of thread engagement.

Summarized, the following statements can be conducted to findings in this paper:

1) The real preload loss of preload is significantly higher than the established guidelines are predicting. These are mainly focusing on seating processes in combination with steel systems. They need to be revised and should be extended. Equations for the loss mechanisms load plastification and creeping need to be developed. While doing so, further and modern materials like aluminum, magnesium or CFRP have to be considered.
2) The main influence for preload loss is thermal load, especially if lightweight materials with temperature-sensitivity and low strength compared to steel are used. Also to consider is the additional preload loss when cooling down after exposure (see Figure 4).
3) Another important influence is the length of the thread engagement. The higher its number, the lower the preload loss. For aluminum in combination with a thermal load, the preload losses are increasing from $t_e = 3 \cdot d$ to $2 \cdot d$ from 52% to 83%. In contrast, the identical steel system losses just 33% of its initial preload ($t_e = 2 \cdot d$). Multiple-thread-engagements are an interesting method for design of applications with reduced preload loss.

Finally, as an outlook to the ongoing work an extension of guidelines has to be mentioned (important for reliable and fast product development). This has also to include investigations on typical roughness situations.

References

Guggolz D (2019) *Auslegungsprozess zur Absicherung des selbsttätigen Losdrehverhaltens von Schraubenverbindungen in realen Bauteilsystemen.* (Design process for validating the self-loosening behavior of bolted joints in real component systems). Aachen: Shaker Publishing Company.

Hörnig T (2016) *Beitrag zur Tragfähigkeit des Gewindeeingriffs bei Schraubenverbindungen im Leichtbau*. (Contribution to the load-bearing capacity of the thread engagement in lightweight bolted joints). Aachen: Shaker Publishing Company.

Hubbertz H (2020) Beitrag zur Auslegungsrechnung von Leichtbauschraubenverbindungen im Hinblick auf die Vorspannkraftrelaxation. (Contribution to design calculation of

lightweight bolted joints with regard to preload relaxation). Siegen: Universi Publishing Company.

Hubbertz H, Friedrich C (2013) Relaxation of clamp force in fastened carbon composite structures with thermal load. In *International Conference on Composites Engineering ICCE-21*. Santa Cruz de Tenerife, 21.07.2013. - 27.03.2013.

Jenne M, Hubbertz H, Friedrich C, Bär C (2015) Improved mechanical preload measurement of bolted joints for lightweight design with CFRP components. In *ASME International Mechanical Engineering Congress and Exposition*. Houston, 13.11.2015 - 19.11.2015.

Peth J (2021) *Einflüsse auf das Vorspannkraftrelaxationsverhalten von Schraubenverbindungen im Leichtbau*. (Influences on preload relaxation behaviour of bolted joint connections in lightweight constructions). PhD Thesis in Progress at MVP. Siegen.

Peth J, Friedrich C (2018) Design Influences of preload relaxation behavior in bolted joints using aluminium parts. In *Recent Developments Conference Integrity - Reliability - Failure*. Lisbon, 22.07.2018 - 26.07.2018.

VDI 2230-1 (2015) *Systematic calculation of highly stressed bolted joints - Joints with one cylindrical bolt*. Berlin: Beuth.

Athens Journal of Technology and Engineering - Volume 9, Issue 3, September 2022 – Pages 213-266

The Interaction of Wind Velocity and Air Gap Width on the Thermal Comfort in Naturally Ventilated Buildings with Multiple Skin Facade

By Enes Yasa[*]

A Multiple (MSF) or Double Skin Facade (DSF) is a building envelope system. It has an external and internal layer that contains buffer space used for controlled windy conditions, ventilation and solar protection. Employing a multiple or double-skin facade for natural ventilation is not an innovative idea, but the background on this mechanism and the impacts of these environmental and designing factors on its performance are still unknown and critically needed. Therefore, with this study, the influences of the Multiple or Double Skin Facade with different width air gaps configurations, alongside the environmental factor on buoyant-driven natural ventilation, are discussed. Naturally ventilated MSFs are often very intriguing in terms of a microclimatic comfort, but an optimum design is crucial to enhance the microclimatic comfort and therefore the proper operation of the entire system. Especially, the development of the system is important when working in a hot climate. There is a significant lack of data within the current literature to demonstrate the complexity and challenges in designing large, naturally ventilated buildings. For these sorts of buildings, it is important to possess the tools to gauge a design's predicted performance to realize successful natural ventilation concepts. However, with the utilization of glass, heat loss during the winter and solar gain during the summer will increase energy loads. At the same time, this will also negatively effect the microclimatic comfort. Through this study, both the effect of the utilization of multiple facades on indoor comfort conditions and thus the effects of distances at different distances from the facade on wind flow and therefore microclimatic comfort at the situation of the Multiple Skin Facades were investigated. This paper demonstrates through a sensitivity analysis, an optimal strategy for completing a CFD simulation of this special building envelope. This study also attempts to research a mechanically ventilated building with DSF configuration—a building in terms of indoor microclimatic thermal comfort. The aim of this study is to work out the effect of wind velocity and wind distribution on naturally ventilated buildings with DSF configuration, to work out if a DSF configuration will provide a far better microclimatic thermal comfort through natural ventilation. This study not only defines and analyzes the dimensional parameters of the air gap to maximize airflows, but also explores the importance of design decisions on system performance, such as the interaction between thermal mass and air gap distances and the building facade.

Keywords: *double skin facade, microclimatic thermal performance, airflow modelling, indoor microclimatic thermal comfort, wind velocity, wind distribution, CFD, natural ventilation performance simulation*

Introduction

A Multiple (MSF) or Double Skin Facade (DSF) are architectural design elements that have increased in popularity in modern building design. They need to be improved as an alternate technology to enhance the microclimatic thermal

[*]Associate Professor, Istanbul University, Turkey.

performance of conventional fully glazed buildings. They also need to be widely used as a solution to scale back the microclimatic thermal instability of inner spaces caused by the growing use of huge glazed areas in buildings. This idea has provided the likelihood of improved sound insulation, pre-heating air for ventilation, and protection from solar shading in urban areas. DSF's can lead to a reduction of winter heating requirements. The building facade plays a crucial role in achieving the microclimatic thermal comfort and energy conservation. A DSF is an envelope system, which has an external and internal layer that contains a buffer space used for controlled ventilation and solar protection.

With the advantages of technological advances, transparency and therefore the use of glass has become a beautiful facade option in architectural design. Building glass facades can provide outdoor views and excellent levels of natural light also because of the potential for natural ventilation. Ventilated facades are already a standard feature of architectural competitions in Europe, but there are still relatively few buildings of which have actually been realized; there is still insufficient experience of their behaviour to be operational. For this reason the CFD analysis might be one among the foremost important tools to predict the behaviour of DSF and help architects make decisions during the planning process (Gratia and De Herde 2007, Ballestini et al. 2007, Zöllner et al. 2002).

The ventilated double skin facade differs from traditional double and triple glazed facades and is characterized by the passage of air through the air gap air space between the inner and outer glass. The movement of air is a crucial departure from more standard glazing systems like double and triple glazed insulating units. Microclimatic thermal mechanisms and its effects on energy and comfort are different. Air flows through it, altering its performance characteristics and dominating from time to time (Lamcour et al. 2012). A ventilated double-skin facade is often defined as a standard single facade that doubles inside or outside with a second, essentially glazed facade. Between these two surfaces there is a ventilated air gap with to a depth of up to about 10 cm from the narrowest place and up to 2 m at the deepest accessible spaces. Air gaps are usually ventilated with natural, mechanical or hybrid ventilation (Waldner et al. 2007). The double skin facade is ventilated with outside air and allows outside air to be ventilated through open windows without causing any disturbance, even in high-rise buildings (Roelofsen, 2002).

In recent years, new building envelope systems are developed so as to enhance microclimatic thermal insulation, to shade solar radiation and to supply appropriate microclimatic thermal and visual comfort conditions. One among these special sorts of envelopes is DSF. DSF are made with two layers of glass separated by a large amount of air space. The space between the glass are often ventilated with three different strategies: mechanical ventilation, natural ventilation or hybrid. The ventilation of the air space between two facade contributes to saving energy both during the summer and therefore the winter time. In fact, in winter, the air between the glass is heated by the sun rays (greenhouse effect) (Gratia and De Herde 2007). Thereby, it provides a reduction in heating costs by improving the microclimatic thermal performance of the facade. In hybrid ventilation systems, fresh air is usually preheated within the

MSF space before entering the HVAC system during the winter months. In summer, air flow from MSF (mechanical or natural) can help lower the temperature inside the cavity. However, when the building is in summer conditions or located in temperate or hot climates, heat gains dominate and thus cooling costs becomes a serious problem.

In the literature there are several examples of using CFD to examine the behavior, characteristics, and energy consumption and comfort status of a DSF (Pappas and Zhai 2008, Safer et al. 2005, Ye et al. 1999). Studies on DSF microclimatic thermal comfort are mostly limited to colder and warmer climatic conditions (Alberto et al. 2017, Chow et al. 2009, Khalvati and Omidvar 2019, Yang et al. 2020, Saroglou et al. 2020, Guardo et al. 2009). However, the use of multiple or double skin facades in hot summer continental climates is not well documented. Additionally, while numerous articles explain how DSFs should improve the microclimatic thermal comfort of a building through principles and ideas, they do not provide calculated or experimental results. Other researchers provided simulation models to specific MSF or DSF typologies, but did not link the facade results level to the microclimatic thermal comfort of the building or link the model to a building energy and comfort model simulation. The significant lack of information that explains the complexity and challenges of designing large, naturally ventilated buildings with MSF or DSF as a means for energy saving with better microclimatic thermal comfort has been addressed in the literature review.

In recent years, the use of multilayer facades has been widely adopted in the design of modern buildings, and the use of more advanced multilayer facades has been investigated, especially for energy savings. However, even if the energy performance side is improved, there is a great need for additional mechanical air conditioners in terms of indoor microclimatic comfort conditions (Gosselin and Chen 2008, Inan et al. 2016, Inan et al. 2017, Ioannidis et al. 2020). Many studies have explored the potential of combining natural ventilation with multiple facades. However, the mechanism behind natural ventilation throughout the facade is still unclear (Inan et al. 2017, Ioannidis et al. 2020). Understanding their optimum designs and the mechanism behind them is critically necessary to broaden relevant studies. In addition, many studies of multiple or double skin facades have ignored the effects of connecting rooms or attached windows, which can lead to overestimation in practical designs (Dama et al. 2017, Wang and Lei 2020). Studying the air flow in the air gap is a major challenge due to the two unique glass facades under combined solar radiation and natural convection in multiple or double skin facades (Souza et al. 2018, Barbosa and Ip 2014, Agathokleous and Kalogirou 2016).

Also, due to some unknown circumstances, previous studies on multiple or double skin facades specifically failed to address the airflow within the inner space (MSF) (DSF) (De Gracia et al. 2013). An accurate CFD study is important to benefit practical applications by allowing the air flow rate to be calculated for natural ventilation in a ventilated air gap, and then unravel the flow details in multiple or dual design (Wang et al. 2019, Nasrollahi and Salehi 2015, Baldinelli 2019). Therefore, an investigation of natural ventilation through different multiple or double skin facades design parameters was administered. This study addressed

the influences of facades and connected rooms configurations alongside the environmental factor of the buoyancy-driven natural ventilation from multiple or double skin facades. The air change rate per hour (ACH) by natural ventilation was addressed over different multiple or double skin facades configuration (Baldinelli 2019).

The Main Objective of this Research

This research presents the foundation of a methodology for modeling natural ventilation airflow in buildings with multiple skin facades to better understand the effect of the shaft air gap and air gap width on the building comfort design and energy performance. This research also investigates the viability of combined shaft-air gap MSF or DSF designs to provide natural ventilation as an energy-efficient solution by means of numerical simulations using CFD coupled with dynamic energy-simulation tools. Actual measured data of the building‘s energy performance based on a full-scale model is not in the scope of this study.

Therefore, the base case is essentially a simulated base case and is not calibrated with an actual model. The simulated combined shaft-air gap strategy is compared with the simulated base case. In addition, the issue of condensation of the facade system has not been taken into account. As there is no exact method of local comfort measurements, the predicted-mean vote was used to evaluate the comfort performance.

The significant lack of information describing the complexity and challenges of designing large, naturally ventilated buildings with DSF as a means to save energy with better microclimatic thermal comfort is addressed in the literature review. Some of these are:

- To determine the effect of difference in convection coefficient on building surfaces.
- To determine if a DSF configuration will provide a better microclimatic thermal comfort through assisted natural ventilation.
- The building interior boundary conditions will use ASHRAE 62.1 and ASHRAE 90.1 specified conditions.
- A methodology for assessing the performance of naturally ventilated DSF buildings through an airflow model will be developed by three-dimensional analysis using CFD.
- Buoyancy, wind, and combined ventilation strategies for a building with operable openings DSF will be evaluated using the turbulence models in the CFD.

The primary goal of this study is to clarify the state-of-the-art performance of buildings with multiple or double skin facades, so that designers can assess the value of these building concepts in meeting design goals for especially microclimatic comfort conditions, ventilation, productivity, and sustainability. Another aim of this study is to investigate the effect of wind velocity and wind distribution on naturally ventilated buildings with multiple or double skin facade

configuration, to determine if a DSF configuration will provide a better microclimatic comfort through natural ventilation in terms of microclimatic comfort. Also, the influences of the double skin facade with different width air gaps configurations, together with the environmental factor on buoyant-driven natural ventilation, are addressed.

Literature Review

Function of Cavities on Multiple or Double Skin Facades

The double skin facade air gap is a space between the exterior and interior glazing. The air gap of a double-skin facade can be airtight or ventilated. An airtight air gap acts as a buffer zone that is often used to maintain indoor temperature in winter. Ventilated air gaps refer to an air gap with an opening in the lower and upper air gap of a double skin facade. It is generally used in summer, where fresh air from outside is given from the lower air gap and ventilated along the upper air gap. This ventilation system takes advantage of a stack effect that allows the air gap air to flow through the upper air gap. The pressure difference between the lower and upper aisle can be used if the wind speed is sufficient, possibly allowing the air to circulate in the air gap. Both methods' stack effect and pressure difference could beneficially reduce the warmth in a double skin facade. The double skin facade air gap can be naturally, mechanically and hybridly ventilated. The depth of the air gap can vary from 10 cm to more than 2.40 m depending on the concept applied. The depth effects the physical properties of the facade and the way the facade is preserved (Waldner et al. 2012, Streicher 2005).

Multiple or double skin facades are generally designed for different operations in summer and winter conditions. During the summer months, MSFs usually operate in "on" mode. This means that vents are made above and below the facade air gap. The air in the air gap removes the excess heat thanks to the convective flow created by the stack effect. This action prevents excessive heat build-up in spaces in an air gap. If this happens, unwanted heat can pass indoors. This can have a significant impact on microclimatic thermal comfort conditions inside the building which creates a greater need for the use of auxiliary cooling systems, thus causing an increase in energy consumption. When the air in the air gap is cleaned, the temperature of the building facade is lowered and the heat transfer from the interior surface to the occupied area is reduced. Accordingly, less heat is transferred from the outside to the inside and less energy is required to cool the space. The widespread use of DSF in winter is used as a closed air gap with no air circulation. For the winter scenario, the DSF air gap is warmer than the outside temperature. As the air in the air gap is heated by the sun, the temperature of the facade increases and the temperature difference across the facade decreases. Accordingly, given a low temperature difference between the interior conditioned area and the adjacent microclimatic thermal zone, less heat is transferred from the inside of the building to the outside. Therefore, Ssignificantly less energy is required to heat the space (Mulyadi 2012).

The air gap allows the air to be circulated through the double-skin air gap. The lower air gap is the air inlet and the upper air gap is the air outlet. The choice of panel type, shading device, air gap geometry and the type, size and location of the air gap openings and ventilation strategy are crucial to the performance of a double-skin facade system (Yoon et al. 2012). When designing a double-skin facade, it is important to determine the type, size and location of the air gap, as these parameters affect the type of air flow and air velocity and therefore the temperatures in the air gap (more important in tall buildings) (Streicher 2005, Mulyadi 2012).

The Physics of Double-Skin Facades

Some research has been done on the microclimatic thermal performance of the double skin facade. Chan et al. (2009) investigated the performance of a double-skin facade in Hong Kong compared to a traditional single-skin facade with absorbent glass. Additionally, by comparing double-skinned and single-skinned facades in a hot and arid climate, Hamza (2008) found that a double-skin facade with reflective glass could provide better energy savings than a single-skin facade with reflective glass. Xu and Yang (2008) investigated the microclimatic thermal performance of a double-skin facade using natural ventilation and solar control louvers. Hien et al. (2005) discovered that a double-skin facade with natural ventilation can reduce energy consumption and improve microclimatic thermal comfort. Kato et al. (2008) examined the effectiveness of the double-skin facade in reducing the cooling load by combining it with the ground-to-air heat exchanger. Moreover, Yoon et al. (2012) proposed the technique of estimating the performance of the double skin facade during the cooling season. In general, the double-skin facade acts as a microclimatic thermal buffer in front of offices. This has two microclimatic thermal effects for offices (Mulyadi 2012, Barták et al. 2001):

1. The air temperature in the double skin facade will often be higher than outside. This will result in lower conductive heat losses (heating season) and higher conductive heat gains (summer) depending on ambient temperatures and solar radiation levels.
2. The extra outside facade glass of the double skin facade will effectively reduce the amount of solar radiation on the interior, thus reducing the solar radiation load of the offices due to the radiation transmission through the windows (Mulyadi 2012, Barták et al. 2001).

Airflows Around Multiple or Double-Skin Facades

Wind causes variable surface pressures in buildings that alter intake and exhaust system flow rates, natural ventilation, in and exfiltration and internal pressures. The average flow patterns and turbulence of wind passing over a building can recirculate exhaust gases to air intakes. Air flow around buildings consists of natural winds that flow around and possibly through buildings. Air

flow around buildings has two effects on building ventilation (Goodfellow and Tahti 2001):

1. Wind pressures applied to exterior building surfaces can affect indoor air movement.
2. The movement of air pollutants outside, which can reduce indoor air quality if brought indoors with insufficient dilution.

The buildings are immersed in an atmospheric boundary layer where the wind is affected by friction with the earth's surface. In this layer of the building envelope, wind speed tends to increase gradually with height and decreases as turbulence levels rise. The surrounding buildings, terrain, and vegetation strongly affect wind and turbulence at a construction site. Wind and turbulence levels are also affected by the microclimatic thermal stratification of the atmosphere, as are the inversion layers at ground level. The major parameters of the wind at a building site depend on the Reynolds (R_e), Karman (K_a), and Richardson (R_i) dimensionless characteristics (Goodfellow and Tahti 2001):

$$R_e=Vl/v\ K_a = J\ [\ (V7)2/V\ R_i = gl/p\ (dp/dZ)\ /\ (d\ V/dZ)\ 2,\ (7.227) \qquad (1)$$

Where Vl/v = building characteristic dimension (height or width), v = kinematic viscosity, V' = velocity fluctuation, V mean velocity, p = air density, dp/dZ = vertical density gradient, and dV/dZ = vertical velocity gradient. Winds traveling past a building will be greatly modified compared with winds in the absence of the building.

The Physics of Airflows within the Multiple or Double Skin Facade Cavities

The main parameter that promotes air movement within the ventilated spaces is pressure differential. This is due to microclimatic thermal buoyancy, the movement of wind around the building, or mechanical action. Multiple or double skin facades (DSFs) accelerate the air movement in the air gap as a result of the greenhouse effect between the building envelope between the two facades, the heated air density decreases and the buoyancy force creates a clump effect and raises the hot air to the upper part by forcing the cold air to enter from the bottom. However, the temperature difference (ΔT) between the inside and outside of the air gap also causes air movement inside the air gap. In this case, the pressure is high at the bottom of the facade and low at the top, creating a reverse flow towards the inlet. The microclimatic thermal uplift (th Δp) inside the facade air gap is explained by the following equation:

$$\Delta pth = \Delta\rho'.\ g\ .\Delta h{\cdot}\Delta Tm\ [Pa] \qquad (2)$$

where:

$\Delta\rho\ '$ = Specific change of air density in relation with temperature change ($kg/m^3{}^\circ K$).

g = Gravitational acceleration ($9{,}81 m/s^2$).

Δh = Effective difference of height of the facade air gap (m).
m ΔT = Mean excess temperature (°K)
The specific change of density (Δρ ′) is derived from the law of gases to the following formula:

$$\Delta\rho' = \frac{\rho}{T_{ab}} \quad = [0.004\ kg/m^3°K] \qquad (3)$$

And the absolute temperature (ab T) is can be explained by:

$$T_{ab} = T_{zu} + \Delta T_m + 273{,}15 \qquad [°K] \quad (4)$$

The wind outside of the facade also has an influence on the airflow inside the air gap of between facade, the pressure created by pressure difference inside the facade and outside is known as “stagnation pressure” (q), which is expressed as:

$$q = \frac{\rho}{2} v^2 \qquad [Pa] \quad (5)$$

where:
ρ = Density of air (kg/m³)
v = Outside air velocity (m/s)

The pressure of the exterior wind (wind p) is given by the specific wind pressure coefficients (cp) which depend on the facade orientation. The values of these coefficients are positive on the pressure zones facing the wind and negative on the suction zones towards the wind direction. The pressure is expressed by the following formula:

$p_{wind} = cp \cdot q \qquad [Pa] \quad (6)$

According to Osterle et al., “the pressure differences between upper and lower openings are regarded as forces acting on the areas of the openings, whereby the motive force is the product of the pressure difference taken in conjunction with the opening area.” This is known as pressure loss (loss Δp), which is formulated as:

$\Delta p = \zeta . Q \qquad [Pa] \quad (7)$

The balance of the volume of air admitted at the inlet (in V) is equivalent to the amount of air leaving the air gap through the outlet (out V), known as the continuity equation, which is expressed basically by:

$$\dot{V}_{in} = \dot{V}_{out} \quad \text{or} \quad A_{in} \cdot v_{in} = A_{out} \cdot v_{out} \qquad [m^3] \quad (8)$$

where:
V = Airflow volume (m³)
A = Opening area (m²)

v = Air velocity (m/s)
This relationship determines that when there is a change in the aperture area, the air velocity must be increased in order to maintain stability balance. Pressure balance concept (loss Δp) is explained as:

$$\Delta p_{loss} = \Delta p_{th} + \Delta p_{wind} \quad \text{[Pa]} \quad (9)$$

The previous fundamental equations give a general idea of air flow from inside the facade to the outside. However, the variation of air flows within a DSF is very complex and depends on the interaction of all elements that contribute to the local and total heat transfer coefficients of the facade that determine how the flow behaves. Therefore, CFD analysis is a very useful tool for computing detailed flow models because the momentum, mass, energy, and radiation equations are discretized and calculated to obtain the flow behavior within the inter-facades.

The two basic types of airflow found in an MSF or DSF are defined as laminar when frictional forces govern over turbulence and inertial forces when high inertia forces are present. Turbulent flows depend on the viscosity of the fluid and the air velocity known as the Reynolds number, which is the relationship between centrifugal force and adhesion. This is explained as:

$$\mathrm{Re} = v \cdot \frac{L}{\nu} \quad (10)$$

where:
v = Air velocity (m/s).
L = Dimension of the change of direction of the air stream (m)
ν = Kinematic viscosity of air [~15.5×106m²/s]

There is a critical Reynolds number value when turbulence occurs. According to Osterle, the critical Re in DSFs is from 10.000 to 20.000 (Oesterle et al. 2001). Von Grabe (2002) stated that, "with natural ventilation inside the air gap, the driving force is the reduction of the density due to the increase of air temperature. This increase is greater near the heat sources, thus near the panes and the shading device. Further on it might be non-symmetrical because of different magnitudes of the heat sources." This means that both the streamline flow created at the facade is higher at the inlet and reduces sharply to half the entire height and eventually increases to a smaller magnitude at the outlet, and also means the input/output relationship plays a key role in determining the standard of streamline flow within the air gap. Inside a double skin facade, the air temperature will mainly depend upon the warmth gains and therefore the amount of air flow. However, during a naturally ventilated double skin facade the air flow itself is especially governed by the temperature difference outside and possibly also by the pressure differences caused by the wind; air flow is usually very unsteady (Park et al. 2004).

Natural ventilation is a crucial aspect of double-skin facade performance, which is said to be microclimatic thermal transmittance and solar heat gain.

Several investigations are performed during which an integrated modeling process was used to define the connection between natural ventilation and therefore the microclimatic thermal performance of double-skin facades. They investigate the microclimatic thermal performance and correlations of double-skin facade with buoyancy-driven airflow employing a numerical model (Pappas and Zhai 2008). Ding et al. examined the performance of a solar naturally ventilated double-skin facade (Ding et al. 2005). Manz and Frank (2005) have simulated the microclimatic thermal performance of double skin facade. Most of these reports have focused on the stack effect or the solar chimney concept design.

Research Methodology

This research helps designers to make better selections of multiple or double skin facade MSF or DSF design features in terms of openings, sizes and locations, air gap depth and height of shaft. DSF microclimatic comfort and energy-performance modelling is a complex problem. An accurate assessment of the physics of airflow and temperatures within the air gap requires detailed analyses of solar radiation transmitted through glazed facades, buoyancy, and wind pressure. Annual building simulation programs cannot provide accurate CFD simulations.

Obtaining Meteorological Inputs and the Modeling Process

The first step in the research procedure on microclimatic thermal comfort of the multiple or double skin facade DSF configurations is to collect climatic data and information on the building site. Entry of the Antalya meteorological data and geographic data pertaining o the climatic region of the building are made by the user. Meteorological data entered to FloEFD software is an index pertaining to Republic of Turkey General Directorate of Meteorology for the outdoor weather temperatures, direction and intensity of wind, intensity of the direct and common solar radiation, and sky cloudiness in the region. These weather data include outdoors weather temperatures, direction and intensity of wind, intensity of the direct and common solar radiation, and sky cloudiness in the region.

Boundary Conditions and Limitations and Assumptions

This study is limited to comparative analyses between three different DSF building configurations considered for application in plot centers of “Hot-Humid Climate”, a characteristic that is dominant in the southern part of Turkey. In order to observe the effect of the variable DSF with the shaft air gap and air gap width on the building comfort design and energy performance on solar radiation and consequently the necessary energy of the building, different microclimatic thermal factors (except solar heat gain) were fixed throughout the research. The calculated internal loads within one typical day for sizing the total internal gains. The total internal gains during a typical day are 300 kW. This gives an indication that the

internal gains constitute a high amount of energy gain that could be used as a positive in winter times and as negative in summer time.

Each floor height of DSF buildings have been considered 4.00 in average. The indoor comfort limit temperature value for the heating and cooling load within the building has been considered 23◦C in all DSF building options.

Entry of the meteorological data and geographical data pertaining to the climatic region of the building are made by the user. Meteorological data entered to FloEFD software is an index pertaining to Republic of Turkey General Directorate of Meteorology for the outdoor weather temperatures, direction and density of wind, density of the direct and common solar radiation, and sky cloudiness in the region.

An important initial concept for CFD analyses is that of boundary conditions. Each of the dependent variable equations requires meaningful values at the boundary of the calculation domain in order for the calculations to generate meaningful values throughout the domain. These values are known as boundary conditions, and can be specified in a number of ways. The specification of boundary conditions for two driving forces of wind and buoyancy effect can be defined as a pressure difference on inlet and outlet. To calculate the stack effect, the energy equation needs to be turned on.

The heat flux coefficient, which is defined as the product of the density, microclimatic thermal conductivity and specific heat capacity quantifies the ability of the material to absorb heat. It has been found to reflect the influence on microclimatic thermal comfort of different surfaces and is therefore used as the basic thermo-physical property defining the materials. The heat flux coefficients for the different layers of each element of the building (walls, roof, floor) are considered as design variables. The thicknesses of the different layers of each building element are also considered as design variables.

The following parameters were taken into account in the analyzed configurations of the double skin facade DSF building; Total volume of room: 7.40 m X 7.60 X 2.85 = 160.2 m^3, thickness: 0.22 m, density: 1,200 kg/m^3, specific heat capacity (Cp): 1,000 J/kg K, microclimatic thermal conductivity: 0.38 W/m K for opaque surfaces; Density: 2,700 kg/m^3, for frame surfaces; specific heat capacity Cp: 953 J/kg K, microclimatic thermal conductivity: 155 W/m K, for transparent surfaces: density: 2,300 kg/m^3, specific heat capacity Cp: 836 J/kg K, microclimatic thermal conductivity: 1.05 W/m K, thickness: 0.05m, turbulence model: (standard model); k-epsilon model, near wall treatment: two-scale wall functions approach, radiation model: discrete transfer method. The materials with different material characteristics used in all DSF; air as fluid, and building envelope, floorings, doors, windows, walls and roofs as building components. The values accepted for fluid air are respectively: Intensity: kg/m^3, Specific heat Cp: J/kg K.

The following parameters given below were analyzed in this research. Building surface temperature values of distribution, building solar heat flux and total surface heat flux (Numerical), temperature, wind flow and wind speed values between DSF and building, building interior surface temperature and wind speed values, wind flow, wind speed and wind direction distribution in interior of building, wind flow changing rate between building temperature zone, heat

transfer rate between building surfaces, total heat flux rate and solar heat flux rate of building, flow temperature in interior of building, perceivable temperature in interior of building, perceivable radiation temperature in interior of building, relative humiditiy in interior of building, PMV and PPD values in building zones.

Creation of the Models and the Analysis Phase in CFD

The geometries of DSF models examined were drawn and the digital mesh networks of the models belonging to each defined DSF option were created, the microclimatic thermal regions of each model were defined and surfaces of the models were created and restricting conditions were decided upon.

Then, geographical and climatic data of different climatic regions were entered into the FloEFD simulation program. Further, data such as permeability and reflectivity of the structure envelope, constructional components and constructional materials were entered. The microclimatic thermal regions, building surfaces and elements thereof previously decided upon during the pre-analys meshing phase were defined. Later, the data comprising the inter-building microclimatic thermal gains were entered and analysis commenced.

As criteria of the case study, for the heating period, average temperature distribution on DSF surface and inner building total temperature gain and loss values, outside air velocity movements, direction of air, layering of air, air change ratio pertaining to DSF buildings zones, for DSF both of building surfaces; overall and average heat transition amount, surface temperatures, pressures, and velocity distributions and wind speed values will be analyzed,

The numerical and visual reports of all such values will be prepared and will rely on such values; evaluations and comments will be made on internal temperature and average temperature distributions on the DSF building surface, overall temperature gain, total temperature loss calculations, investigation of architectural solutions for better cooling and ventilation as well as their effects on cooling and ventilation.

In the CFD FloEFD software where the analysis study is performed, information on the building envelope such the thickness, density, specific heat, microclimatic thermal conductance coefficient, sun radiation absorbency, sun radiation reflectivity, surface roughness and number of layers are defined, whereas layers in the floorings together with (if present) separate stratifications are defined in the ground floor, second floor and roof slab. The thickness, density, specific heat, microclimatic thermal conductance coefficient, sun radiation absorbency, sun radiation reflectivity, surface roughness and number of layers of the material used in the flooring are examined. On the other hand, the data used in the simulation program are defined by entering the values of volume ambient temperatures, boundary conditions for surfaces and microclimatic thermal zones, absorbency of surfaces, reflectivity, density, specific heat and microclimatic thermal conductance. The correct type of fluid flow is a very important aspect of the CFD simulation as well.

There are two radically different states of flows that are easily identified and distinguished: laminar flow and turbulent flow. Laminar flows are characterized

by smoothly varying velocity fields in space and time in which individual ―laminar―move past one another without generating cross currents. These flows arise when the fluid viscosity is sufficiently large to dampen out any perturbations to the flow that may occur due to boundary imperfections or other irregularities. These flows occur at low-to-moderate values of the Reynolds number 5. In contrast, turbulent flows are characterized by large, nearly random fluctuations in velocity and pressure in both space and time.

These fluctuations arise from instabilities that grow until nonlinear interactions cause them to break down into finer and finer whirls that eventually are dissipated (into heat) by the action of viscosity. Turbulent flows occur in the opposite limit of high Reynolds numbers. The solver needs for this study are more likely to be turbulent due to irregularities of the surface. There are usually regions with and without turbulence in the same space. The turbulence model must be able to deal with laminar and transitional flow at the same time and the RNG k-e model of turbulence appears to be the most suitable choice among other models in CFD.

HVAC System and Components for Case Study

The building is equipped with a typical HVAC system that follows the following process. The outdoor air flows into the air handling unit through a filter to dilute and remove air contaminants. However, the energy required to condition this outdoor air could be of significant effect on the total-consumed load. The floor heating system is used in winter. Following this process, the air is heated or cooled with respect to the difference between the ambient temperature and the required room temperature. The assumptions are made according to the following:

Infiltration

The infiltration rate is assumed because the accurate air change rate through infiltration usually depends on many factors such as the outside air velocity, the pressure distribution around the building, the tightness of the windows, etc. So, it cannot be precisely predicted. The assumption is based on a referred office building example in the ASHRAE Handbook 2009. This example assigned an infiltration rate of 0.1 h^{-1} depending on the building tightenness and insulation. Likewise, the example in the studied building has the same degree of tightens and is well insulated. Thus, the infiltration rate is assigned as 0.1 h^{-1} in the winter period. In summer the infiltration rate should be higher, due to the uncertainty of the occupants' behaviours for opening the windows.

Interior Gains

The heat gains from office appliances are assigned according to ASHRAE Research 1482-RP (ASHRAE 1999). It mentioned that flat panel monitors of 30-inches in size has an average power consumption of 80W. Printer's power consumption during a printing cycle varies from 80 to 150 W depending on the model, print capacity, and speed. An average heat gain of 90 W was assumed for each monitor; that is in total 90 monitors with total gains of 7860 W. Also, an

average heat gain of 110 W was assumed for each printer which is in total 10 printers with total gains of 860 W.

Ventilation Rate

The minimum required fresh air is calculated according to ASHRAE Standard 62-1999. Based on one person's needs, the quantity of fresh air inside an office is 20 CFM, which is equal to 35m3/hr. Since the first floor zone is occupied by 85 employees, the minimum required fresh air is 3000 m^3/hr (ASHRAE 1999).

Wind Speed, Wind Direction, and Mean Wind Speed Profile

The natural wind speed varies in time and space; the character of its variation is highly random and the wind flow is highly turbulent. All CFD analysis had conducted 16 different configurations under different radiations and velocities. But in this study, it is used two different exterior flow velocity 5 m/s, 15 m/s.

Geometry Model of Validation for CFD Validation

For achieving model validation, an iterative process of calibrating the model took place; comparing the model to actual system behaviour. This process was repeated until sufficient model accuracy was reached. The calibration process is performed manually by making small changes to the values of the parameters and re-running the simulation to see the results. The calibration methodology with the parameters that were checked iteratively. After 45 simulation trials, satisfying results were obtained for the model (Figure 1).

Figure 1. *Convergence of Residuals of the Model*

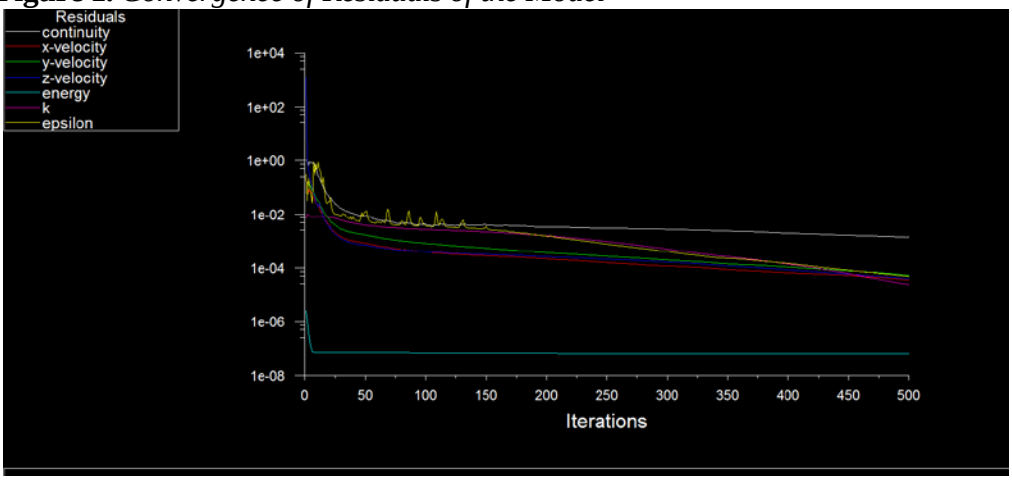

The CFD simulations provides a good prediction with an average absolute error of 2.85% for the 80 cm air gap and 3.95% for the 100 cm air gap distance. The maximum errors for each case are found at 3.2 m in the air gap. Errors are generally higher at the bottom (1.2 m) and top (3.2 m) locations than in the middle.

This research of the CFD model was validated in a laboratory test conducted by Inan and Basaran (2019). The geometry model was conducted according to the experiment (Figure 3). The building chosen as the reference in the study model is

considered as having 2 storeys, with a floor height of 4.00 m, with exterior building dimensions of 7.80 m x 7.80 x 7.80 m and model dimensions of 7.40m x 7.60 x 2.85m (Figures 2-3).

Figure 2. *Model of Building with DSF*

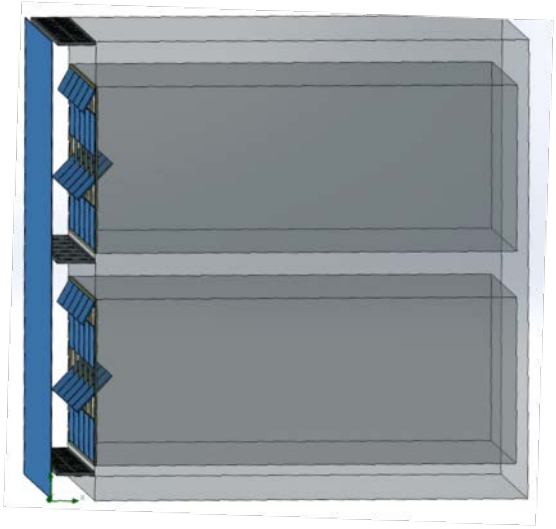

Figure 3. *Model of Double-Skin Facade*

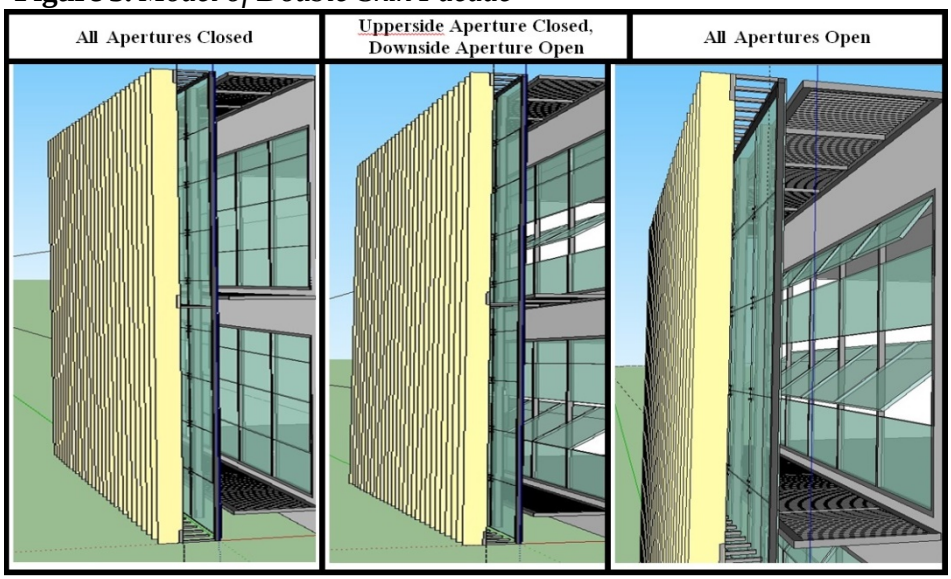

The performed configurations in this research are the following: DSF-1 (air gap width 80 cm with all operable windows are closed); DSF-1 (air gap width 80 cm with all operable windows are open); DSF-1 (air gap width 80 cm with bottomside operable window open, upperside closed); DSF-1 (air gap width 80 cm with bottomside operable window closed, upperside open); DSF-2 aAir gap width 160 cm with all operable windows are closed); DSF-2 (air gap width 160 cm with all operable windows are open); DSF-2 (air gap width 160 cm with bottomside operable window open, upperside closed); DSF-2 (air gap width 160 cm with bottomside operable window closed, upperside open); DSF-3 (air gap width 240

cm with all operable windows are closed); DSF-3 (air gap width 240 cm with all operable windows are open); DSF-3 (air gap width 240 cm with bottomside operable window open, upperside closed); DSF-3 (air gap width 240 cm with bottomside operable window closed, upperside open); DSF-4 with shaft (air gap width 240 cm with all operable windows are closed); DSF-2 with shaft (air gap width 160 cm with all operable windows are open); DSF-2 with shaft (air gap width 160 cm with bottomside operable window open, upperside closed); DSF-2 with shaft (air gap width 160 cm with bottomside operable window closed, upperside open) (Figure 3).

Mesh Modelling

The relative number of cells of the mesh is a vital parameter that strongly influences the computational time. Increasing the number of cells can often increase computational time by an order of magnitude. Also the grid dimensions influence the accuracy of CFD results and the value of y+. The parameter y+ is critical to the correct use of turbulence models. Before conducting the simulations, different meshes were analysed, for 2D and 3D models, in order to find the minimum amount of cells that can guarantee the invariability of the results. A vital of mesh feature is that the y+ value must be less than, or close to, 1 for the first grid close to the walls. This permitted the use of k-ε with enhanced wall treatment, and k-ω models as turbulent models. The ventilation of the building is purely driven by buoyancy force in the air gap. That is why it is important to have sufficient fine mesh to resolve the microclimatic thermal comfort boundary layer on both facades. The better mesh sizes with $y+ < 1$ was determined for the glazing facades. The grid sensitivity is examined over five mesh sizes which were consecutively refined by around 1.8 at each dimension.

Figure 4. *Computational Domain Mesh System of the Building with Double-Skin Facade*

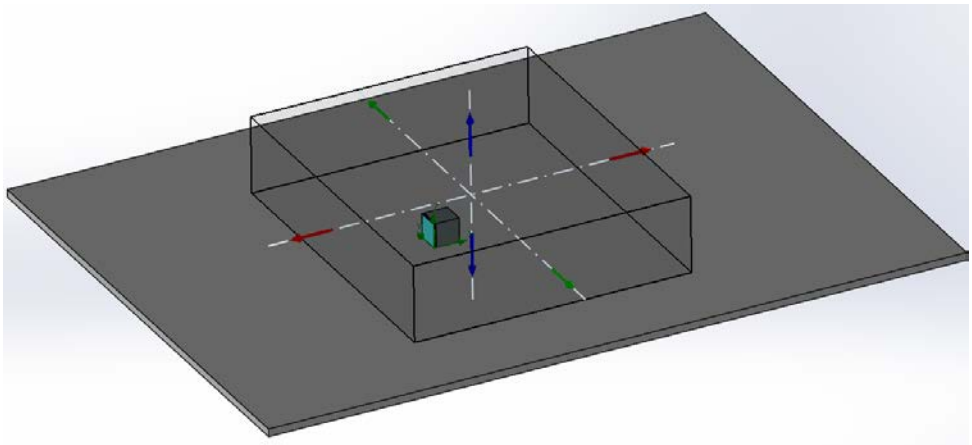

The computational domain mesh consisted of about 13 million polyhedral cells. The computational time was 45 s per iteration. The *y+* value was close to 1; The calibration methodology with the parameters that were checked iteratively. After 45 simulation trials, satisfying results were obtained for the model (Figure 4).

Governing Equations for CFD

Numerical simulations were carried out using the commercial CFD software FloEFD. A finite-volume based fluid dynamics solver. The general form of transport equations for incompressible flow can be expressed as:

Momentum equation,

$$\frac{\partial \vec{V}}{\partial t} + \left(\vec{V} \cdot \nabla\right)\vec{V} = \Gamma \nabla^2 \vec{V} - \frac{1}{\rho}\nabla p \qquad (11)$$

The equations for viscous flow that have been derived in the preceding sections apply to a viscous flow, i.e., a flow which includes the dissipative, transport phenomena of viscosity and microclimatic thermal conduction.

$$x\text{-component}: \quad \frac{\partial(\rho u)}{\partial t} + \nabla \cdot (\rho u \vec{V}) = -\frac{\partial p}{\partial x} + \frac{\partial \tau_{xx}}{\partial x} + \frac{\partial \tau_{yx}}{\partial y} + \frac{\partial \tau_{zx}}{\partial z} + \rho f_x \qquad (12)$$

$$y\text{-component}: \quad \frac{\partial(\rho v)}{\partial t} + \nabla \cdot (\rho v \vec{V}) = -\frac{\partial p}{\partial y} + \frac{\partial \tau_{xy}}{\partial x} + \frac{\partial \tau_{yy}}{\partial y} + \frac{\partial \tau_{zy}}{\partial z} + \rho f_y \qquad (13)$$

$$z\text{-component}: \quad \frac{\partial(\rho w)}{\partial t} + \nabla \cdot (\rho w \vec{V}) = -\frac{\partial p}{\partial z} + \frac{\partial \tau_{xz}}{\partial x} + \frac{\partial \tau_{yz}}{\partial y} + \frac{\partial \tau_{zz}}{\partial z} + \rho f_z \qquad (14)$$

The equations for inviscid flow inviscid flow is, by definition, a flow where the dissipative, transport phenomena of viscosity, mass diffusion and microclimatic thermal conductivity are neglected. The governing equations for an unsteady, three-dimensional, compressible inviscid flow are obtained by dropping the viscous terms in the above equations.

Continuity equation,

$$\frac{\partial \rho}{\partial t} + \nabla \cdot \left(\rho \vec{V}\right) = 0 \qquad (15)$$

Energy conservation equation,

$$\frac{\partial T}{\partial t} + \left(\vec{V} \cdot \nabla\right) T = \Gamma \nabla^2 T + S_T \qquad (16)$$

Where fluid velocity $\vec{V}$ at any point in the flow field is described by the local velocity components u, v, and w. Γ is a general diffusion coefficient, t represents time, and S_T is the energy source term (Pasut and De Carli 2012).

Results and Discussion

Evaluation of Air Gap Effects for Double Skin Facade on Building Regarding Post-Process Analysis of Visual Data

In this study, only air gap width 80 cm—all openings-open and closed configurations will be considered as post analysis visual data.

Air Gap Width 80 cm - All Openings-Open Configurations for Wind Velocity 5 m/s - Air Flow Temperature in Interior of Building (°C)

Figure 5. *Air Flow Temperature in Interior of Building (°C) for Wind Velocity 5 m/s*

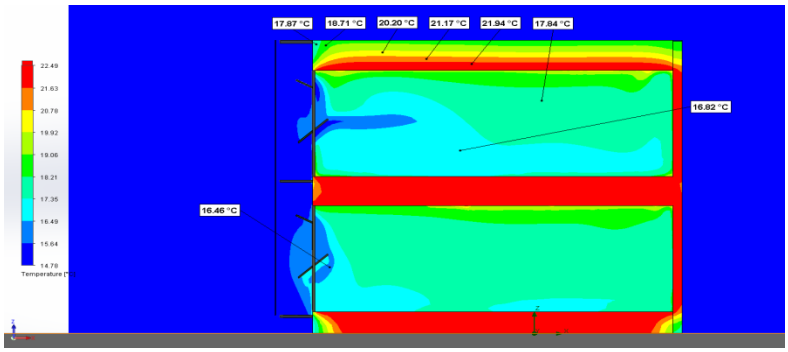

In the configuration where both openings on the interior facade of the building are open, interior temperature values are between 17 °C - 20 °C on entry of the flow between two facades toward the interior space from the openings on the building while the peripheral temperature is 15 °C, exterior flow velocity is 5 m/s, fixed indoor temperature is 23 °C. It has been observed that when both openings on the building are open, the flow from both openings reduces the indoor temperature value of the building by between 3 °C and 6 °C (Figure 5).

Air Gap Width 80 cm - All Openings-Open Configurations for Wind Velocity 5 m/s - Interior Facade Temperature Distribution Vertical (Between Two Facades) (°C)

Figure 6. *Interior Facade Temperature Distribution-Vertical (Between Two Facades) (°c) for Wind Velocity 5 m/s*

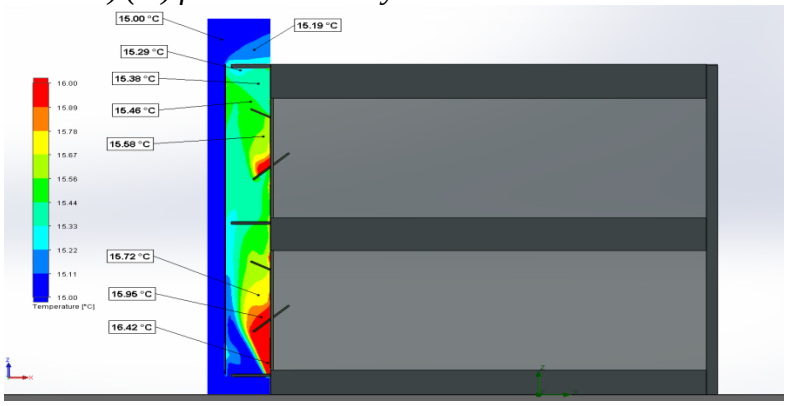

In the configuration where both openings on the interior facade of the building are open, as a result of the examination of the temperature values between two facades, the flow temperature from the opening toward the interior space has been observed 16 °C, and about 15 °C at the upper spaces while the peripheral temperature is 15 °C, exterior flow velocity is 5 m/s, fixed indoor temperature is 23 °C (Figure 6).

Air Gap Width 80 cm - All Openings-Open Configurations for Wind Velocity 5 m/s - Interior Facade Temperature Distribution-Horizontal (Between two Facades) (°C)

] *(°c) for Wind Velocity 5 m/s*

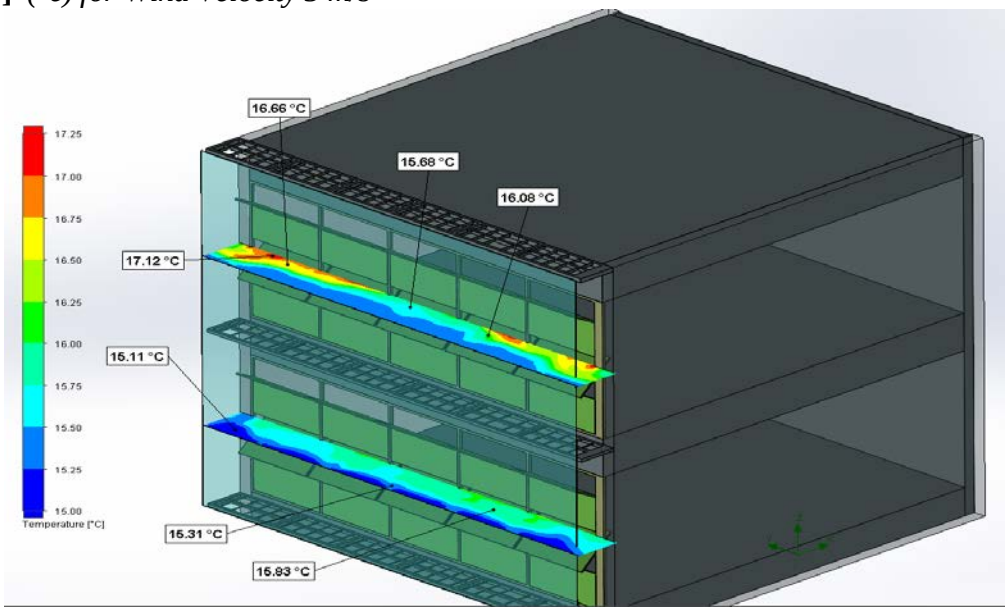

In the configuration where both openings on the interior Ffcade of the building are open, as a result of the examination of the temperature values between two facades, the flow temperature from the opening toward the interior space has been observed 15 °C on the ground floor, and about 17 °C at the upper spaces of the ground floor while the peripheral temperature is 15 °C, exterior flow velocity is 5 m/s, fixed indoor temperature is 23 °C (Figure 7).

Air Gap Width 80 cm - All Openings-Open Configurations for Wind Velocity 5 m/s - Wind Velocity-Wind Distribution in DSF and Around Building (°C)

Figure 8. *Wind Velocity - Wind Distribution in DSF and Around Building for Wind Velocity 5 m/s*

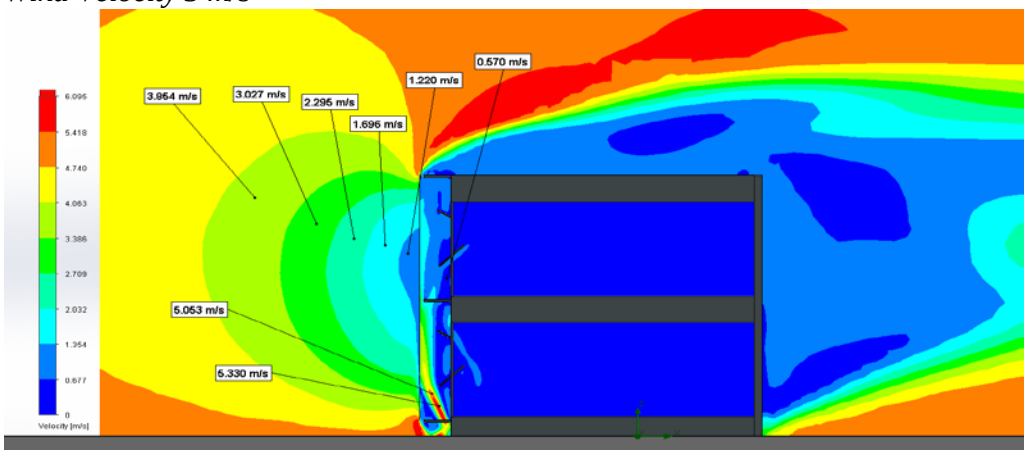

In the configuration where both openings on the interior facade of the building are open, examining the exterior flow velocity values it has been observed that the exterior flow velocity fell toward the exterior surface of the building, and the flow velocity increased due to the chimney effect between the two facades while the peripheral temperature is 15 °C, exterior flow velocity is 5 m/s, and fixed indoor temperature is 23 °C. It has been seen that the velocity between two facades increased to values of 5 m/s on the ground floor space while the exterior flow velocity is 2-3 m/s (Figure 8).

Air Gap Width 80 cm - All Openings-Open Configurations for Wind Velocity 5 m/s - Interior Facade Wind Velocity-Wind Distribution in Interior of Building

Figure 9. *Interior Facade Wind Velocity-Wind Distribution (Between two Facades) m/s for Wind Velocity 5 m/s*

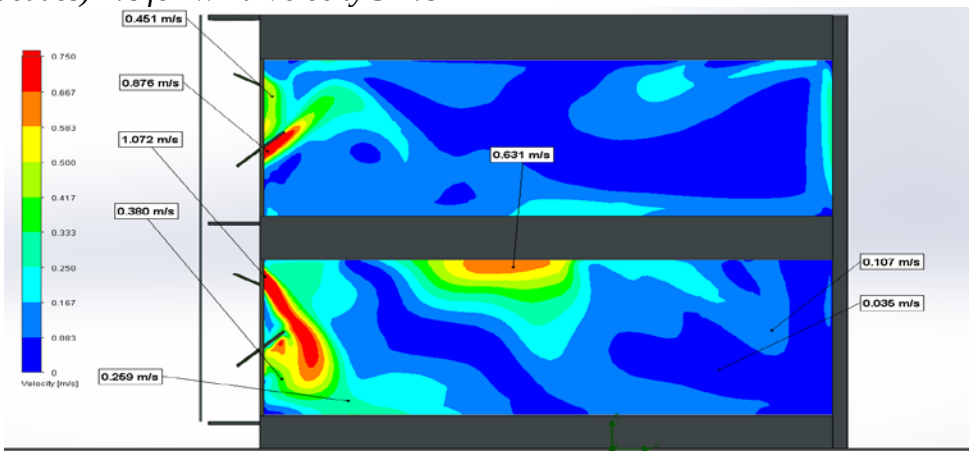

In the configuration where both openings on the interior facade of the building are open, the building interior flow velocity has been observed that the flow toward the interior from the openings on the building change the building

flow and temperature values when the exterior flow velocity is 5 m/s while the peripheral temperature is 15 °C, exterior flow velocity is 5 m/s, and fixed indoor temperature is 23 °C. It has been observed that while the ground floor indoor flow values are about 0.75 m/s close to the openings, the flow velocity values inward at the vicinity of the opening are about 0.2-0.3 m/s (Figure 9).

Air Gap Width 80 cm - All Openings-Open Configurations for Wind Velocity 5 m/s - Outside Facade Temperature Values of Distribution (°C)

Figure 9. *Outside in Front of Facade Building Temperature Values of Distribution (°C) for Wind Velocity 5 m/s*

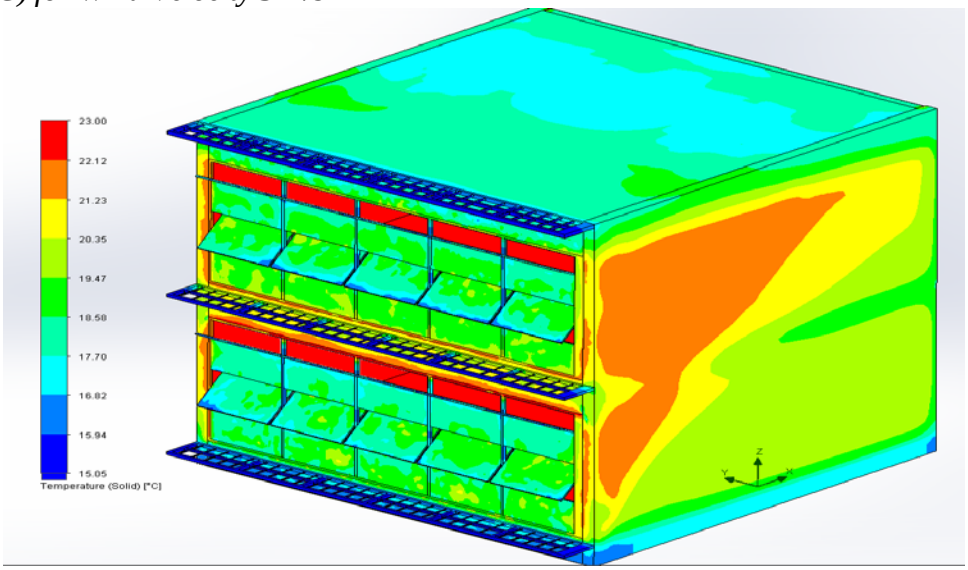

In the configuration where both openings on the building interior facade are open, it has been seen that the temperature values of transparent surfaces with openings, particularly to the bottom rose to 18 °C, and that the transparent surface temperature value of the transparent surface of the opening to the top rose to 23 °C while the exterior temperature is 15 °C, exterior flow velocity is 5 m/s, fixed indoor temperature is 23 °C. Besides, the building side surface temperature distribution average has been observed between 20 -21 °C (Figure 9).

Air Gap Width 80 cm - All Openings-Open Configurations for Wind Velocity 5 m/s - PMV and PPD Values in Building Zones

Figure 10. *PMV and PPD Values in Building Zones of Bottom Side Openings Level for Wind Velocity 5 m/s*

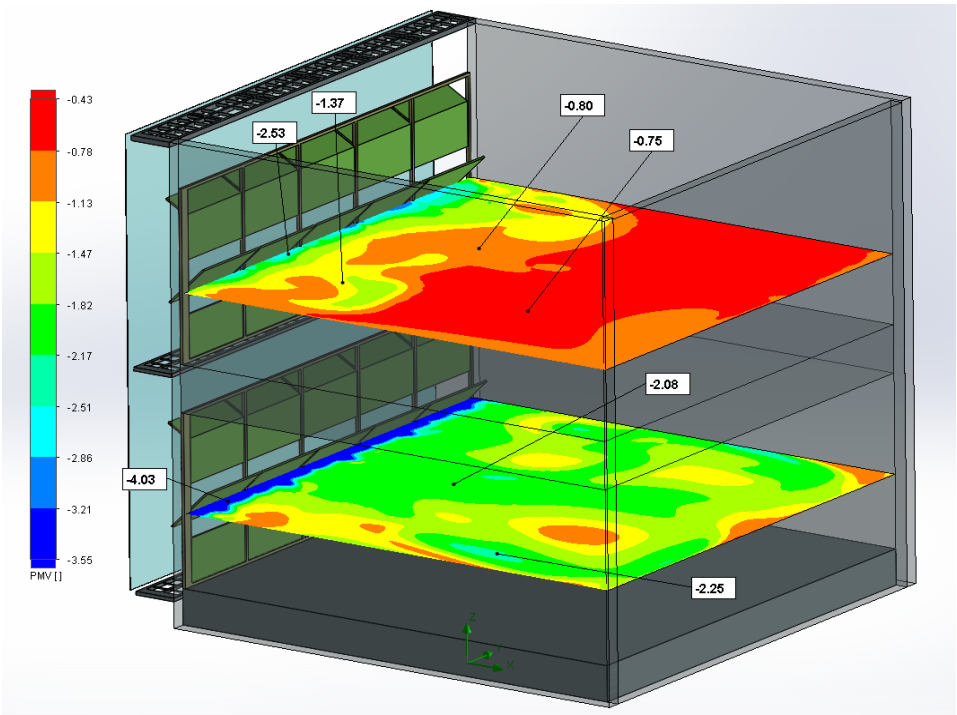

Figure 11. *PMV and PPD Values in Building Zones of Upper Side Openings Level for Wind Velocity 5 m/s*

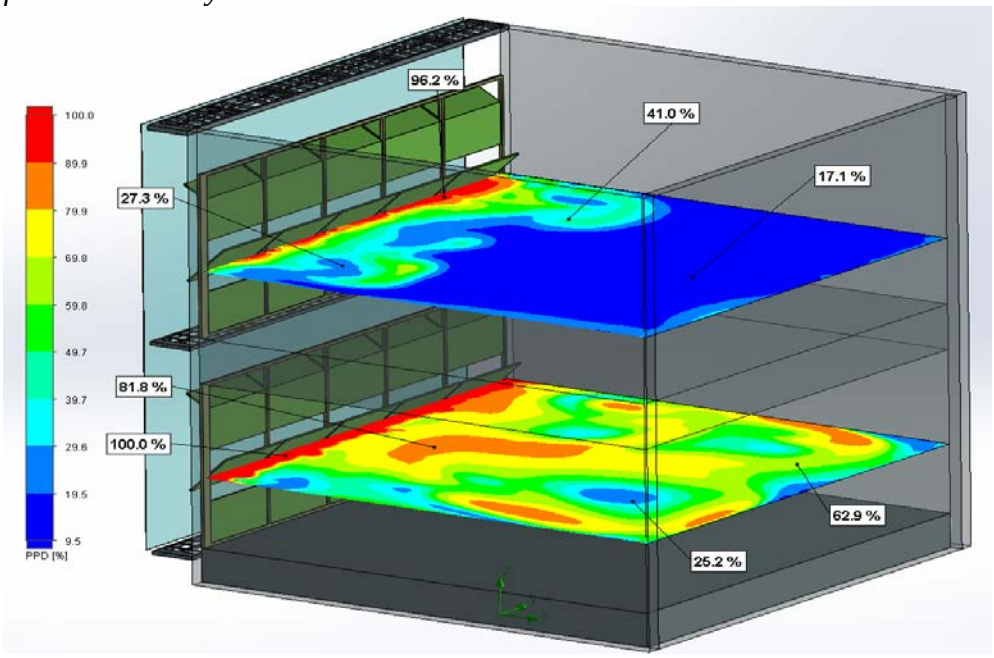

In the configuration where both openings on the interior facade of the building are open, the PMV values were observed between -1.15 and -2.55 at ground floor 1.8 m level while the peripheral temperature is 15 °C, exterior flow velocity is 5 m/s, and fixed indoor temperature is 23 °C. It was observed between values -0.40 and -1.80 at 1.8 m elevation upstairs.

Examining PPD values in the same configuration and levels, values between 30% and 60% have been observed at 1.8 m level of the ground floor, values between 10% and 20% at spaces mostly behind the opening area of the interior space, and values between 40-50% at locations close to the opening space (Figures 10-11).

Air Gap Width 80 cm - All Openings-Open Configurations for Wind Velocity 5 m/s - Relative Humiditiy in Interior of Building (%)

Figure 12. *Relative Humiditiy in Interior of Building (%) for Wind Velocity 5 m/s*

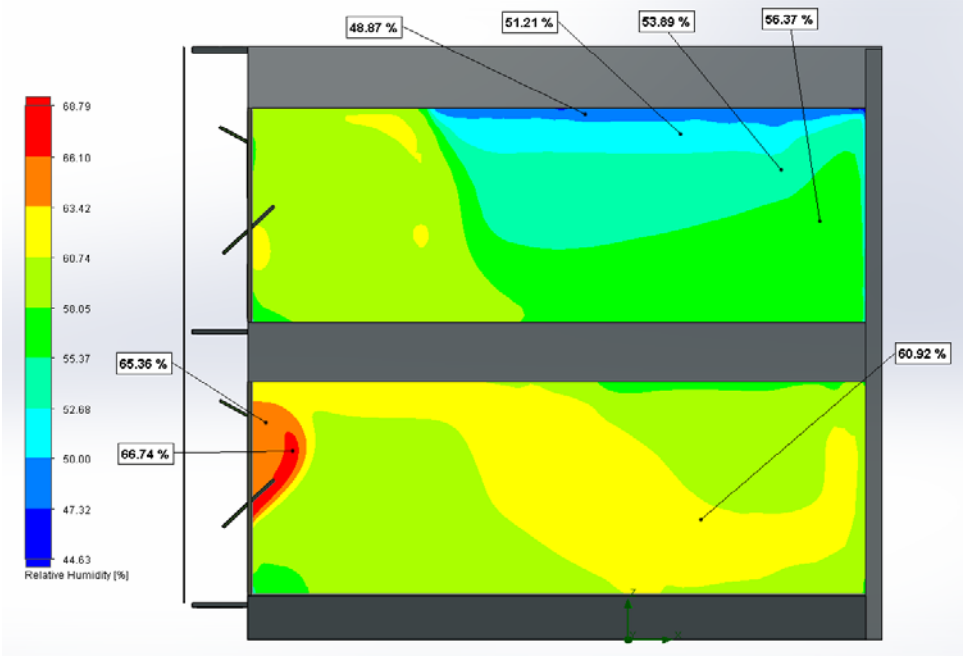

In the configuration where both openings on the interior facade of the building are open, the building ground floor relative humidity values average has been observed about 62% at locations close to the openings and about 50% in further inside areas while the peripheral temperature is 15 °C, exterior flow velocity is 5 m/s, and fixed indoor temperature is 23 °C and while the average ground floor inner space relative humidity values are about 60% (Figure 12).

Air Gap Width 80 cm - All Openings-Open Configurations for Wind Velocity 15 m/s - Air Flow Temperature in Interior of Building (°C)

Figure 13. *Air Flow Temperature in Interior of Building (°C) for Wind Velocity 15 m/s*

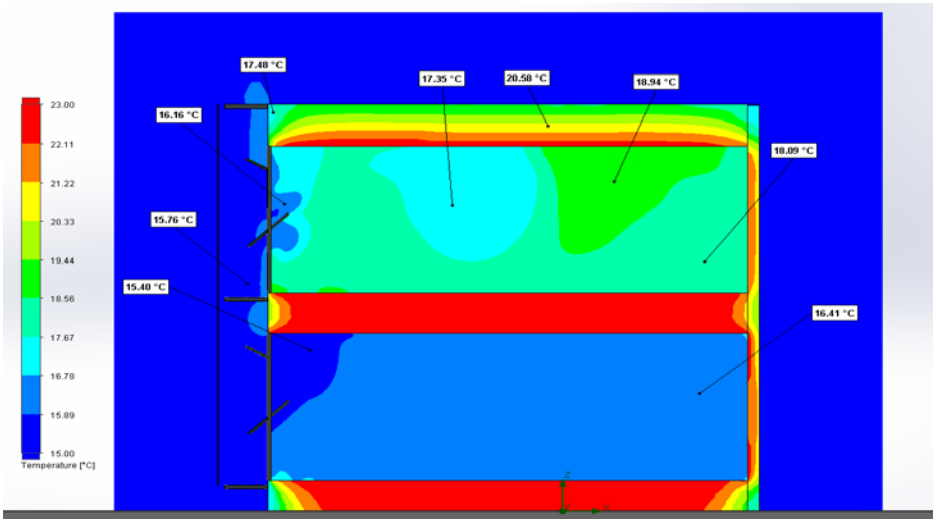

In the configuration where both openings on the interior facade of the building are open, ground floor average interior space flow temperature values have been observed between 15 °C - 16 °C on entry of the flow between two facades toward the interior space from the openings on the building while the peripheral temperature is 15 °C, exterior flow velocity is 5 m/s, fixed indoor temperature is 23 °C. The upstairs interior space average temperature values are between 17 °C - 19 °C (Figure 13).

Air Gap Width 80 cm - All Openings-Open Configurations for Wind Velocity 15 m/s - Interior Facade Temperature Distribution (Between Two Facades) (°C)

Figure 14. *Interior Facade Temperature Distribution-Vertical (Between two Facades) (°C) for Wind Velocity 15 m/s*

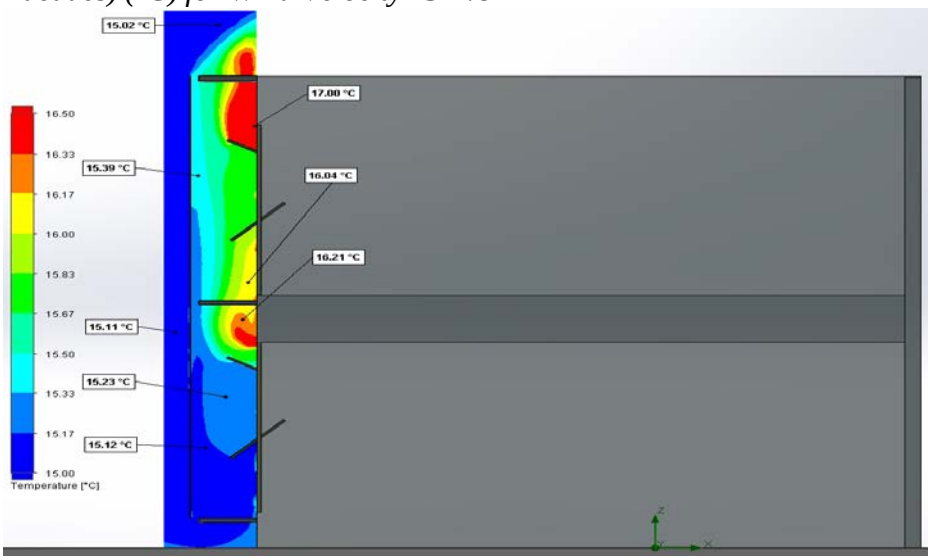

In the configuration where both openings on the interior facade of the building are open, it has been observed that the flow temperature values between the two facades at ground level was 15-16 °C and that it increased to 17 °C at upper floors while the peripheral temperature is 15 °C, exterior flow velocity is 15 m/s, and fixed indoor temperature is 23 °C (Figure 14).

Figure 15. *Interior Facade Temperature Distribution-Horizontal (Between two Facades) (°C) for Wind Velocity 15 m/s*

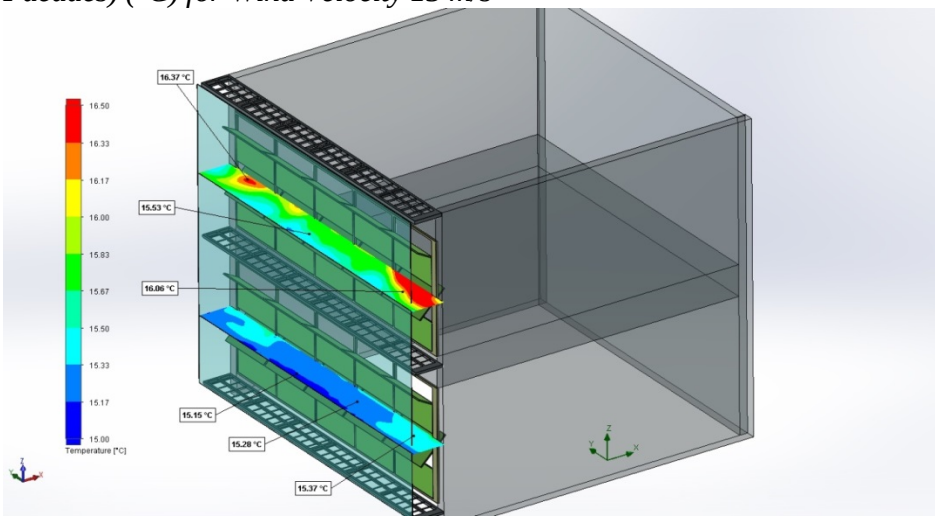

In the configuration where both openings on the interior facade of the building are open, as a result of the examination of the temperature values between two facades, the flow temperature both on the ground floor and on the opening toward the interior space have been observed 15 °C, and about 17 °C at the upper spaces of the ground floor, while the peripheral temperature is 15 °C, exterior flow velocity is 15 m/s, fixed indoor temperature is 23 °C (Figure 15).

Air Gap Width 80 cm - All Openings-Open Configurations for Wind Velocity 15 m/s - Wind Velocity-Wind Distribution in DSF and Around Building (°C)

Figure 16. *Wind Velocity-Wind Distribution in DSF and Around Building for Wind Velocity 15 m/s*

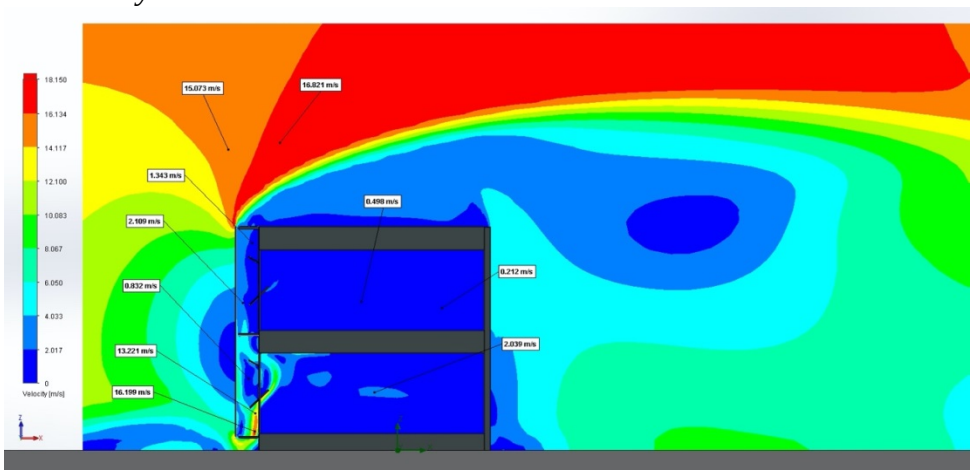

In the configuration where both openings on the interior facade of the building are open, the wind velocity values between two facades have been observed to fall down to 2-4 m/s while the exterior velocity values are about 8-10 m/s at building level while the peripheral temperature is 15 °C, exterior flow velocity is 15 m/s, fixed indoor temperature is 23 °C.

While it has been observed that the building exterior flow velocity value is 5 m/s, the flow velocity value approached the exterior flow level; and it has been observed in the 15 m/s exterior flow fixed value analysis that the instant flow velocity values between two facades fell down from about 15 m/s to 2-4 m/s. In this case, it has been observed that the wall effect of the exterior Facade reduced velocity values quite high in transition to between interior facade.

Besides, where exterior flow velocity is 15 m/s, it has been observed that the flow amount passing from the openings at the upper floor interior space was less compared to the 5 m/s velocity value (Figure 16).

Figure 17. *Wind Velocity-Wind Distribution of Interior Building for Wind Velocity 5 m/s*

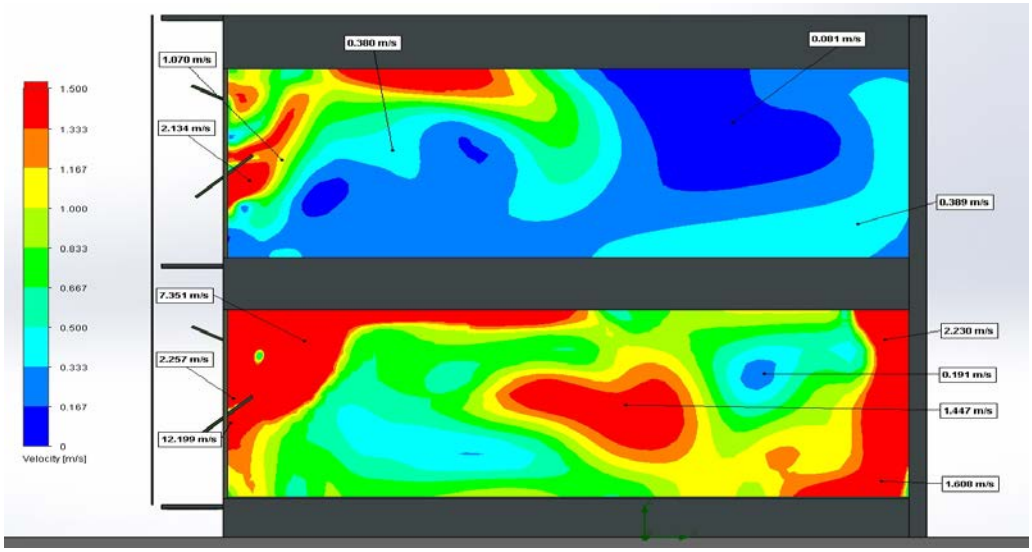

In the configuration where both openings on the interior facade of the building are open, the building interior flow velocity has been observed that the flow toward the interior from the openings on the building change the building flow and temperature values when the exterior flow velocity is 5 m/s while the peripheral temperature is 15 °C, exterior flow velocity is 5 m/s, and fixed indoor temperature is 23 °C. It has been observed that while the ground floor indoor flow values are about 1.5 m/s close to the openings, the flow velocity values inward at the vicinity of the opening are about 0.4-0.7 m/s (Figure 17).

Air Gap Width 80 cm - All Openings-Open Configurations for Wind Velocity 15 m/s - Outside Facade Temperature Values of Distribution (°C)

Figure 18. *Outside in Front of Facade Building Temperature Values of Distribution (°C) for Wind Velocity 15 m/s*

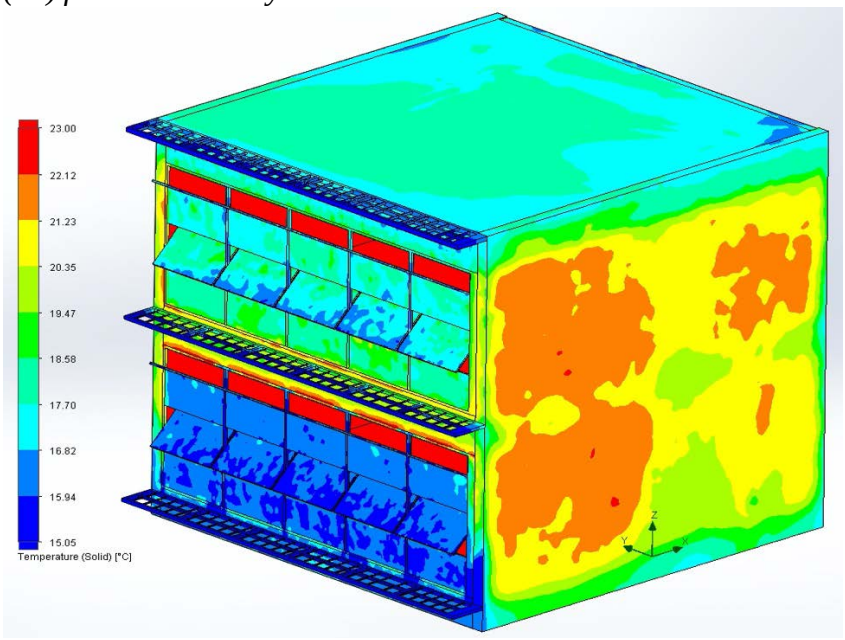

In the configuration where both openings on the interior facade of the building are open, the building exterior surface temperature distribution values, particularly ground floor building facade and indoor facade transparent surface temperature values have been observed 15 °C and upper floor level opening area transparent surface temperature value about 17-18 °C, while the peripheral temperature is 15 °C, exterior flow velocity is 15 m/s, fixed indoor temperature is 23 °C. Besides, the building side surface temperature distribution average has been observed between 20-21 °C (Figure 18). As to the exterior flow fixed value analysis with exterior flow velocity value 15 m/s while building interior facade transparent surface temperature distribution average values are 19-20 °C while building exterior flow velocity value is 5 m/s, it has been observed that the average values of building interior Facade transparent surface temperature distribution fell down to 15 m/s. It has been observed that the increase in the exterior flow velocity caused a fall on the average double skin facade interior facade temperature values (Figure 18).

Air Gap Width 80 cm - All Openings-Open Configurations for Wind Velocity 15 m/s - PMV and PPD Values in Building Zones

Figure 19. *PMV and PPD Values in Building Zones of Bottom Side Openings Level for Wind Velocity 15 m/s*

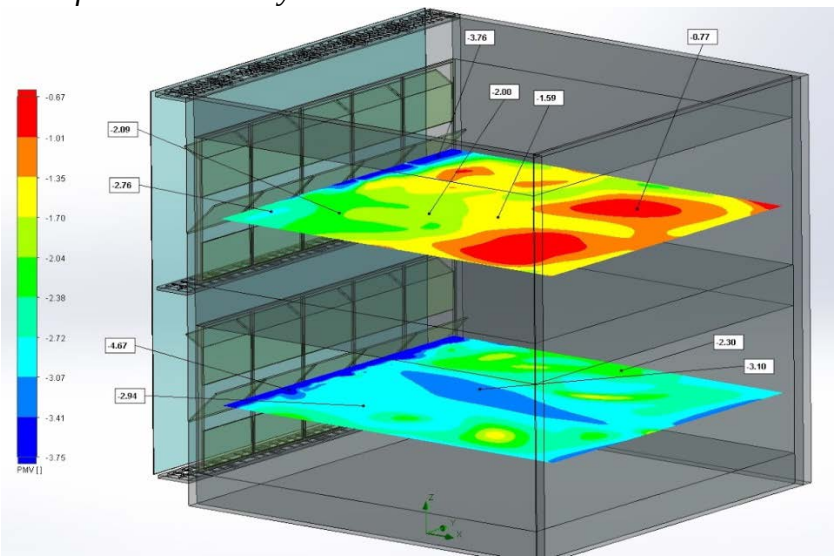

Figure 20. *PMV and PPD Values in Building Zones of Upper Side Openings Level for Wind Velocity 15 m/s*

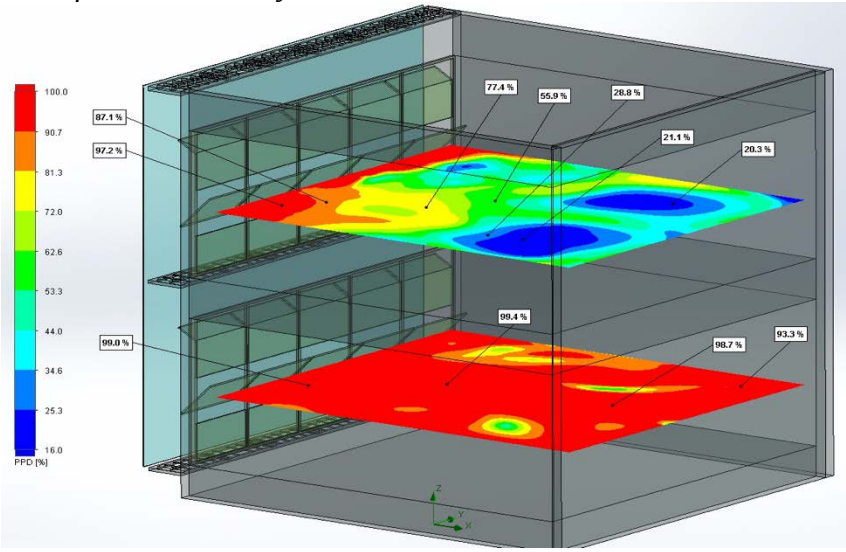

In the configuration where both openings on the interior facade of the building are open, the PMV values were observed between -2.30 and -2.90 at ground floor 1.8 m level while the peripheral temperature is 15 °C, exterior flow velocity is 5 m/s, and fixed indoor temperature is 23 °C. It was observed between values -0.90 and -2.00 at 1.8 m elevation upstairs.

Examining PPD values in the same configuration and levels, values of 90% have been observed at 1.8 m level of the ground floor, values between 70% and 80% at spaces mostly behind the opening area of the interior space, and values between 40-50% at locations close to the opening space (Figures 19-20).

Air Gap Width 80 cm - All Openings-Open Configurations for Wind Velocity 15 m/s - Relative Humiditiy in Interior of Building (%)

Figure 21. *Relative Humiditiy in İnterior of Building (%) for Wind Velocity 15 m/s*

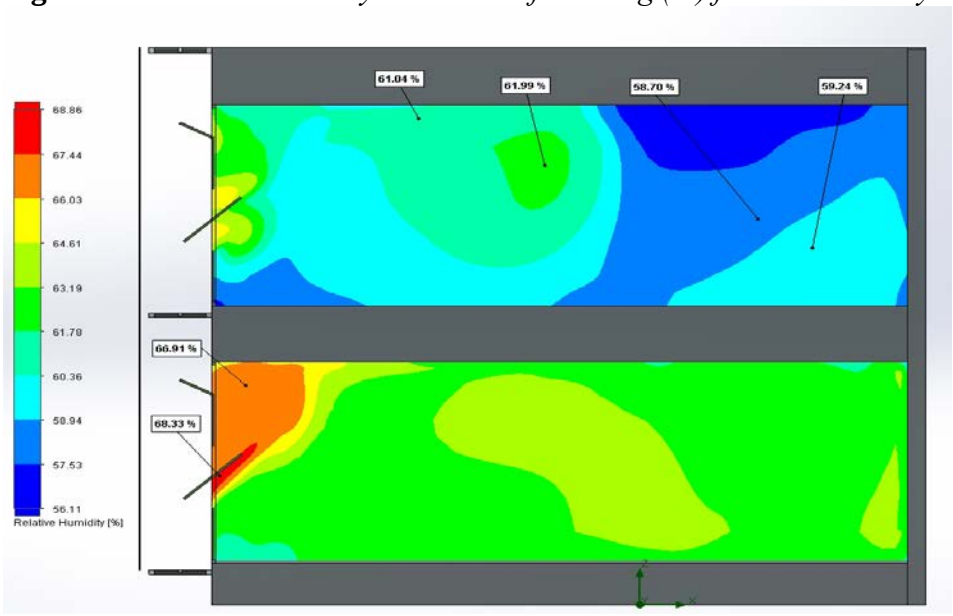

In the configuration where both openings on the interior facade of the building are open, the building ground floor relative humidity values average has been observed about 60% at locations close to the openings and about 50% in further inside areas while the peripheral temperature is 15 °C, exterior flow velocity is 5 m/s, and fixed indoor temperature is 23 °C, and average ground floor interior relative humidity values are about 65% (Figure 21).

Air Gap Width 80 cm - All Openings-Closed Configurations for Wind Velocity 5 m/s - Air Flow Temperature in Interior of Building (°C)

Figure 22. *Air Flow Temperature in Interior of Building (°C) for Wind Velocity 5 m/s*

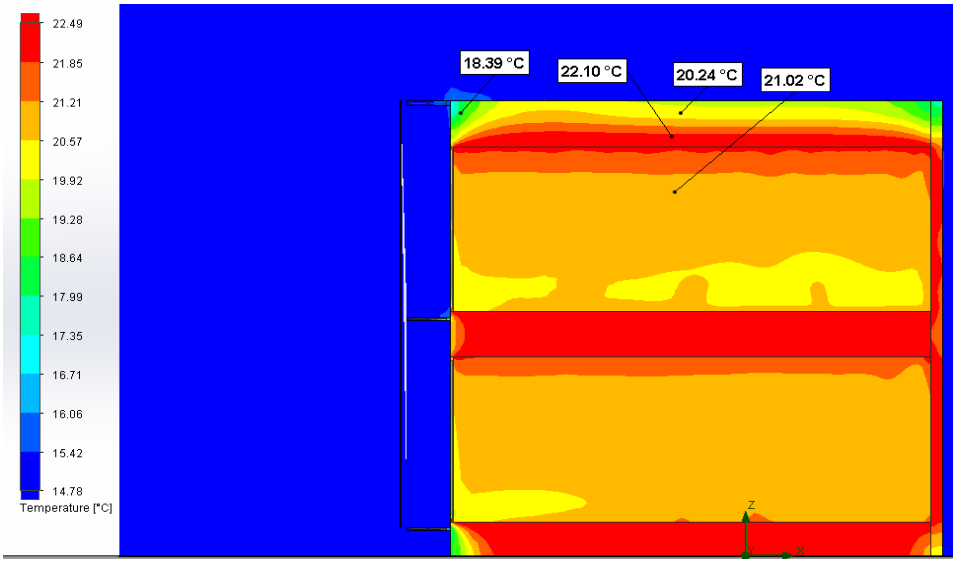

In the configuration where both openings on the interiorfFacade of the building are totally closed, interior temperature values are between 18 °C - 22 °C while the peripheral temperature is 15 ^{0}C, exterior flow velocity is 5 m/s, fixed indoor temperature is 23 °C (Figure 22).

Air Gap Width 80 cm - All Openings-Closed Configurations for Wind Velocity 5 m/s - Interior Facade Temperature Distribution (Between Two Facades) (°C)

Figure 23. *Interior Facade Temperature Distribution-Vertical (Between Two Facades) (°C) for Wind Velocity 5 m/s*

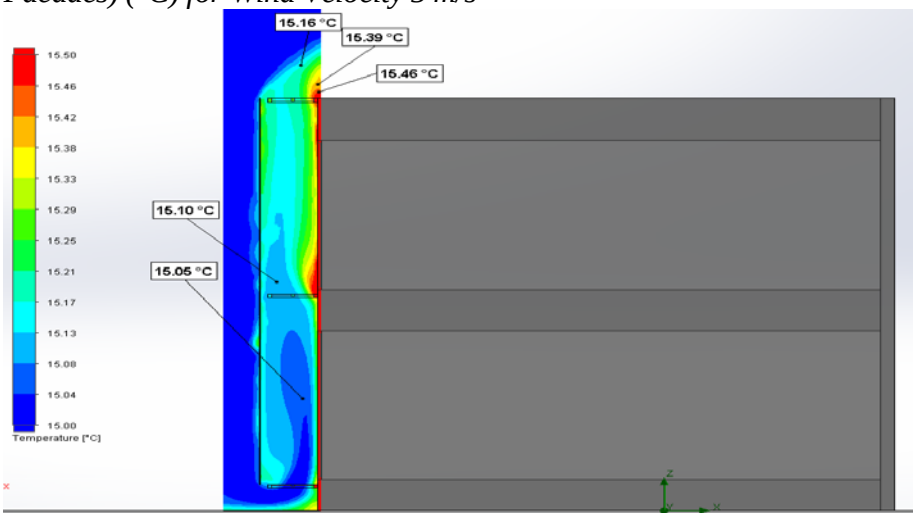

Figure 24. *Interior Facade Temperature Distribution-Horizontal (Between Two Facades) (°C) for Wind Velocity 5 m/s*

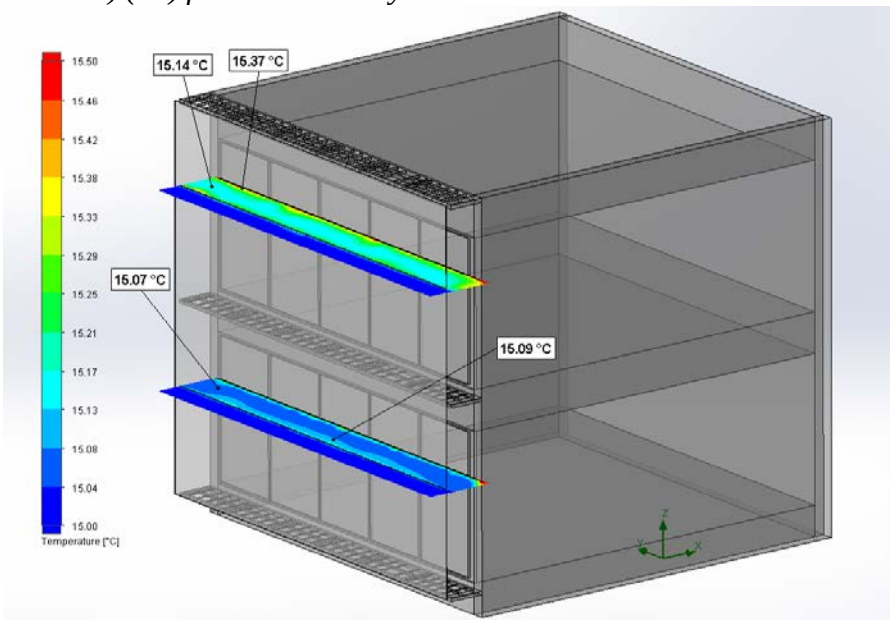

In the configuration where both openings on the interior facade of the building are totally closed, the flow temperature from the opening toward the interior space has been observed 15 °C, and about 15 °C at the upper spaces while the peripheral

temperature is 15 °C, exterior flow velocity is 5 m/s, fixed indoor temperature is 23 °C (Figures 23-24).

Air gap Width 80 cm - All Openings-Closed Configurations for Wind Velocity 5 m/s - Interior Facade Wind Velocity-Wind Distribution (Between Two Facades) m/s

Figure 25. *Wind Velocity-Wind Distribution in DSF and Around Building for Wind Velocity 5 m/s*

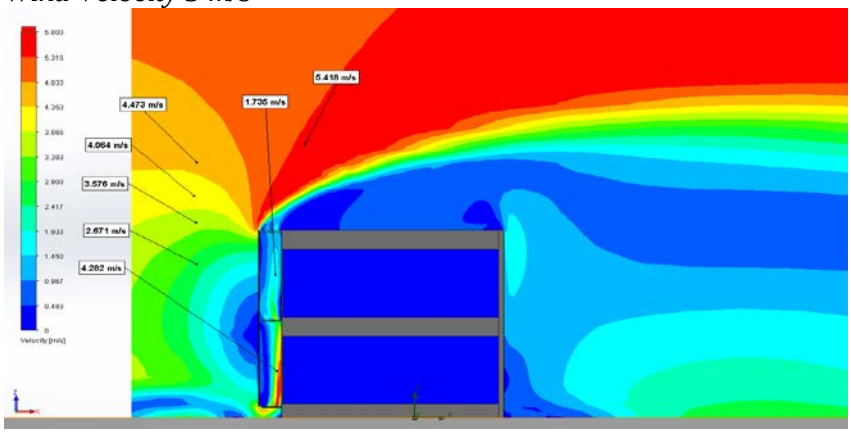

In the configuration where both openings on the interior facade of the building are totally closed, the wind velocity values between two facades particularly at the entry spaces with openings on the building have been observed up to 5 m/s while the peripheral temperature is 15 °C, exterior flow velocity is 5 m/s, and fixed indoor temperature is 23 °C, and exterior windward flow speed is 2m/s-2.5 m/s at levels with openings on building. Flow speed increases at once due to the chimney effect between two facades. At the downwind space of the building, flow velocity values were observed about 1.8 m/s (Figure 25).

Figure 26. *Wind Velocity-Wind Distribution of Interior Building for Wind Velocity 5 m/s*

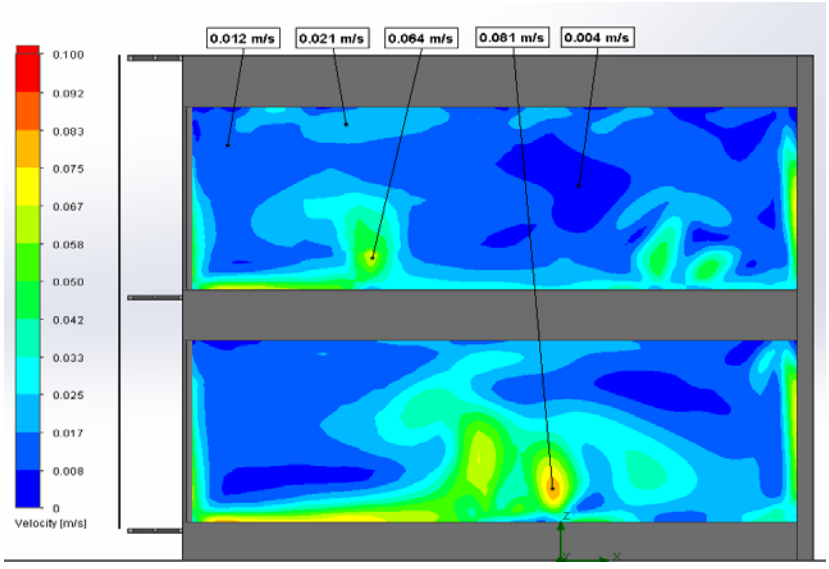

In the configuration where both openings on the interior facade of the building are totally closed, the building interior flow velocity has been observed at levels of 0.02-0.05 m/s while the peripheral temperature is 15 °C, exterior flow velocity is 5 m/s, and fixed indoor temperature is 23 °C, and exterior flow speed is 5 m/s because the building openings are totally closed and since there is no incoming flow in the volume (Figure 26).

Air gap Width 80 cm - All Openings-Closed Configurations for Wind Velocity 5 m/s - Outside Facade Temperature Values of Distribution (°C)

Figure 27. *Outside in Front of Facade Building Temperature Values of Distribution (°C) for Wind Velocity 5 m/s*

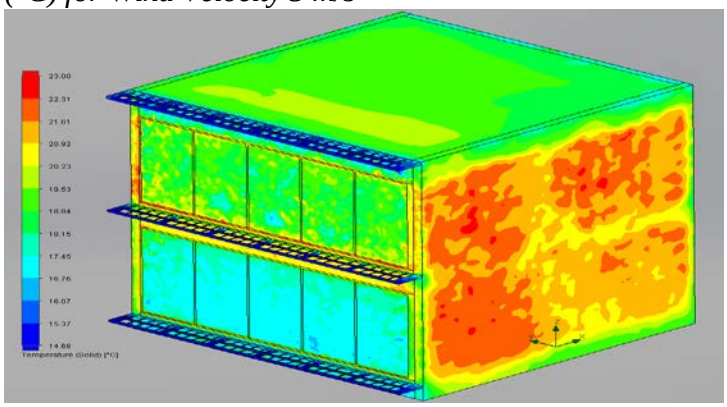

In the configuration where both openings on the interior facade of the building are totally closed, the building exterior surface temperature values, particularly ground floor and upstairs region side facade surface temperature values, are about 21 °C - 22 °C, while the peripheral temperature is 15 °C, exterior flow velocity is 5 m/s, fixed indoor temperature is 23 °C (Figure 27).

Air Gap Width 80 cm - All Openings-Closed Configurations for Wind Velocity 5 m/s - PMV and PPD Values in Building Zones

Figure 28. *PMV and PPD Values in Building Zones of Bottom Side Openings Level for Wind Velocity 5 m/s*

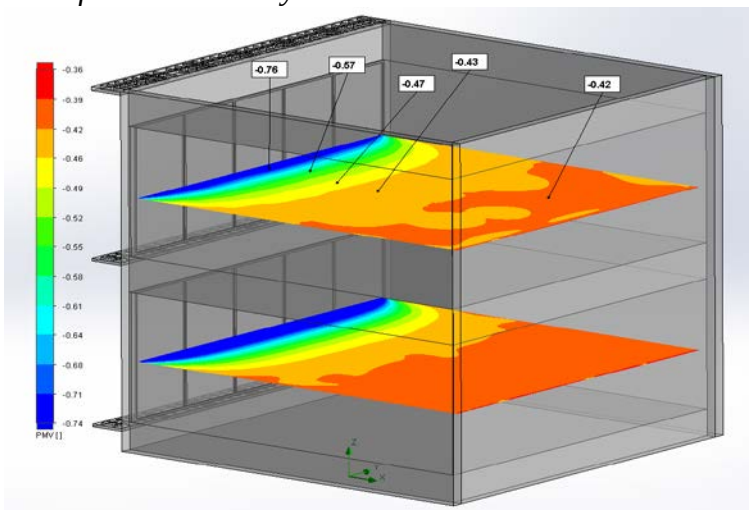

Figure 29. *PMV and PPD Values in Building Zones of Upper Side Openings Level for Wind Velocity 5 m/s*

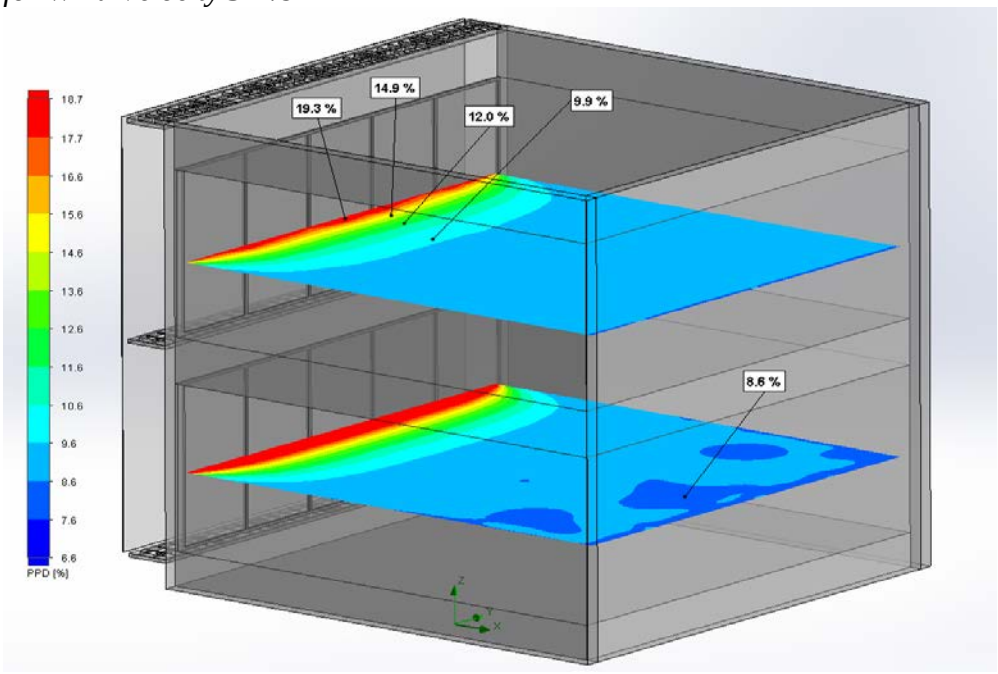

In the configuration where openings on the interior facade of the building are totally closed, the PMV values were observed about -0.75 at the space close to the building interior facade transparent surface, and about -0.35 at farther internal spaces at ground floor 1.8 m level while the peripheral temperature is 15 °C, exterior flow velocity is 5 m/s, and fixed indoor temperature is 23 °C. It was observed between values 0.75 and -0.45 at 1.8 m elevation upstairs. In the same configuration and levels, the PPD values were observed 18% close to the transparent surface of the building interior facade surface, about 10% further into the interior space, is occasionally 8% at ground floor 1.8 m level. At 1.8 m level of the upper floor, 10% and 18% values were observed at this time respectively at the spaces of the interior space behind the opening and spaces close to the opening (Figures 28-29).

Air Gap Width 80 cm - All Openings-Closed Configurations for Wind Velocity 5 m/s - Relative Humiditiy in Interior of Building (%)

Figure 30. *Relative Humiditiy in Interior of Building (%) for Wind Velocity 5 m/s*

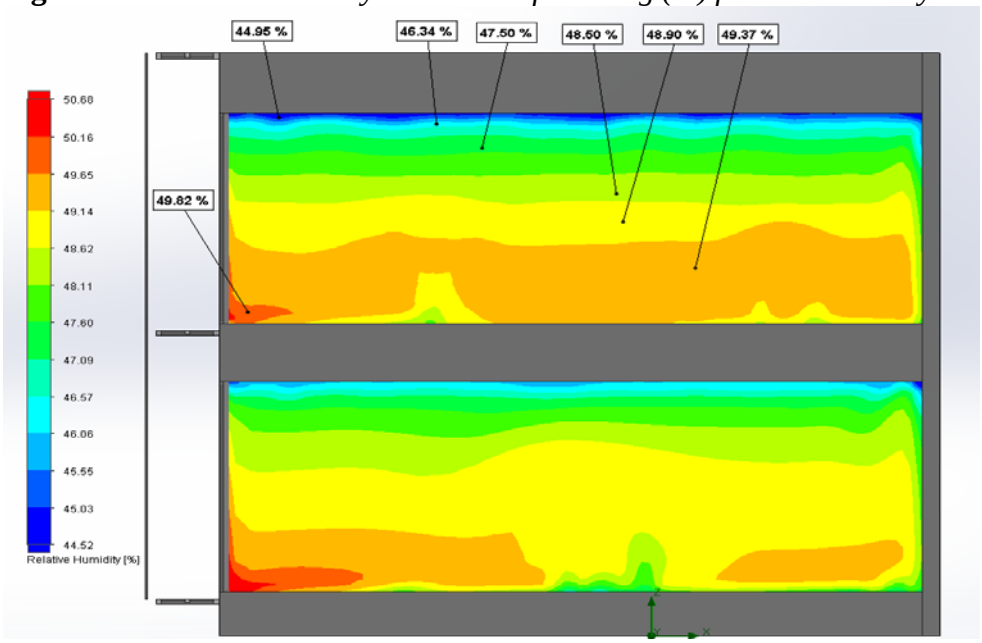

In the configuration where both openings on the interior facade of the building are totally closed, the building ground floor and upper floor interior space relative humidity values average has been observed about 48% while the peripheral temperature is 15 °C, exterior flow velocity is 5 m/s, and fixed indoor temperature is 23 °C. (Figure 30).

Air Gap Width 80 cm - All Openings-Closed Configurations for Wind Velocity 15 m/s - Air Flow Temperature in Interior of Building (°C)

Figure 31. *Air Flow Temperature in Interior of Building (°C) for Wind Velocity 15 m/s*

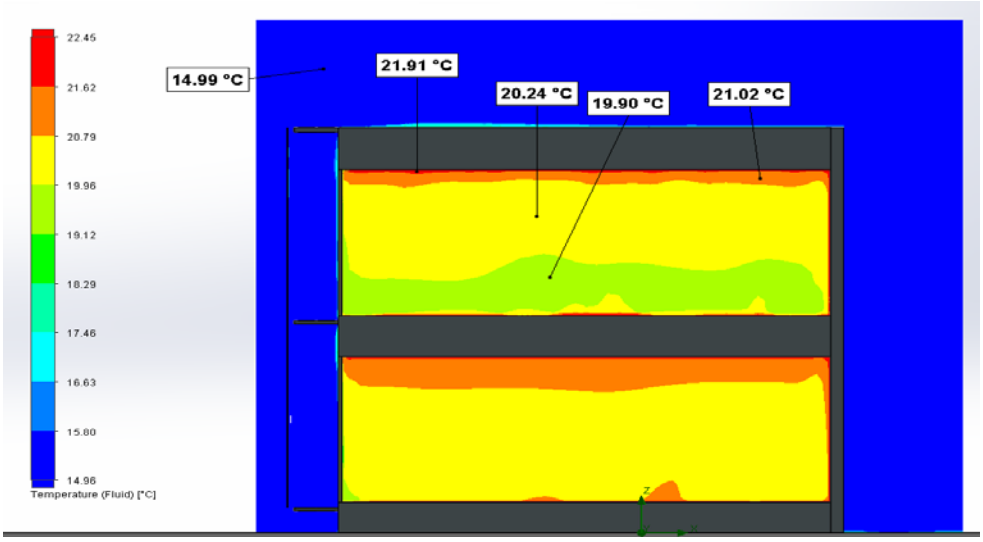

In the configuration where both openings on the interior facade of the building are totally closed, the interior space temperature values of ground floor interior space flow temperature average has been observed between 20 °C - 21 °C while the peripheral temperature is 15 °C, exterior flow velocity is 5 m/s, and fixed indoor temperature is 23 °C, and exterior flow speed is 5 m/s because the building openings are totally closed and there is no incoming flow. The upstairs interior space average temperature values are about 20 °C (Figure 31).

Air Gap Width 80 cm - All Openings-Closed Configurations for Wind Velocity 15 m/s - Interior Facade Temperature Distribution (Between two Facades) (°C)

Figure 32. *Interior Facade Temperature Distribution-Vertical (Between Two Facades) (°C) for Wind Velocity 15 m/*s

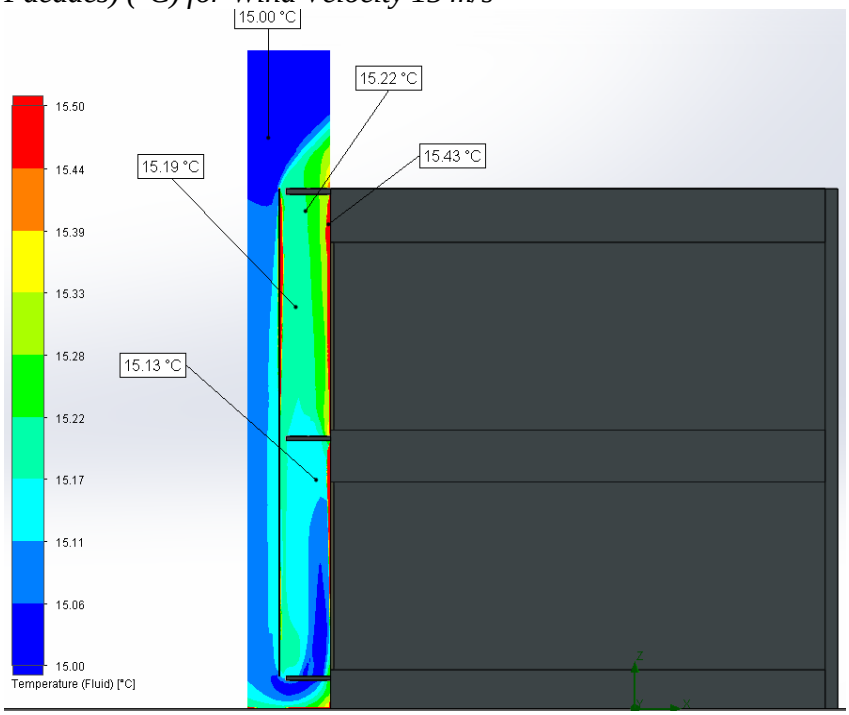

In the configuration where both openings on the interior facade of the building are totally closed, it has been observed that flow temperature value increases in proportion with upward flow from the double facade to the exterior facade surface toward between the two facades at ground level while the peripheral temperature is 15 °C, exterior flow velocity is 15 m/s, and fixed indoor temperature is 23 °C (Figure 32).

Figure 33. *Interior Facade Temperature Distribution-Horizontal (Between Two Facades) (°C) for Wind Velocity 15 m/s*

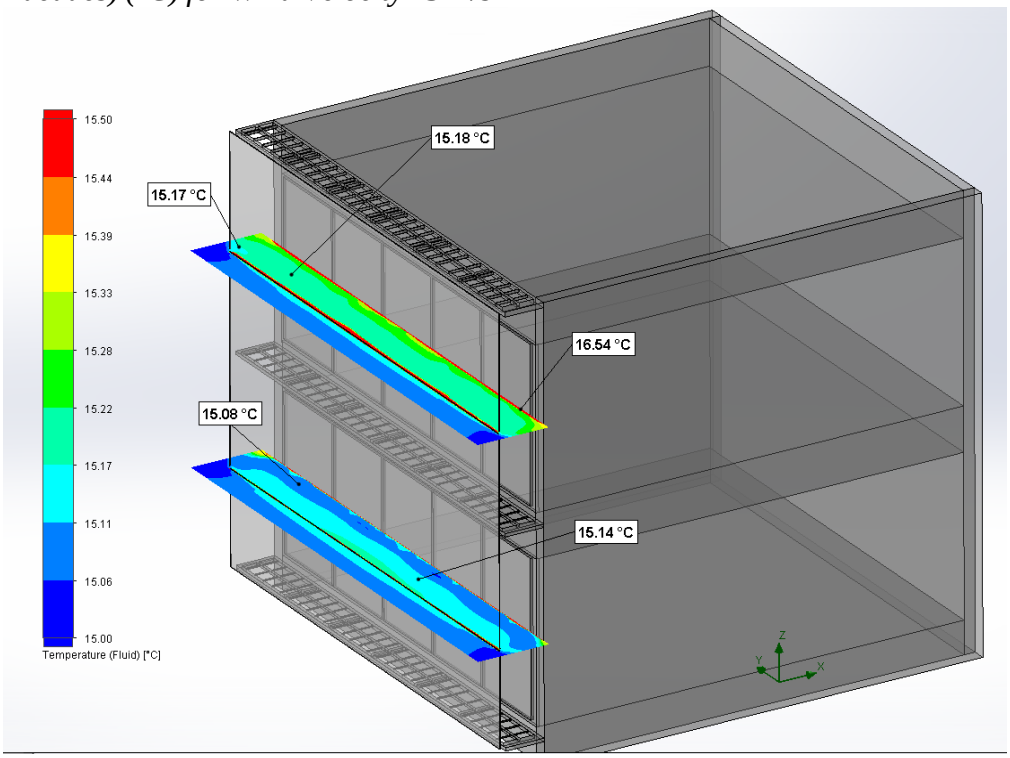

In the configuration where both openings on the interior facade of the building are totally closed, it has been observed that the flow temperature value of flow from double facade exterior facade surface toward between the two facades at ground level was 15 °C, and the upper space ground floor level was about 17 °C while the peripheral temperature is 15 °C, exterior flow velocity is 15 m/s, and fixed indoor temperature is 23 °C (Figure 33).

Air Gap Width80 cm - All Openings-Closed Configurations for Wind Velocity 15 m/s - Interior Facade Wind Velocity-Wind Distribution (°C)

Figure 34. *Wind Velocity-Wind Distribution in DSF and Around Building for Wind Velocity 15 m/s*

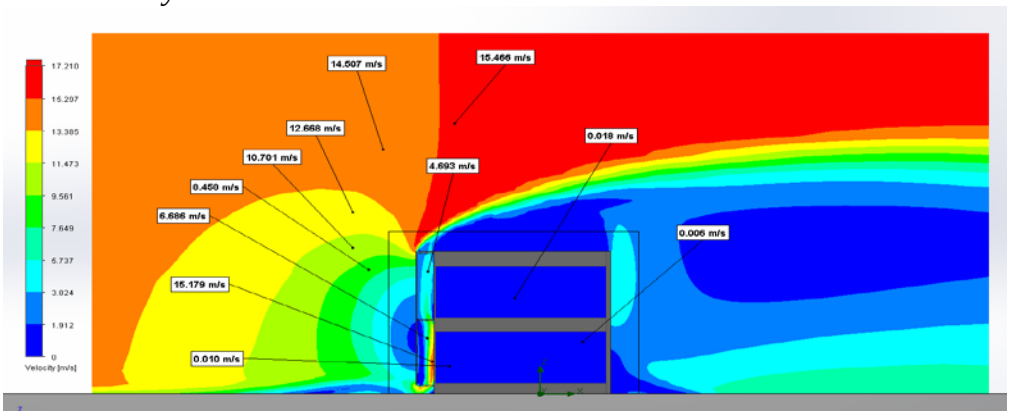

Figure 35. *Wind Velocity-Wind Distribution in DSF for Wind Velocity 15 m/s*

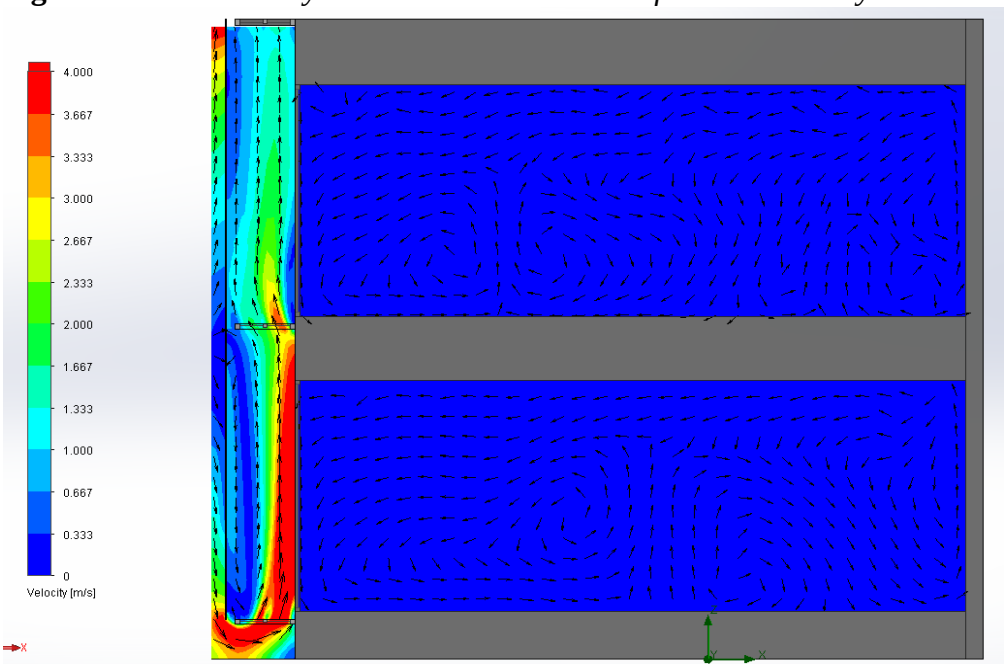

In the configuration where both openings on the interior facade of the building are totally closed, the wind velocity values between two facades have been observed to increase up to 17 m/s instantly at ground level, and reduce down to 4-5 m/s at the upper floor level, while the peripheral temperature is 15 °C, exterior flow velocity is 15 m/s, fixed indoor temperature is 23 °C, and exterior flow speed is 10-12m/s at building level (Figures 34-35).

Figure 36. *Wind Velocity-Wind Distribution Interior of Building for Wind Velocity 15 m/s*

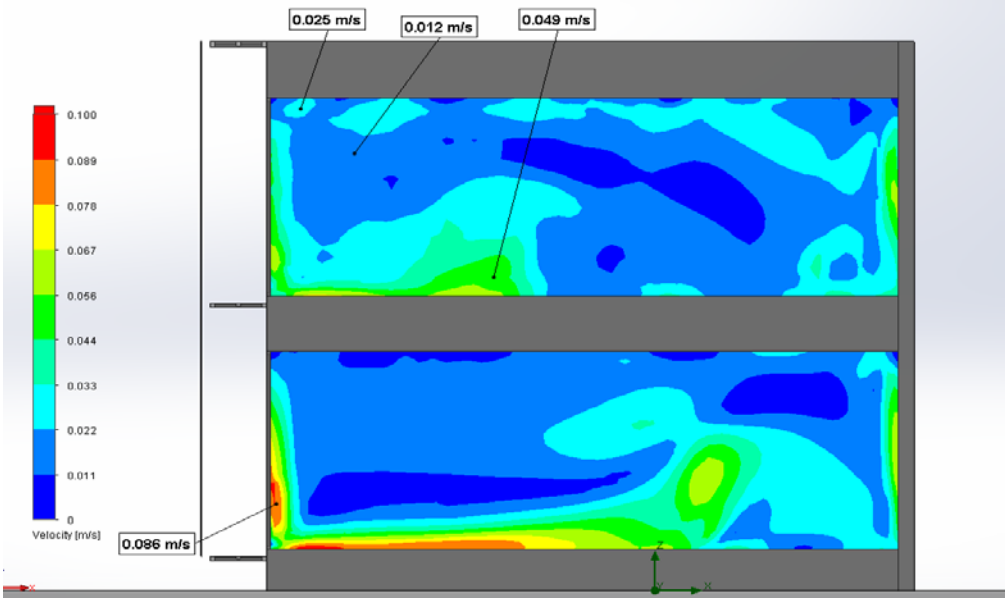

Figure 37. *Section of Wind Velocity-Wind Distribution of Interior of Building for Wind Velocity 15 m/s*

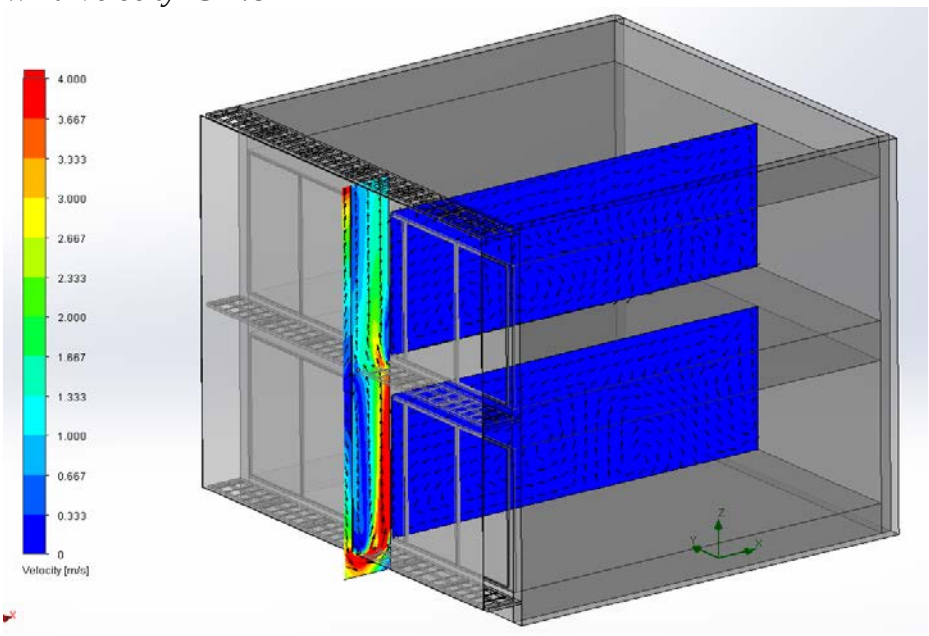

In the configuration where all openings are totally closed, it has been observed that while the building exterior flow velocity value is 15 m/s , the interior space flow velocity values were about 0.02-0.03 m/s on average (Figures 36-37).

Air Gap Width 80 cm - All Openings-Closed Configurations for Wind Velocity 15 m/s - Outside Facade Temperature Values of Distribution (°C)

Figure 38. *Outside in Front of Facade Building Temperature Values of Distribution (°C) for Wind Velocity 15 m/s*

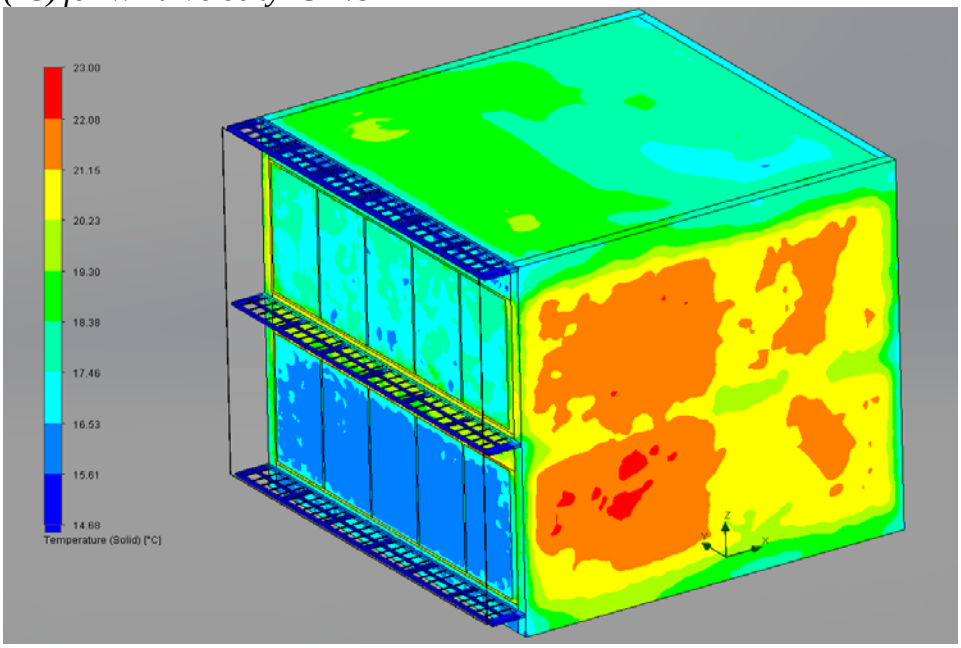

In the configuration where both openings on the interior facade of the building are totally closed, the building's exterior surface temperature distribution values, particularly ground floor building facade and indoor facade, have transparent surface temperature values that have been observed at 14-15 °C and upper floor level opening area transparent surface temperature value about 19 °C while the peripheral temperature is 15 °C, exterior flow velocity is 15 m/s, fixed indoor temperature is 23 °C. Besides, the building side surface temperature distribution average has been observed between 20-21 °C (Figure 38). As to the exterior flow fixed value analysis with exterior flow velocity value 15 m/s while building interior facade transparent surface temperature distribution average values are 19-20 °C while building exterior flow velocity value is 5 m/s, it has been observed that the average values of building interior facade transparent surface temperature distribution rise up to 22 m/s. It has been observed that the increase in the exterior flow velocity caused a fall on the average double skin Facade interior Facade temperature values (Figure 39).

Air Gap Width 80 cm - All Openings-Closed Configurations for Wind Velocity 15 m/s - PMV and PPD Values in Building Zones

Figure 40. *PMV and PPD Values in Building Zones of Bottom Side Openings Level for Wind Velocity 15 m/s*

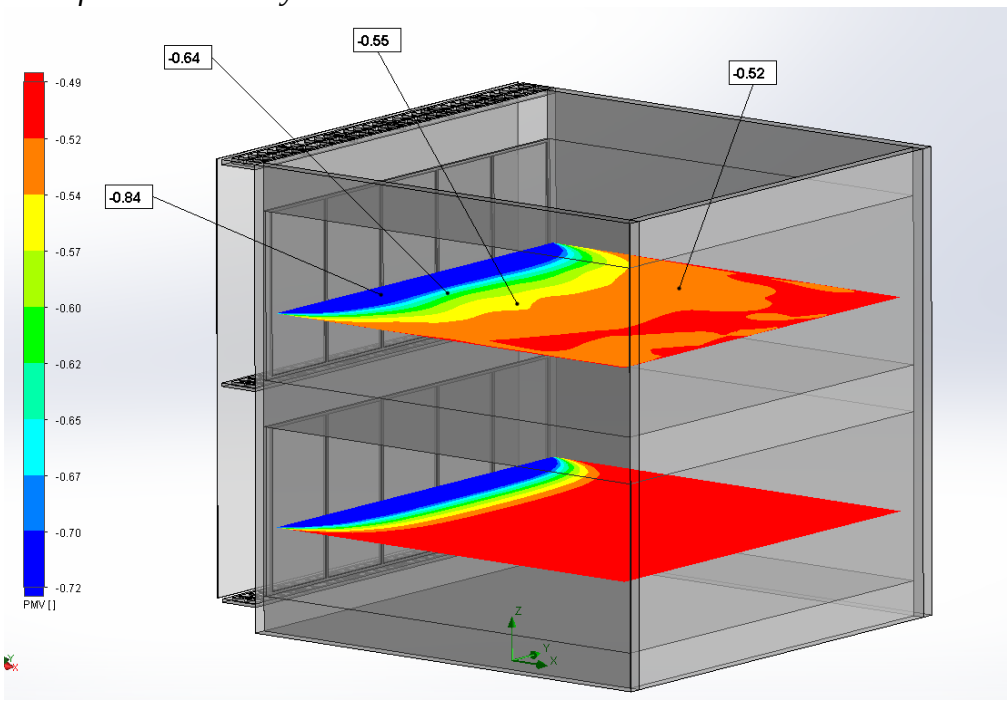

Figure 41. *PMV and PPD Values in Building Zones of Upper Side Openings Level for Wind Velocity 15 m/s*

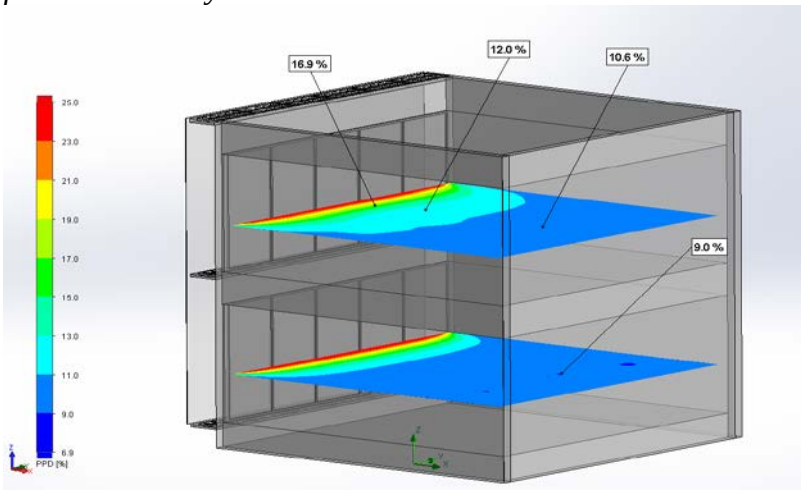

In the configuration where both openings on the interior facade of the building are totally closed, the PMV values were observed between -0.75 and -0.60 at the space close to the building interior facade transparent surface, and about 0.35 backwards at ground floor 1.8 m level while the peripheral temperature is 15 °C, exterior flow velocity is 15 m/s, and fixed indoor temperature is 23 °C. It was observed that the internal space average PMV value is about -0.52 at 1.8 m elevation upstairs.

Examining PPD values in the same configuration and levels, values of 10% have been observed at 1.8 m level of the ground floor, values between 11% and 13% at spaces mostly behind the opening area of the interior space, and values between 20-25% at locations close to the opening space (Figures 39-41).

Air Gap Width80 cm - All Openings-Closed Configurations for Wind Velocity 15 m/s - Relative Humiditiy in Interior of Building (%)

Figure 42. *Relative Humiditiy in Interior of Building (%) for Wind Velocity 15 m/s*

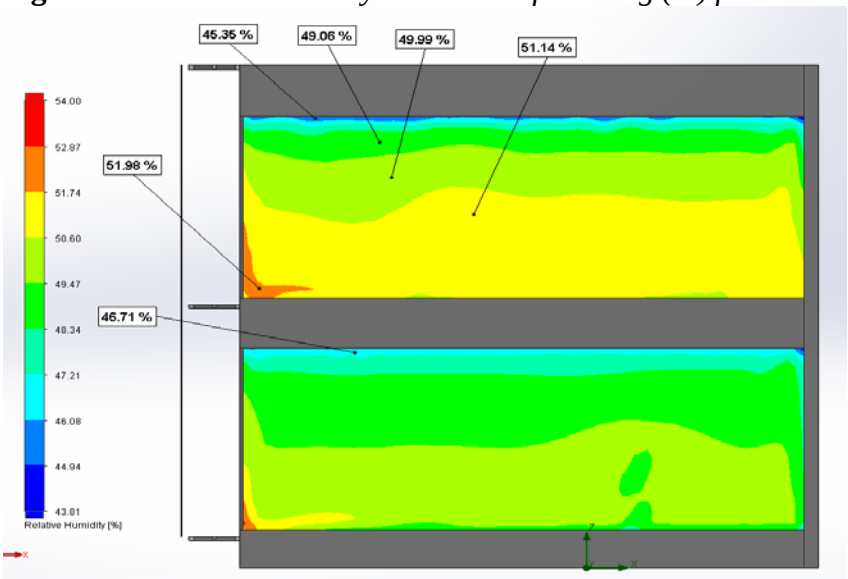

In the configuration where both openings on the interior facade of the building are totally closed, the building's ground floor relative humidity values average has been observed about 48% and upper floor interior space relative humidity values average about 52% at spaces close to the openings while the peripheral temperature is 15 °C, exterior flow velocity is 15 m/s, and fixed indoor temperature is 23 °C (Figure 42).

Evaluation of the Effects of Wind Speed Between Multiple Facades for 5 m/s Wind Flow Speed Conditions, Building Interior Operative Temperature, Mean Relative Humidity, Air Diffusion Performance Index Values on Microclimatic Comfort

An examination of the building's wind flow values on the ground floor in analysis studies with an exterior wind flow speed of 5 m/s has shown that in configurations where all cavities are open, there are configurations with highest flow amounts and flow rates within the space. However, in the case where all cavities are open in the three configurations, it is seen that the configuration with the highest flow and flow rate into the space is DSF 1 where the width between two facade is 80 cm (Figure 43).

Figure 43. *Ground Floor Interior Wind Velocity - For Wind Speed 5 m/s*

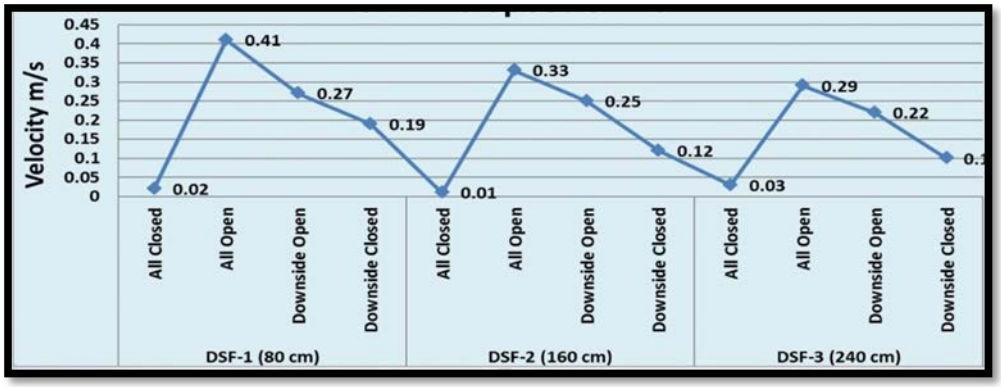

In analyses with exterior wind flow rate 5 m/s on the ground floor plane in DSF-1 configuration, the flow into the space increased the indoor fixed flow rate value to 0.4 m/s value, and it was observed that the increase reduced the fixed indoor temperature value, which was 23 °C at the same time, to 19.27 °C (Figure 44). Furthermore, an examination of other analysis results regarding the cavities on the inner facade showed that the case where the downside open case on the facade ensured increased flow and speed indoor compared to the alternative case in terms of indoor flow rate and amount values (Figure 43).

Figure 44. *Ground floor Interior Operative Temperature (t0) - For Wind Speed 5 m/s*

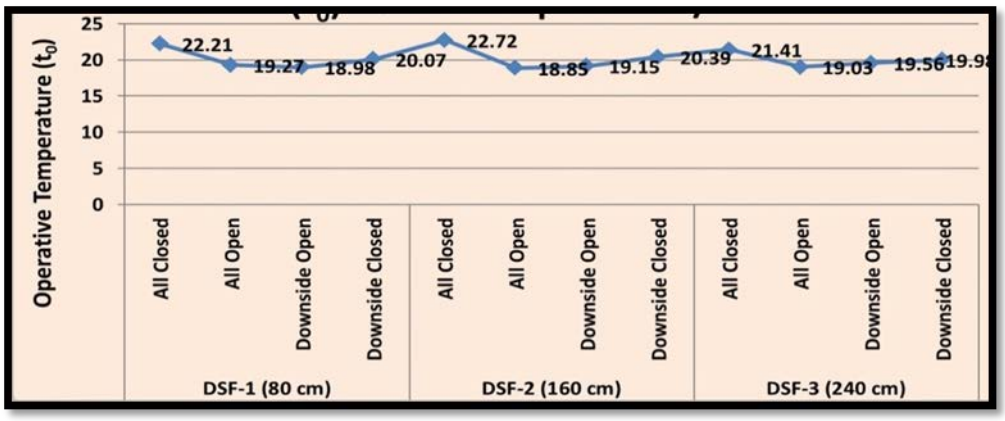

An examination of the indoor relative humidity values on the ground floor plane in analysis studies with an exterior wind flow rate of 5 m/s has shown that the case with the lowest relative humidity comfort value (48%) is seen in configurations where all cavities are closed on the Facade (Figure 44).

Figure 45. *Ground Floor Mean Relative Humidity (%) - For Wind Speed 5 m/s*

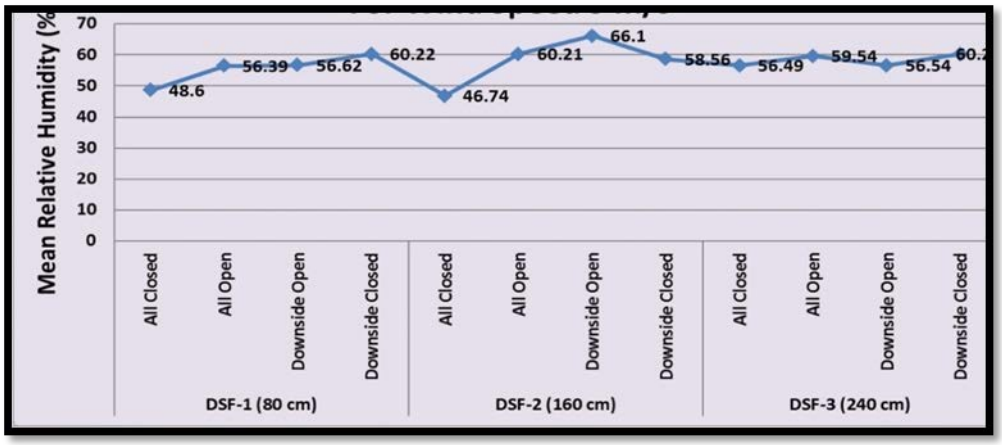

ADPI (Air Diffusion Performance Index) is defined as the percentage of locations in the occupied space which meet the comfort criteria based on velocity and temperature measurements taken at a given number of uniformly distributed points. This ADPI value has proven to be a valid measure of an air diffusion system. The higher the ADPI rating, the higher the quality of room air diffusion within the space, Generally an ADPI of 80 is considered acceptable.

In examination of the acceptable comfort level of the flow to indoor of all ground floor indoor configurations in analysis studies where exterior wind flow rate is 5 m/s, it was seen that ASHRAE acceptable indoor comfort flow percentage according to standard 55 is 80% and above, ADPI percentage is 33% in DSF-1, 46% in DSF-2 and 70% in DSF-3 according to acceptable reference where cavities on the building inner facade are completely open, while ADPI percentage rose to

90% and above in downside closed upside open, or upside open configurations (Figure 46).

Figure 46. *Ground floor Air Diffusion Performance Index (%) - For Wind Speed 5 m/s*

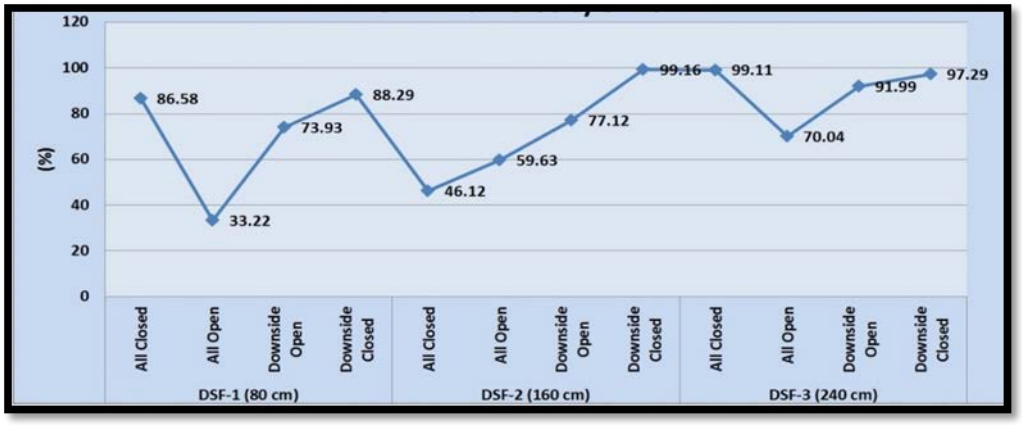

An examination of the building wind flow values on the first floor plane in analysis studies with an exterior wind flow rate of 5 m/s has shown that in configurations where all cavities are open, there are configurations with highest flow amounts and flow rates within the space. However, in the case where all cavities are open in the three configurations, it is seen that the configuration with the highest flow and flow rate into the space is DSF 2 where the widthbetween two facades is 160 cm (Figure 47).

Figure 47. *First floor İnterior Wind Velocity - For Wind Speed 5 m/s*

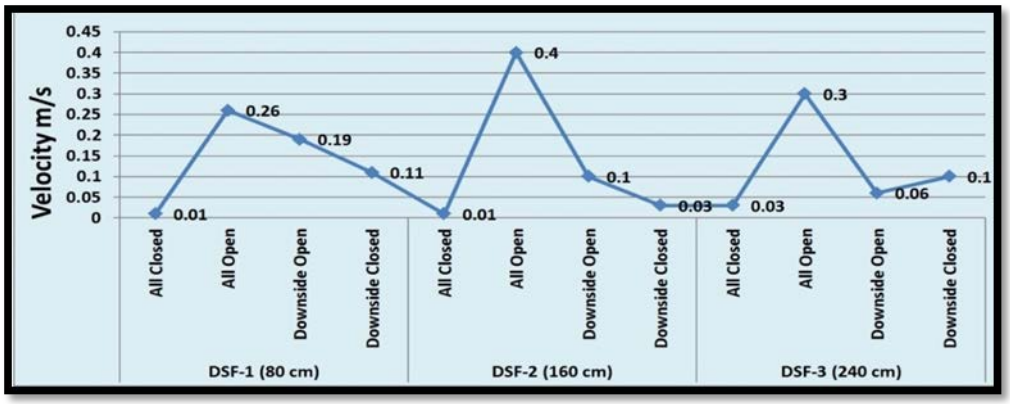

In analyses with exterior wind flow rate 5 m/s on the first floor plane in DSF-1 configuration, the flow into the space increased the indoor fixed flow rate value to 0.3 m/s value, and it was observed that the increase reduced the fixed indoor temperature value, which was 23 °C at the same time, to 18.78 °C (Figure 48).

Figure 48. *First floor Interior Operative Temperature (t0) - For Wind Speed 5 m/s*

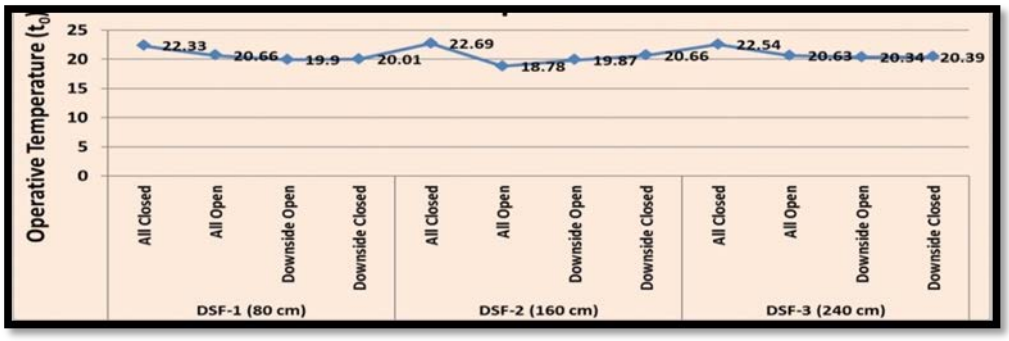

An examination of the indoor relative humidity values on the ground floor plane in analysis studies with an exterior wind flow rate of 5 m/s has shown that the case with the lowest relative humidity comfort value (48%) is seen in configurations where all cavities are closed on the facade (Figures 48-49).

Figure 49. *First Floor Mean Relative Humidity (%)- For Wind Speed 5 m/s*

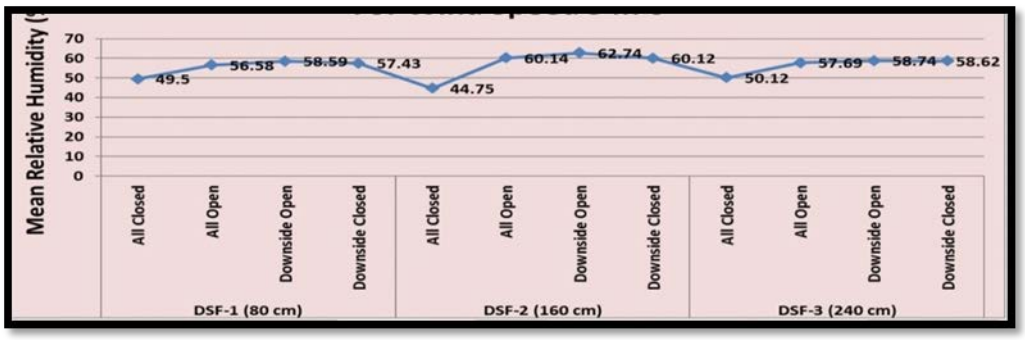

On examination of the acceptable comfort level of the flow to indoor of all first floor indoor configurations in analysis studies where exterior wind flow rate is 5 m/s, it was seen that according to acceptable reference of standard 55 of ASHRAE acceptable indoor comfort flow percentage of 80% and above; 80% and above ADPI levels of performance was observed in configurations other than all closed ones (Figure 50).

Figure 50. *First Floor Air Diffusion Performance Index (%)-For Wind Speed 5 m/s*

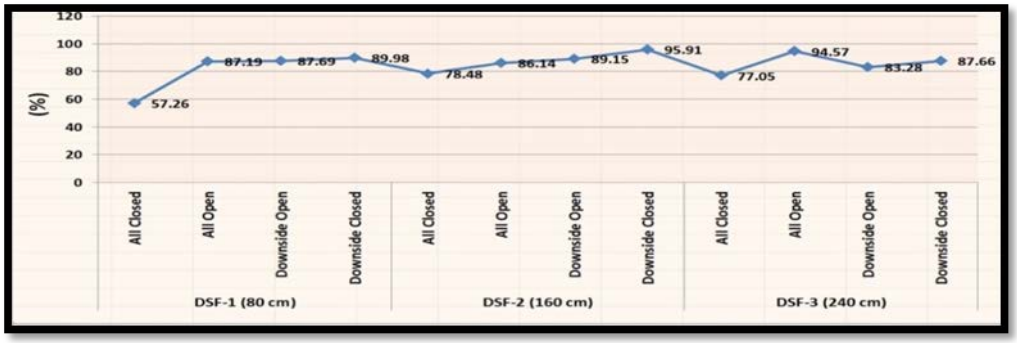

An examination of the building's wind flow values on the ground floor plane in analysis studies with an exterior wind flow rate of 15 m/s has shown that the option downside open on the facade is the configuration with highest flow amount and flow rate into the space. However, in DSF-2 configuration, the highest flow and highest speed (0.88 m/s) to indoor in DSF-2 configuration was seen in all open option. An examination of the DSF-3 configuration analysis results shows that the option downside open is the configuration with highest flow amount and flow rate (0.79 m/s) into the space (Figures 50-51). Nevertheless, the case whereby the flow rate is highest to the interior space has been seen in the all open configuration where exterior wind speed is 5 m/s.

Evaluation of the Effects of Wind Speed Between Multiple Facades for 15 m/s Wind Flow Speed Conditions, Building Interior Operative Temperature, Mean Relative Humidity, Air Diffusion Performance Index Values on Microclimatic Comfort

Figure 51. *Ground Floor Interior Wind Velocity - For Wind Speed 15 m/s*

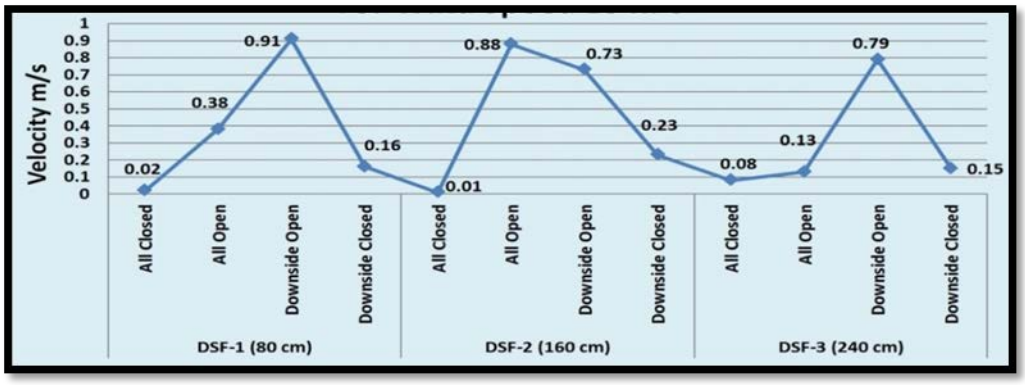

In analyses with exterior wind flow rate 15 m/s on the ground floor plane in the downside open option with the highest indoor flow amount and flow rate in DSF-1 configuration, the fixed flow indoor increased the flow rate to 0.9 m/s, and it was observed that the increase reduced the fixed indoor temperature value, which was 23 °C at the same time, to 17.74 °C (Figure 52).

Figure 52. *Ground floor Interior Operative Temperature (t0) - For Wind Speed 15 m/s*

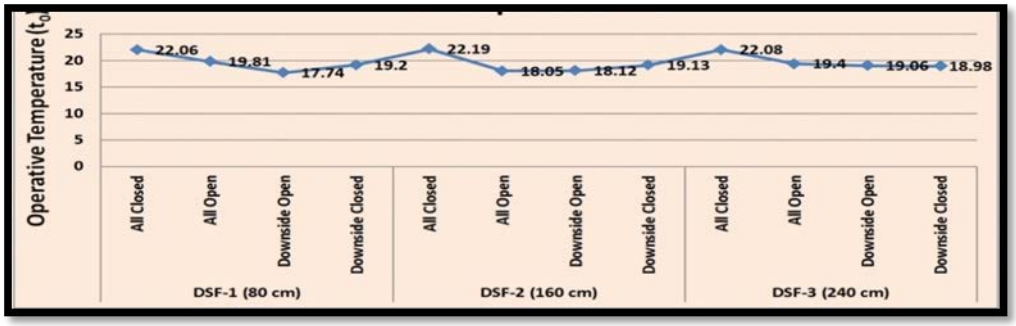

In the analysis works where exterior wind speed is 15 m/s, examination of the indoor relative humidity values on the ground floor plane showed that the case

whereby the relative humidity comfort values are the lowest (46%) is the configurations whereby all cavities on the facade are closed (Figure 53).

Figure 53. *Ground Floor Mean Relative Humidity (%) - For Wind Speed 15 m/s*

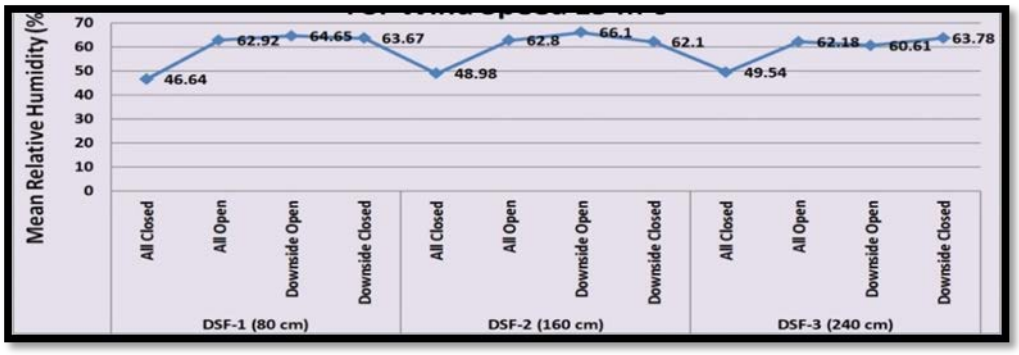

On examination of the acceptable comfort level of the flow to indoor of all ground floor indoor configurations in analysis studies with an exterior wind speed of 15 m/s, it was seen that according to ASHRAE standard 55 reference stipulating acceptable indoor comfort flow percentage of 80% and above, ADPI percentage is 89% in DSF-1 in downside closed case, ADPI percentage is 89% in DSF-2 in downside open case and of 89% and above in DSF-3 in both downside open and downside closed configurations (Figure 54).

Figure 54. *Ground floor Air Diffusion Performance Index (%)-For Wind Speed 15 m/s*

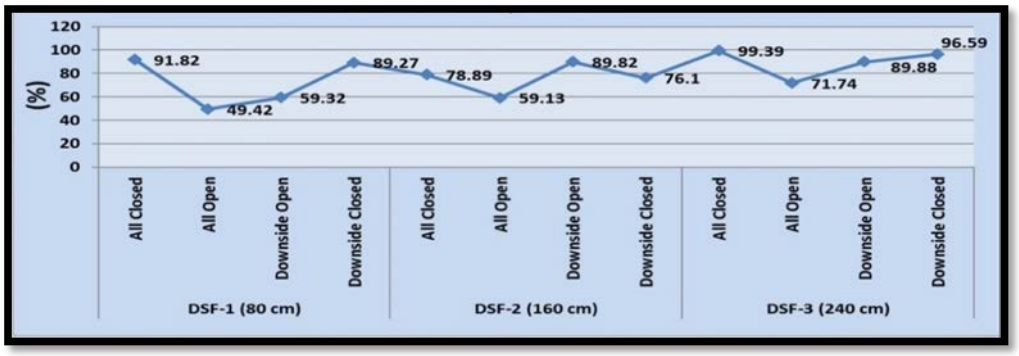

An examination of the building wind flow values on the first floor in analysis studies with an exterior wind flow rate of 15 m/s has shown that the configurations with the highest flow amount and flow speed (0.63 m/s) into the space is DSF-3, the downside open configuration of the cavities on the facade. Nevertheless, an examination of the analysis study results where exterior wind flow speed is 5 m/s, it was observed that the configuration with highest flow reaching highest speeds is the all open configurations of the facade. In analysis studies with an exterior wind flow speed of 15 m/s, it has been seen that the highest flow speed and flow amount (0.39 m/s) is in DSF-2 all open configurations on the first floor (Figure 55).

Figure 55. *First Floor Interior Wind Velocity - For Wind Speed 15 m/s*

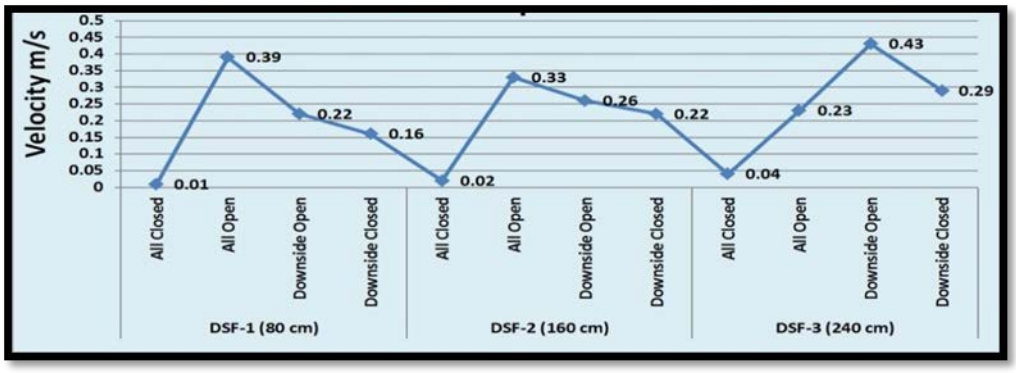

In analyses with exterior wind flow speed 15 m/s, it has been observed that the flow into the space on the first floor plane in DSF-3 configuration increased the indoor fixed flow rate value of the downside open configuration to 0.63 m/s value, and that the increase reduced the fixed indoor temperature value, which was 23 °C at the same time, to 18.09 °C (Figure 56).

Figure 56. *First floor Interior Operative Temperature (t0) - For Wind Speed 15 m/s*

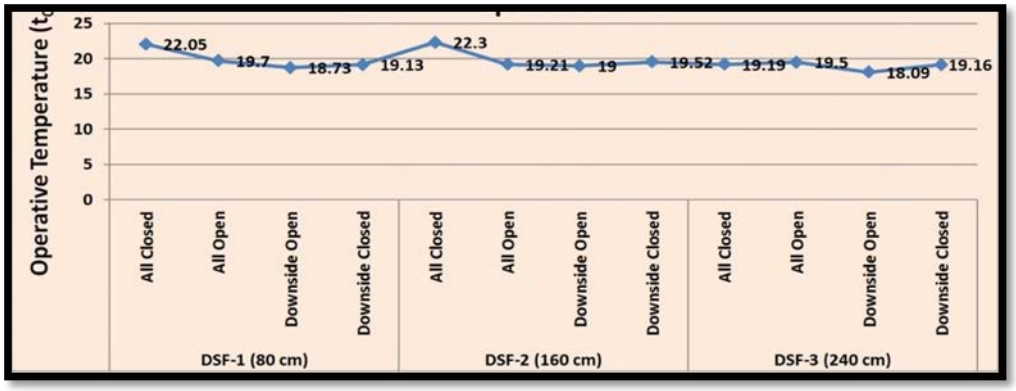

In the analysis works where exterior wind speed is 15 m/s, examination of the indoor relative humidity values on the ground floor plane showed that the case whereby the relative humidity comfort values are the lowest (48%) is the configurations whereby all cavities on the facade are closed (Figure 45). As to the examination of the relative humidity values in configurations where there is inward flow, the lowest values are observed approximately at 57% level in all open case (Figure 57).

Figure 58. *First Floor Mean Relative Humidity (%)- For Wind Speed 15 m/s*

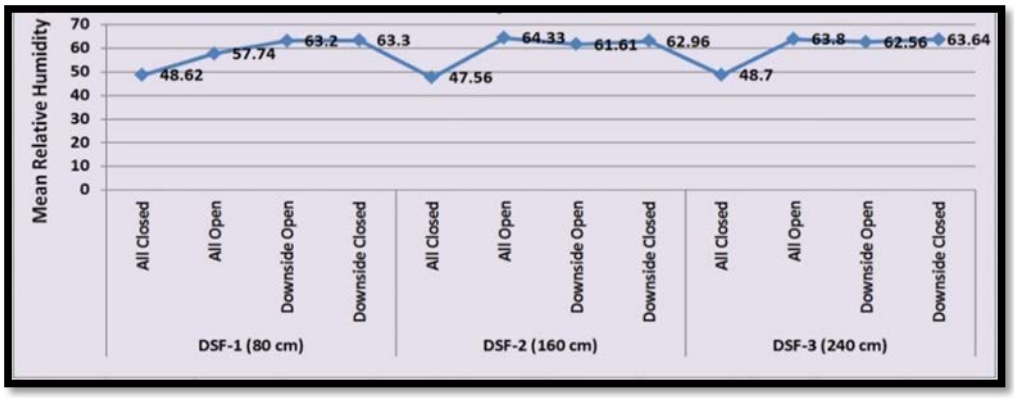

On examination of the acceptable comfort level of the flow to indoor of all first floor indoor configurations in analysis studies where exterior wind flow rate is 15 m/s, it was seen that according to acceptable reference of standard 55 of ASHRAE acceptable indoor comfort flow percentage of 80% and above; 80% and above ADPI levels of performance were observed in all configurations other than all closed and all opened ones (Figure 52). Nevertheless, on examination of the first floor indoor ADPI percentages where exterior wind flow rate is 15 m/s, it was seen that 80% and above values were obtained in configurations other than all closed ones (Figure 59).

Figure 59. *First Floor Air Diffusion Performance Index (%) - For Wind Speed 15 m/s*

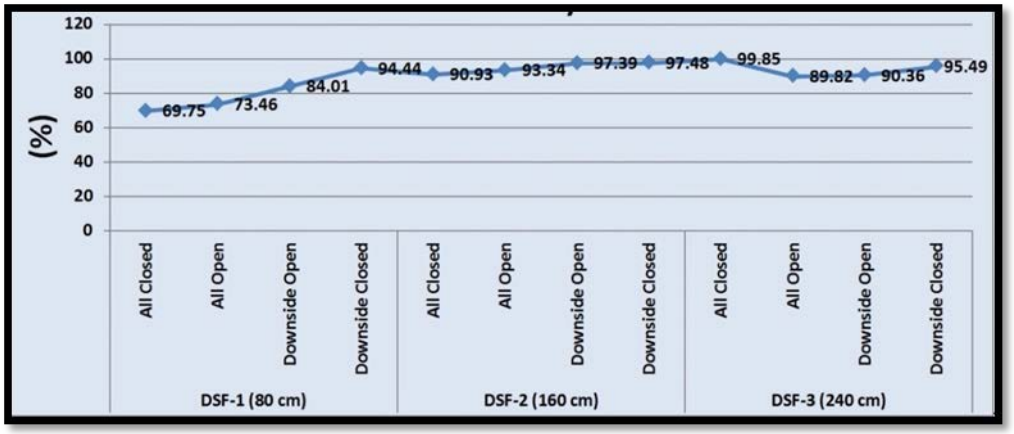

Solar Heat Flux and Total Heat Transfer Rate Values from the Interior Facade for Air Gap Width 80 cm Configurations

In building configuration where DSF Widthbetween two facade is 80 cm and all building surface openings are closed, the building surface area is 320 m^2, and the surface area between two facades is 58.4 m^2.

In the configuration where both openings on the interior facade of the building are totally closed, the solar heat flux value was 0.315 W/m^2 over the 320

m^2 interior surface of the building while the peripheral temperature is 15 °C, exterior flow velocity is 5 m/s and fixed indoor temperature is 23 °C, and the solar heat flux value over the interior surface of the building was 0.625 W/m^2 over the building interior surface while the total heat transfer rate value is 101 W/m^2 and exterior wind velocity speed was 15 m/s.

In the configuration where the openings on the interior facade of the DSF building are totally closed, the wind flow velocity average between two facades has been 1.8 m/s while the peripheral temperature is 15 °C, exterior flow velocity is 5 m/s, and fixed indoor temperature is 23 °C, and the average wind flow velocity value between two facades has been observed 4.9 m/s where the exterior wind flow is 15 m/s.

ACH Value for Air Gap Width 80 cm Configurations

ACH (Air Change Per Hour) Value is (1 ACH = 46 m^3/h; Total volume 46 m^3). In the configuration where both openings on the interior facade of the building are totally closed, ACH ratio at 58.4 m^2 between two facades is 1.996, and the total flow rate value is 91.80 while the peripheral temperature is 15 °C, exterior flow velocity is 5 m/s, fixed indoor temperature is 23 °C. ACH ratio at 58.4 m^2 between two facades is 5.872 and the total flow rate value is 270 while the exterior flow velocity is 15 m/s.

In the configuration where both openings on the interior facade of the building are open, the wind velocity values between two facades have been observed to fall down to 2-4 m/s while the exterior velocity values are about 8-10 m/s at building level while the peripheral temperature is 15 °C, exterior flow velocity is 15 m/s, fixed indoor temperature is 23 °C.

While it has been observed that the building exterior flow velocity value is 5 m/s, the flow velocity value approached the exterior flow level; and it has been observed in the 15 m/s exterior flow fixed value analysis that the instant flow velocity values between two facades fell down from about 15 m/s to 2-4 m/s. In this case, it has been observed that the wall effect of the exterior Facade reduced velocity values quite high in transition to between interior Facade. Besides, where exterior flow velocity is 15 m/s, it has been observed that the flow amount passing from the openings at the upper floor interior space was less compared to the 5 m/s velocity value.

Microclimatic Thermal Comfort and Temperatures of the Interior Wall

Since the air inside the double skin facade air gap is warmer than the outdoor air during the heating period, the interior part of the facade can maintain temperatures that are closer to the microclimatic thermal comfort levels. On the other hand, it is really important that the system and space between the double facade should well designed, so efficient heat extraction ensures that the temperatures inside the air gap do not increase dramatically, leading to high operative temperatures.

In the configuration where both openings on the interior facade of the building are open, the wind velocity values between two facades have been observed to fall down to 2-4 m/s, while the exterior velocity values are about 8-10 m/s at building level; while the peripheral temperature is 15 °C, exterior flow velocity is 15 m/s, fixed indoor temperature is 23 °C.

While it has been observed that the building exterior flow velocity value is 5 m/s, the flow velocity value approached the exterior flow level; and it has been observed in the 15 m/s exterior flow fixed value analysis that the instant flow velocity values between two facades fell down from about 15 m/s to 2-4 m/s. In this case, it has been observed that the wall effect of the exterior facade reduced velocity values quite high in transition to between interior facade.

Besides, where exterior flow velocity is 15 m/s, it has been observed that the flow amount passing from the openings at the upper floor interior space was less compared to the 5 m/s velocity value. In the configuration where both openings on the interior facade of the building are open, the building interior flow velocity has been observed that the flow toward the interior from the openings on the building change the building flow and temperature values when the exterior flow velocity is 5 m/s while the peripheral temperature is 15 °C, exterior flow velocity is 5 m/s, and fixed indoor temperature is 23 °C. It has been observed that while the ground floor indoor flow values are about 1.5 m/s close to the openings, the flow velocity values inward at the vicinity of the opening are about 0.4-0.7 m/s.

Conclusions

One of the main advantages of the double skin facade systems is that they can allow natural (or fan supported) ventilation. Different types can be applied in different climates, orientations, locations and building types in order to provide fresh air before and during the working hours. The selection of a double skin facade type can be crucial for temperatures, air velocity, and the quality of the introduced air inside the building. If designed well, the natural ventilation can lead to a reduction in energy use during the occupation stage and improve the comfort of the occupants. In this study, discussed analysis studies where the exterior flow rate is 5 m/s and 15 m/s and the flow temperature is 15 °C, it has been observed that the exterior flow and conditions have different values in terms of their effects on the ground floor or upper floor indoor space comfort, three different DSF configurations discussed, and different air gap scenarios of each configuration on the facade. The obtained results presented as a natural ventilation and microclimatic comfort of occupants

On examination of the indoor flow rate and operative temperature values of both the ground floor and upper floor where exterior flow is 5 m/s, it has been observed that the flow to the interior volume is the highest in the option were cavities are all open and in all three configurations (DSF-1, DSF-2, DSF-3) and the highest of the flow rate values were seen. It was seen that the indoor flow rate values are about 0.4 m/s, and the flow reduced the indoor temperature values by 4-5 °C. Accordingly, an examination of to what extent the flow indoors affects

indoors ADPI comfort percentage levels revealed that 80% and above values suggested by ASHRAE-55 standard were reached in downside closed options on the Facade in all three configurations (DSF-1, DSF-2, DSF-3).

However, it was observed that ADPI percentage is about 40-45% in all open options. 80% and above values for the upper floor indoor space ADPI comfort percentage have been seen in downside open and downside closed options. A comfort evaluation for the ground floor indoor space relative humidity percentages has shown that upper floor relative humidity percentage values are at higher levels. While values between 50% and 55% are obtained on the ground floor, the relative humidity percentage values for indoors on the upper floor are from 56% to 62%.

On examination of the indoor flow rate and operative temperature values of both the ground floor and upper floor, it has been observed this time that very different values and options emerge compared to analyses where exterior flow is 5 m/s. It has been seen that the highest indoor space flow rate values were realized at about 0.9 m/s in all three configurations (DSF-1, DSF-2, DSF-3) in downside open option for the cavities on the facade. The flow to the ground floor indoor space at this level of speed reduced the indoor temperature level down to about 17 °C.

An examination of to what extent the exterior flow affects indoors ADPI comfort percentage levels revealed that 80% and above values suggested by ASHRAE-55 standard were reached in downside closed option on the acade in DSF-1, and in downside open option of the facade cavities in DSF-2, and that 80% and above values were reached in both downside open and downside closed options in DSF-3. 80% and above values for the upper floor indoor space ADPI comfort percentage have been seen in downside open and downside closed options.In this study, detailed CFD calculations on three main different DSF, the influence of geometrical characteristics on airflows also was studied as a different aperture effects case compared with each DSF.

Although air gap width on DSF and windows openings or closed condition relatively influences on the amount of natural ventilation, it will directly change the value of ACH and indoor airflow coverage. For future studies on natural ventilated double-skin facade, closed window status can be disregarded, but a reasonable air gap width and dimension on DSF would be more practical because it provides a better indoor air distribution. Although there is more air in the wider air gap, when the air flow velocity values are compared, faster air flow was observed in the narrower air gap. Therefore, the use of both narrow and wide air gap of multiple facade in summer climatic conditions may be advantageous in terms of cooling the air warmed by solar radiation and natural ventilation.

Indoor and outdoor climate simulations have to be carried out already at an early design stage and then be refined during the actual design. This will ensure improved indoor and outdoor climate performance of the building. In order to achieve and improved microclimatic thermal environment it is essential to (a) validate the calculation methods, (b) carry out simulations on a component level in order, to gain the necessary background to the possibilities and limitations of the system, (c) prioritize the performance and quality requirements to be fulfilled and (d) carry out simulations on a different DSF width air gaps configurations and on a building level. Accordingly, the future Research s on should address the

performance characteristics of innovative materials used in multiple building facades, the number of layers and material relations, the relationship between DSF and the mechanical air conditioning used in the building.

Acknowledgments

This research project was supported by the Scientific and Technological Research Council of Turkey (TUBITAK) Foundation under grant number 1059B191400407.

References

Agathokleous RA, Kalogirou SA (2016) Double skin Facades (DSF) and building integrated photovoltaics (BIPV): a review of configurations and heat transfer characteristics. *Renewable Energy* 89(Apr): 743–756.

Alberto A, Ramos NMM, Almeida RMSF (2017) Parametric study of double-skin facades performance in mild climate countries. *Journal of Building Engineering* 12(Jul): 87–98.

ASHRAE (1999) *ANSI/ASHRAE Standard 62-1999, Ventilation for acceptable ındoor air quality*. Atlanta: American Society of Heating, Refrigerating, and Air-Conditioning Engineers, Inc.

ASHRAE Handbook 2009. Refrigerating and Air-Conditioning Engineers, Inc. American Society of Heating.

Baldinelli G (2009) Double skin Facades for warm climate regions: analysis of a solution with an integrated movable shading system. *Building and Environment* 44(6): 1107–1118.

Ballestini G, De Carli M, Masiero N, Tombola G (2007) Possibilities and limitations of natural ventilation in restored industrial archaeology buildings with a double-skin Facade in mediterranean climates. *Building and Environment* 40(7): 983–995.

Barbosa S, Ip K (2014) Perspectives of double skin Facades for naturally ventilated buildings: a review. *Renewable and Sustainable Energy Reviews* 40(Dec): 1019–1029.

Barták M, Dunovská T, Hensen J (2001) Design support simulation for a double-skin Facade. In *1st International Conference on Renewable Energy in Buildings, Sustainable Buildings and Solar Energy 2001*. Prague.

Chan A, Chow T, Fong K, Lin Z (2009) Investigation on energy performance of double skin Facade in Hong Kong. *Energy and Buildings* 41(11): 1135–1142.

Chow T, Lin Z, Fong K, Chan L, He M (2009) Microclimatic thermal performance of natural airflow window in subtropical and temperate climate zones – A comparative study. *Energy Conversion and Management* 50(8): 1884–1890.

Dama A, Angeli D, Larsen OK (2017) Naturally ventilated double-skin Facade in modeling and experiments. *Energy and Buildings* 144(Jun): 17–29.

De Gracia A, Castell A, Navarro L, Oró E, Cabeza LF (2013) Numerical modelling of ventilated Facades: a review. *Renewable and Sustainable Energy Reviews* 22(Jun): 539–549.

Ding W, Hasemi Y, Yamada T (2005) Natural ventilation performance of a double-skin Facade with a solar chimney. *Energy and Buildings* 37(4): 411–418.

Goodfellow H, Tahti E (2001) *Industrial ventilation design guidebook*. Academic Press.
Gosselin J, Chen Q (2008) A dual airflow window for indoor air quality improvement and energy conservation in buildings. *HVAC&R Research* 14(3): 359–372.
Gratia E, De Herde A (2007) Greenhouse effect in double-skin Facade. *Energy and Buildings* 39(2): 199–211.
Guardo A, Coussirat M, Egusquiza E, Alavedra P, Castilla R (2009) A CFD approach to evaluate the influence of construction and operation parameters on the performance of Active Transparent Facades in Mediterranean climates. *Energy and Buildings* 41(5): 534–542.
Hamza N (2008) Double versus single skin Facades in hot arid areas. *Energy and Buildings* 40(3): 240–248.
Hien WN, Liping W, Chandra AN, Pandey AR, Xiaolin W (2005) Effects of double glazed Facade on energy consumption, microclimatic thermal comfort and condensation for a typical office building ın Singapore. *Energy and Buildings* 37(6): 563–572.
Inan T, Basaran T (2019) Experimental and numerical investigation of forced convection in a double skin Facade by using nodal network approach for Istanbul. *Solar Energy* 183(May): 441–452.
Inan T, Başaran T, Erek A (2017) Experimental and numerical investigation of forced convection in a double skin Facade. *Energies* 10(9): 1364.
Inan T, Başaran T, Ezan MA (2016) Experimental and numerical investigation of natural convection in a double skin Facade. *Applied Thermal Engineering* 106(Jun): 1225–1235.
Ioannidis Z, Rounis E-D, Athienitis A, Stathopoulos T (2020) Double skin Facade integrating semi-transparent photovoltaics: experimental study on forced convection and heat recovery. *Applied Energy* 278(Nov): 115647.
Kato H, Yoon G, Tanaka H, Hatate Y, Yoshida M, Torigoe Y, et al. (2008) Effectiveness of reducing heating and cooling load by using double skin Facade coupling the earth-to-air heat exchanger. In *7th International Conference on Sustainable Energy Technology*. Seoul.
Khalvati F, Omidvar A (2019) Summer study on microclimatic thermal performance of an exhausting airflow window in evaporatively-cooled buildings. *Applied Thermal Engineering* 153: 147–158.
Lancour X, Deneyer A, Blasco M, Flamat G, Wouters P (2012) *Ventilated double Facades: classification & illustration of Facade concepts*. Available at: http://www.bbri.be/activefacades/new/download/Ventilated%20Doubles%20Facades%20-%20Classification%20&%20illustrations.dvf2%20-%20final.pdf.
Manz H, Frank T (2005) Microclimatic thermal simulation of buildings with double-skin Facades. *Energy and Buildings* 37(11): 1114–1121.
Mulyadi R (2012) *Study on naturally ventilated double-skin Facade in hot and humid climate*. PhD Dissertation. Japan: Nagoya University.
Nasrollahi N, Salehi M (2015) Performance enhancement of double skin Facades in hot and dry climates using wind parameters. *Renewable Energy* 83(Nov): 1–12.
Oesterle E, Lieb R-D, Lutz M, Heusler W (2001) *Double skin Facades – Integrated planning*. Munich, Germany: Prestel Verlag.
Pappas A, Zhai Z (2008) Numerical investigation on microclimatic thermal performance and correlations of double skin Facade with buoyancy-driven airflow. *Energy and Buildings* 40(4): 466–475.
Park C, Augenbroe G, Messadi T, Thitisawat M, Sadegh N (2004) Calibration of a lumped simulation model for double-skin facade system. *Energy and Building* 36(11): 1117–1130.

Pasut W, De Carli M (2012) Evaluation of various CFD modelling strategies in predicting airflow and temperature in a naturally ventilated double skin Facade. *Applied Microclimatic Thermal Engineering* 37(May): 267–274.

Roelofsen P (2002) *Ventilated Facades: climate Facade versus double-skin Facade*. European Consulting Engineering Network.

Safer N, Woloszyn M, Roux JJ (2005) Three-dimensional simulation with a CFD tool of the airflow phenomena in single floor double-skin Facade equipped with a venetian blind. *Solar Energy* 79(2): 193–203.

Saroglou T, Theodosiou T, Givoni B, Meir IA (2020) Studies on the optimum double-skin curtain wall design for high-rise buildings in the Mediterranean climate. *Energy and Buildings* 208(Feb): 109641.

Souza LCO, Souza HA, Rodrigues EF (2018) Experimental and numerical analysis of a naturally ventilated double-skin Facade. *Energy and Buildings* 165(Apr): 328–339.

Streicher W (2005) *Best practice for double skin Facades (EIE/04/135/S07.38652)*. WP 1 Report "State of the Art". BESTFACADE.

Von Grabe J (2002) A prediction tool for the temperature field of double Facades. *Energy and Buildings* 34(9): 891–899.

Waldner R, Flamant G, Prieus S, Erhorn-Kluttig H, Farou I, Duarte R, et al. (2012) *BESTFACADE: best practice for double skin Facades*. Available at: http://www.bestfacade.com/pdf/downloads/WP5%20Best%20practice%20guidelines%20report%20v17final.pdf.

Wang H, Lei C (2020) A numerical investigation of combined solar chimney and water wall for building ventilation and microclimatic thermal comfort. *Building and Environment* 171: 106616.

Wang Y, Chen Y, Li C (2019) Airflow modeling based on zonal method for natural ventilated double skin Facade with Venetian blinds. *Energy and Buildings* 191(Part 2): 211–223.

Xu X, Yang Z (2008) Natural ventilation in the double skin Facade with venetian blind. *Energy and Buildings* 40(8): 1498–1504.

Yang S, Cannavale A, Di Carlo A, Prasad D, Sproul A, Fiorito F (2020) Performance assessment of BIPV/T double-skin Facade for various climate zones in Australia: effects on energy consumption. *Solar Energy* 199(Mar): 377–399.

Ye P, Harrison SJ, Oosthuizen PH (1999) Convective heat transfer from a window with a venetian blind: detailed modeling. In *ASHRAE Transactions*, 1031–1037.

Yoon G, Kato H, Okumiya M (2012) Study on the microclimatic thermal performance of double-skin Facade: part 1. Proposal of prediction technique for microclimatic thermal performance on cooling season. *Journal of Environmental Engineering* 77(674): 251-257.

Zöllner A, Winter ERF, Viskanta R (2002) Experimental studies of combined heat transfer in turbulent mixed convection fluid flows in double-skin-Facades. *International Journal of Heat and Mass Transfer* 45(22): 4401–4408.